# Variation in Nitrate Sources and Delivery in Space and Time within the 389 ha Lake Okaro Catchment

A thesis

submitted in partial fulfilment

of the requirements for the degree

of

**Master of Science (Research) in Environmental Sciences**

at

**The University of Waikato**

by

**CLAIRE ELIZABETH EYBERG**


THE UNIVERSITY OF
WAIKATO
*Te Whare Wānanga o Waikato*

2020

# Abstract

The eutrophication of surface water is a global issue, with excessive nitrate concentrations reducing water quality and affecting water supplies, ecosystem health and its recreational use. In New Zealand, the degradation of freshwater quality has largely been attributed to nitrate leaching from intensive landuse, in particular from intensively grazed pastoral systems.
As agricultural activity in catchments can contribute a large proportion of the nutrient pollution in surface waters, an understanding of nitrogen dynamics is therefore vital in managing the downstream effects of diffuse nitrogen inputs. Nitrate isotopes ($\delta^{15}N$, $\delta^{18}O$) have been increasingly used for determining nitrate cycling and source identification. Together with water isotopes ($\delta^{2}H$, $\delta^{18}O$), these conservative tracers can provide the necessary tools for determining the transport mechanisms of nitrate.

Lake Okaro has suffered from water quality degradation for several decades, and has been the focus of intense lake restoration projects focused on nutrient management. The 389 ha agriculture-dominated catchment exemplifies New Zealand's complex physiographic landscape.

Results from high-resolution monitoring of streamflow during storm events demonstrates the potential to capture dynamic shifts in distinct water sources, but can be limited by insufficient monitoring of ancillary parameters, or a lack of pre-event characterisation of streamflow. Spatial sampling indicated characteristic fractionation processes for sites of similar environments, likely due to enhanced plant and microbial processing of carbon and nitrogen. This spatial sampling demonstrates that even in small catchments, there may be a significant degree of heterogeneity in water and nitrate flows, in both space and time.

Nitrate contributions were much lower in summer relative to autumn and winter during baseflow or non-storm flow. Storm events contributed a disproportionate amount of nitrate, but the effect was most notable in winter.

During baseflow, or non-stormflow, in the main inflow stream in the Lake Okaro catchment, nitrate had $\delta^{15}N$ and $\delta^{18}O$ values indicative of a soil nitrogen origin (+5.8 ‰ to +7.3 ‰, and -0.5 ‰ to +1.7 ‰, respectively).

The dominant nitrate sources shifted during rain events, with streamflow in the winter event having $\delta^{15}N$ and $\delta^{18}O$ values indicative of urine, whereas the summer event observed $\delta^{18}O$-enriched baseflow signatures. Water isotope ratios indicated the winter event was dominated by event water. The differing seasonal responses to rainfall suggest nitrate inputs during storms in this catchment are strongly linked to seasonal nitrate availability in water flow paths.

Patterns observed in temporal and spatial data collected require more investigation around potential reasons or mechanisms of fractionation. Further refinement of the Okaro catchment flows and cycling of nitrogen will help create more catered management techniques.

# Acknowledgements

Firstly, I have to thank my supervisor Troy Baisden for his relentless support and encouragement. I greatly appreciate your patience and providing me with the 'bigger picture' when I fell down a research rabbit hole, which was a lot.
Rachel Murray, the LGR whisperer, if it wasn't for you I'd have no results to write about. I appreciate all your time in the field helping me sample, but more importantly for letting us stop for Fanta McFloats on the way back. A similar thanks to Chris Eager for all the time spent in the field and lab helping me figure things out, your vast field experience was very welcomed. Meti, I have really enjoyed working together and can't wait to read your PhD. A massive thank you to my friend Andrew Douie for staying with me overnight to sample in the rain when no-one else would. Likewise, to Allycia Van de Laar for helping sample in the rain. More thanks to the many other talented and knowledgeable people at the University of Waikato who have assisted me: Simon Stewart, Chris McBride, Dean Sandwell, Grant Tempero, and the patient lab technicians, Lee, Bex and Warrick. Others from UoW who have helped me tremendously, Christine White and Hannah Te Puia. Thanks to all my fellow Masters students, especially Kendal.
I extend a huge thank you Birchall family and team for being incredibly accommodating and helpful during our site visits. As well as BOPRC, and especially James Dare for sending through a range of data. A very appreciative thanks to MBIE and UoW for the study award.

Ben, thank you for being my solace during this time. I am forever indebted for all the home-cooked meals and snacks you brought in to my study nest. Katrina and Jeremy, thank you for looking after me, checking I was still alive and taking me for icecream. Laura, thank you for always being there, no matter the distance. Bryony, I don't have enough space in this thesis to thank you for all the support and encouragement you have given me. My many other friends who have kept an eye on me from a far and sent their love and thoughts… I would mention you all individually, but there is just not enough space.
I thank my family for always being there for me. My brothers, David and Steven, who I have missed seeing dearly. To Ursula, I am so glad to have you in our lives. To my Dad, my number one supporter and champion in everything, I couldn't have done any of this with you.

# Table of Contents

# List of Figures

# List of Tables

# Chapter One

# Introduction

## 1.1 Background

The eutrophication of surface water is a global issue, with excessive nitrate concentrations reducing water quality and affecting water supplies ecosystem health and its recreational use (Vitousek et al., 1997; Stark and Richards, 2008; Galloway et al, 2008). In New Zealand, the degradation of freshwater quality has largely been attributed to nitrate leaching from intensive landuse, in particular from intensively grazed pastoral systems (MfE, 2019; Burkitt et al., 2017). Nitrate is the dominant contaminant of groundwater in New Zealand (Close et al., 2016).

As agricultural activity in catchments can contribute a large proportion of the nutrient pollution in surface waters, an understanding of nitrogen dynamics is therefore vital in managing the downstream effects of diffuse nitrogen inputs (Blaen et al., 2017). Variations in nitrate concentrations cannot be captured sufficiently by monthly sampling, and impairs the ability to study the biogeochemical conditions associated with both the transport and transformations of nitrate (Burkitt et al., 2017). When it comes to nitrogen loading calculations, this pairing of higher resolution discharge with discrete water quality sampling can hugely affect the accuracy of estimates (Burkitt et al., 2017).

During storm events, stream water quality can vary substantially, and periods of the poorest water quality may only be experienced for a short duration of the event (Kirchner et al., 2004). Therefore, there is a requirement for high-frequency monitoring over a series of storms to quantify the response of water quality to rainfall under various conditions, as well as to capture these transitory environmentally-significant episodes (Chappell, Jones, Tych, 2017).

The range of water quality parameters that can be measured in-situ has increased, which is enhancing understanding of the variation in water quality at the finer scale of storm events (Lloyd et al., 2016). Photometric UV/VIS sensors can be used in both surface and groundwater monitoring, providing high-resolution nitrate concentrations (Huebsch et al., 2015).

While nitrate concentrations are affected by numerous variables, it is the flow of water that is the dominant driver of nitrate flux (Feng, Schilling, and Chan, 2013). High-frequency monitoring of water quality parameters and their relationship with hydrological fluxes can be used to infer nitrate pathways and potential sources (Lloyd et al., 2016). Storm events are responsible for a disproportionate amount of nutrient transport in catchments, therefore characterising a catchment's response during storms and understanding how this drives mobilisation of nitrates is necessary for nutrient management (Lloyd et al., 2016). Water isotopes (2H and 18O) can provide information on sources of water carrying these nutrients.

Identification of the source of nitrate contamination is an important step in nitrate management, as then the input of nitrates can be reduced or controlled (Zhang et al., 2018). Over the last few decades, dual nitrate isotopes (15N and 18O) have been increasingly used for source identification and transformations of nitrate, as these isotopes can have different isotopic compositions and ratios that reflect this, respectively (Kendall 1998; Wells et al., 2016; Rayner et al., 2019).

Isotopic fractionations of nitrogen can be influenced by vegetation extent and type, soil structure and dynamics, landuse, or other factors that alter biogeochemical processes that affect nitrogen transformation (Zhang et al., 2018).

As source signatures can partly overlap and may be altered through complex fractionation processes, the combination of nitrate isotopic data

with other data types, such as hydrological, physiochemical, and water isotopes, can further resolve of these signals of nitrate (Zhang et al., 2018). Organising landscape in to units can provide insight in to local physiochemical and hydrological processes, and differences between these units, that can otherwise be concealed by a lumped catchment response to environmental drivers (McGlynn and McDonnell, 2003). Water quality can vary over twice as much due to differences in landscape characteristics than to differences in land use (Rissman et al., 2018).

In New Zealand's complex landscape, taking this in to account is particularly imperative. As such, groups have begun to adopt a physiographic classification approach coupled with mapping of Physiographic Units (PGU), as a tool for managing processes and control points at farm scale to reduce water quality degradation (Rissman et al., 2018).

Analysing spatially and temporally variable data in the context of their physiographic environmental allows for enhanced interpretation of nitrate sources and transformations, as well as the ability to incorporate this coupled information in to the managing of sub-catchment parcels of land for environmental protection.

## 1.2 Study Area

The Okaro catchment is in the Bay of Plenty region of the North Island, approximately 20 km southeast of Rotorua. It is located in the Waiotapu geothermal area, which resides at the southern fringe of the Okataina Volcanic Complex and within the central Taupo Volcanic Zone (Hardy, 2005; Environment Bay of Plenty, 2006).

Lake Okaro is the smallest lake (31 ha) of the 12 in the Rotorua area, with a catchment size of 389 ha (Scholes, 2009; Özkundakci, Hamilton and Scholes, 2010). The Okaro catchment has a small rural community centred around agriculture (Environment Bay of Plenty, 2006).

### 1.2.1 Environmental Background

***Environmental Issues***

Lake Okaro has experienced degraded water quality over the past several decades. It is suggested the lake has been eutrophic since at least the 1960's, with anecdotal evidence indicating the water quality deteriorated significantly in the late 1970's (Forsyth et al., 1988; Environment Bay of Plenty, 2006).

Since 1997, cyanobacteria and algal blooms have occurred annually, and often regularly over the year (Environment Bay of Plenty, 2006; Scholes, 2009). This has been predominantly been due to increased nutrient inputs from the Okaro catchment, as well as internal cycling of nutrients during seasonal periods of stratification (c. 8 months of the year) and the resulting anoxia in the bottom waters (Özkundakci, Hamilton and Scholes, 2010). The main input of nitrogen in to Lake Okaro is from the pastoral land use which dominates the catchment (Environment Bay of Plenty, 2006).

Some improvement has been seen in the lake's water quality since its poorest in the late 1990's (Trophic Level Index (TLI) of 6), with TLI even reaching the Action Plan target of a TLI of 5 or less. Since 2014 there has been a gradual increase of TLI score observed (Figure 1.1) returning it to a classification of supertrophic (TLI>5). These TLI scores are most strongly correlated with total nitrogen and chlorophyll-*a* concentrations (Figure A.1) so appears to be most affected by total nitrogen concentrations (as algal growth and resultant chlorophyll-a concentrations is related to nutrient availability).

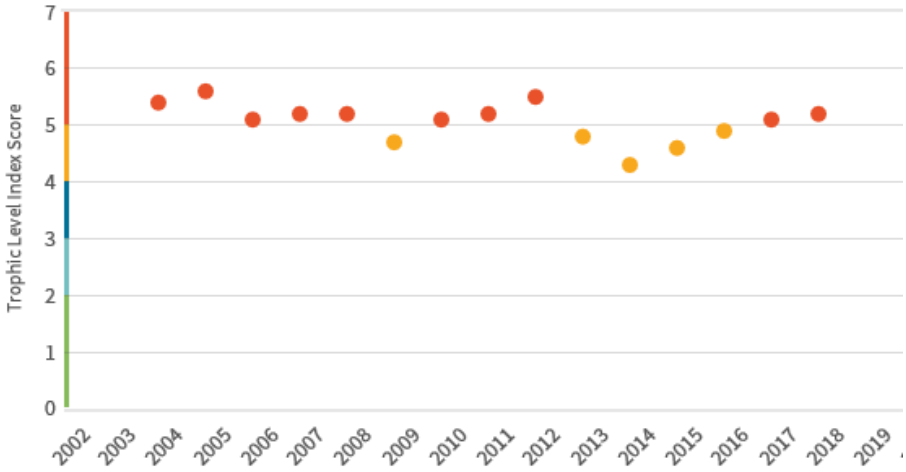


**Figure 1.1.** Trophic Level Index scores of Lake Okaro between 2004 and 2018, based off average in-lake sample concentrations of total nitrogen, total phosphorous, Secchi depth and chlorophyll-*a* (LAWA, 2020)

Much of the improvement to lake quality has been through concerted effects by the Bay of Plenty Regional Council and the local farming to mitigate nutrient inputs in to the lake. However, recent TLI scores highlight the need for further, more targeted mitigation to reduce nutrient inputs, especially that of nitrogen.

### *Land use and cover*

The Lands and Survey Department cleared land in the Okaro Lake catchment in the 1950's, with the purpose of developing it for agricultural use (Cross, 1963; Environment Bay of Plenty, 2006). The Okaro catchment is dominated by agricultural landuse (Figure 1.2). This shows the dominant landuse for each parcel, and does not incorporate sections of forestry development within farm land

Rotomahana Station is the largest farm (556 ha) in the Okaro catchment, and predominantly grazes sheep but also supplies grazing area for cattle from their sister farm (BFEA, 2003). Some areas have been converted to new forestry (Landcorp Farming Limited, 2017).

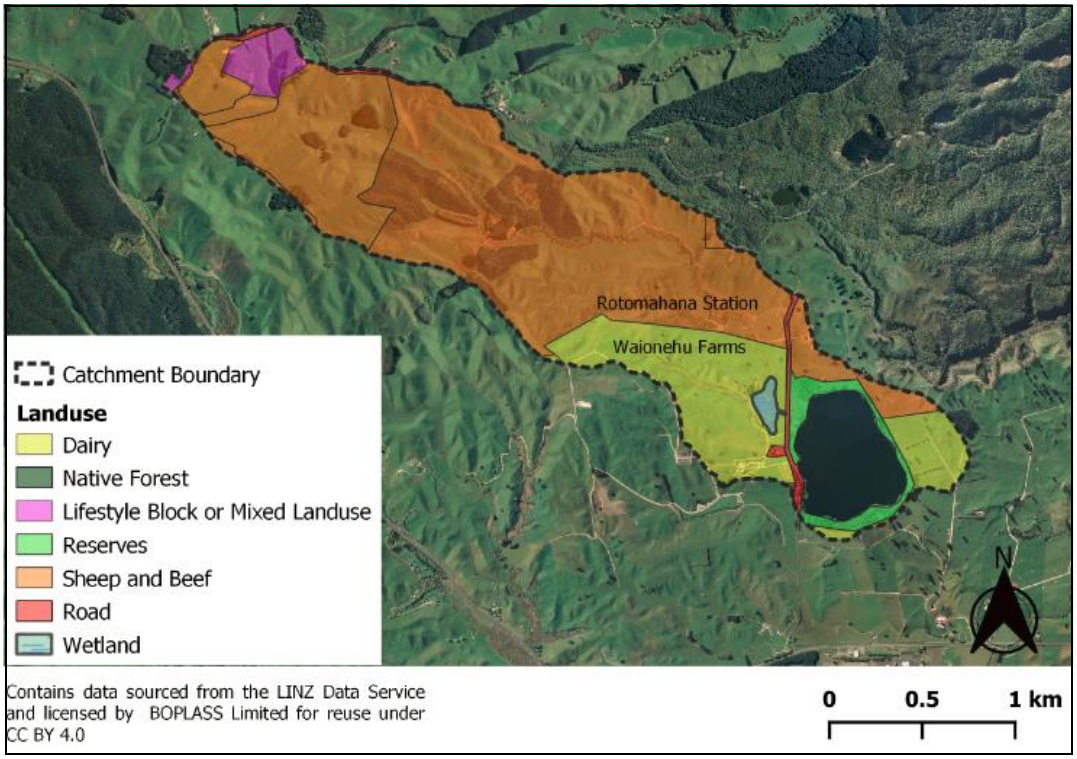


**Figure 1.2.** Main landuses of land parcels in the Okaro catchment in 2017, indicating main farms draining in to Lake Okaro.

Waionehu Farm (also referred to as Birchall Farm) has approximately 60ha of their dairy farm located in the Okaro catchment, near the inflow in to the lake on the west to north-western margin. The farm is approximately a system 2.5, as supplementary feeding is required due to the steep contours of much of their pastures (S. Birchall, personal communication, 3 September, 2019).

The Lake Okaro Recreation Reserve (managed by Rotorua District Council, shown as light green in Figure 1.2) includes the smaller wetland, old stream channels, public access and amenities, and natural wetlands and wildlife habitat at the lake edge (Environment Bay of Plenty, 2006). It is a popular destination for tourists to visit and camp, and recreational uses of the lake mainly involve boating activities, such as fishing and water skiing (Environment Bay of Plenty, 2006).

Before the catchment was largely cleared of native vegetation in order to be developed for farming, the land was dominated by manuka and bracken (Cross, 1963).

Since this initial clearance, the catchment has gradually had a reduction on pasture cover, largely to retirement of land for riparian planting and conversion to exotic forestry (Table 1.1. **Land cover in the Okaro catchment (adapted from Scholes (2009)**.

**Table 1.1.** Land cover in the Okaro catchment (adapted from Scholes (2009)

| Land Cover (%) | 1978 | 1996 | 2003 | 2018† |
|---|---|---|---|---|
| Pasture | 100 | 95.7 | 90.6 | 82.2 |
| Exotic forest | 0 | 0.7 | 6.3 | 9.6 |
| Native vegetation | 0 | 3.6 | 2.1 | 8.2 |

† Based off the land cover database v5 data from LRIS Portal

The riparian margin of the northern stream used to consist of poplars, willow, blackberry and scrub, and while some remains, much of it has been replaced with native riparian vegetation (Environment Bay of Plenty, 2006).

### *Mitigation and Management*

To address the issues of lake quality degradation, an Action Plan was made for the Lake Okaro catchment in 2006, with the aim to reduce the lake's TLI to below 5 and improve water quality and ecological health of the lake (Environment Bay of Plenty, 2006; Özkundakci, Hamilton and Scholes, 2010). The actions outlined in the plan to reduce nutrient inflows in to the lake were construction of a wetland, in-lake phosphorus removal, riparian restoration and protection, and implementation of best farming management practises (Environment Bay of Plenty, 2006; Özkundakci, Hamilton and Scholes, 2010). There is no in-lake mitigation of nitrogen, and therefore the onus is on managing the external loads of nitrogen to the lake. It is best practise to control both nutrients, as this will still reduce growth of nuisance algae or cyanobacteria.

The wetland system that was completed in 2006, consists of two wetlands, a larger wetland which flows in to a smaller wetland in the lake reserve, with a combined area of 2.3 ha (Hudson et al., 2009). The primary stream is diverted in to the main wetland through a 184 $Ls^{-1}$ rated pipe, whereas the

secondary stream flows directly in to the main wetland, as do farm drains (Tanner et al., 2007). A weir at the primary stream intake allows for a proportion of stormflow to bypass the wetland (to prevent scouring or inundation), and flow along the old stream channel and in to the lake directly (Hudson et al., 2009).

The wetland was designed to remove nutrients through sedimentation and denitrification, with potential for further removal through sorption and plant uptake (Tanner et al., 2007). A shallow depth, native wetland sedges and incorporation of additional carbon through pine dust was implemented to enhance the denitrification process (Tanner et al., 2007). The initial estimate of total nitrogen removal capability being 45% from the inflows (165–210 kgN $yr^{-1}$) (Tanner et al., 2007), and an assessment of wetland performance (undertaken 3 years after its completion) indicated that the nutrient reduction estimates and targets were exceeded overall (Hudson and Nagels, 2011). Detention bunds were installed upstream to reduce maximum flows reaching the diversion weir and minimising bypass flow, as well as allowing time for a reduction in flow for sediment settling.

Removal of available phosphorus from the lake was first attempted in 2003, through an Alum application trial, but had short-lived improvement (Gibbs et al., 2007; Özkundakci, Hamilton and Scholes, 2010). In 2007, a different P-inactivating material, modified zeolite, was applied as a sediment-capping agent to the lake where the depth exceeded 5 m, which saw a marked reduction in hypolimnion phosphorus concentrations (Özkundakci, Hamilton and Scholes, 2010).

Riparian restoration and protection of waterways had already begun before the initiation of the Action Plan as this was outlined in the Regional Water and Land Plan to be completed by 2012, and is now fully completed (Environment Bay of Plenty, 2006). Works to satisfy this included fencing for livestock exclusion, removal of certain exotic vegetation to plant native species and additional planting to stream and lake margins (Özkundakci, Hamilton and Scholes, 2010). Planting of native vegetation around the

crater pond (now stormwater detention pond) on the north stream was undertaken by the Department of Conservation (Environment Bay of Plenty, 2006).

Waionehu Farm follows an environmental plan and applies best management practises, which include implementation of a herd home, once a day milking and careful pasture rotation to minimise pugging and nitrate leaching in wet conditions (Birchall, pers comms, 2019). Improvements have also been made to their management of farm dairy effluent, including a solids trap and muck spreader, large capacity effluent pond and irrigating effluent depending on soil moisture to avoid runoff (Birchall, pers comms, 2019). The riparian margins have been revegetated and fenced off for stock exclusion for all stream channels on this farm (Environment Bay of Plenty, 2006), and the farm has retired 5 ha of land around the wetland and lake (Birchall, pers comms, 2019).

Rotomahana Station is owned by Pāmu (Landcorp Farming Ltd), who are a part of the Okaro Community Lake Restoration Group, and have their own environmental policies and plans, which have included new forestry development on existing farm land (BFEA, 2003; Landcorp Farming Limited, 2017). Nutrient loss has been reduced through altered fertiliser application (such as use of serpentine rather than urea), no break-feeding, minimal cultivation and a relatively low stocking rate (BFEA, 2003). Riparian protection has been implemented on 18.1 ha around streams and wetland, .4 ha of perennial and ephemeral stream channels, and around three sinkholes created by the 1886 AD Tarawera eruption (BFEA, 2003). Part of their remedial work has included installation of a storm water riser to detain up to 12,000 $m^2$ of water during high flow events (BFEA, 2003).

Nutrient budgets for farms in the Okaro catchment have been calculated, and this is monitored using Overseer®, a farm-scale model that determines input and output nutrient values from a range of criteria, such as stocking rates, fertiliser, effluent management and environmental factors (Özkundakci, Hamilton and Scholes, 2010).

### 1.2.2 Catchment Characteristics

#### *Landscape, Geology and Soils*

Lake Okaro formation began c. 700 years, soon after the Kaharoa eruption (1314 ±12 AD), by a phreatic or steam-driven eruption, followed by two secondary hydrothermal eruptive episodes (Hardy, 2005; Montanaro et al., 2020), but was originally thought to be formed by geothermal explosion (Lloyd, 1959). Under this Okaro breccia is 2-5 m of tephra deposits from various volcanic eruptions from the Okataina Volcanic Complex, including Kaharoa and Taupo tephra, as well as paleosols (buried horizons) as a result of these ash deposits (Figure 1.3) (Cross, 1963; Hardy, 2005).

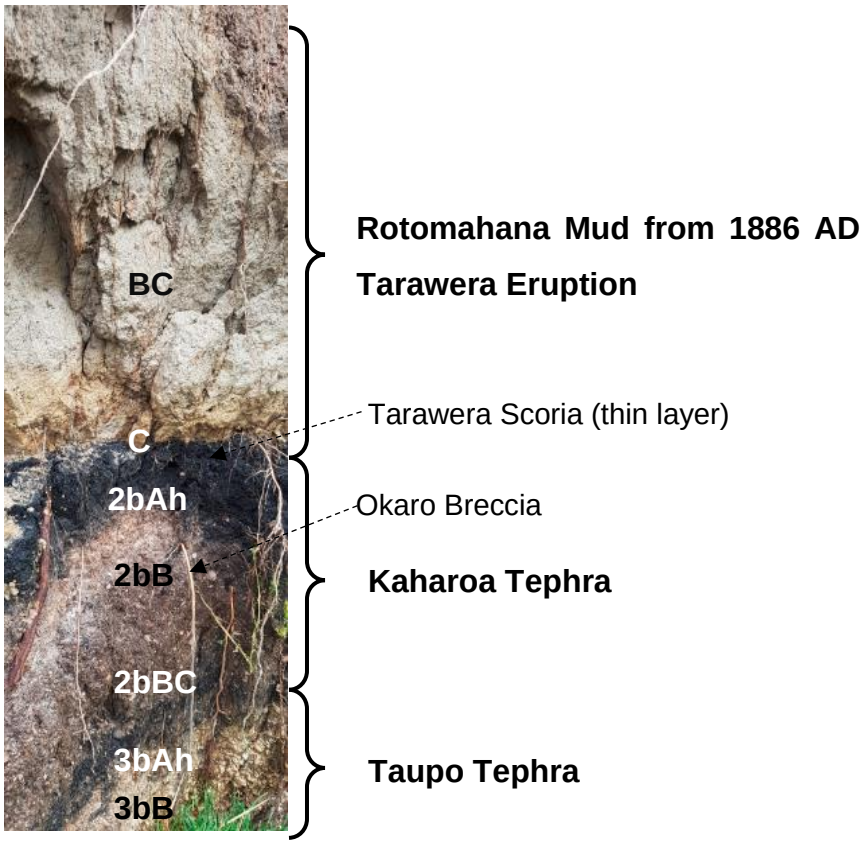


**Figure 1.3.** Horizons of exposed soil profile on the north-western valley floor of the Okaro catchment, with estimated horizon notation and descriptions based off information from Hardy (2005) and Lowe (2006).

The poorly sorted breccia deposits from the Okaro eruptions consist of large lapilli to pumice blocks and welded ignimbrite amongst fine mud material (approximately a third of material smaller than 0.5 mm), giving this layer a

low permeability (Hardy, 2005). A thin paleosol covers the Okaro breccia, which is then overlain by a variable depth (approximately 0.1 – 1m) of grey, uncompacted Rotomahana Mud that was deposited on the Okaro catchment during the 1886 AD Tarawera eruption (Hardy, 2005).

Exposed soil profiles around the catchment display varying thicknesses of the different soil horizons or deposits (Figure A.11), indicating the variability in soil profiles due to distance from the various eruption sites as well as deposition and erosion dynamics of the different landforms (i.e. on the hills versus valley floors).

A unit of weakly compacted ash and pumice flows, known as the Earthquake Flat Pyroclastics, has formed the base topography of the Okaro catchment (Nairn, 2002). The series of stream-driven eruptive episodes formed over 30 craters in a complex field, further contributing to the catchment's topographic features (Montanaro et al., 2020) The north-northwest of the lake has areas of volcanically-derived hummocky terrain (Figure A.12.) (Montanaro et al., 2020). Large-scale rill erosion is most prevalent north to northwest of Lake Okaro, providing conduits for preferential flow of rainwater (Hardy, 2005). Cessation of the rapid rill formation after the 1886 AD eruption is believed to be due to the low permeability of the Okaro breccia, as the rilling is exclusively in the then freshly deposited Rotomahana Mud mantle (Hardy, 2005). This flow of eroded material sediment originally caused degradation, but later as the erosion slowed, the result was 0.1 m of aggradation of the valley floors (Hardy, 2005).

Soils found in the catchment include Okaro-Rotomahana complex, Rotomahana silt loam varieties, Rotomahana hill soils and Rotomahana shallow sandy loams (Figure A.19). Clay minerals (kaolinite and montmorillonite) have been identified and suggests the material has undergone substantial weathering (Hardy, 2005).
Rotomahana mud is a tephra with an atypical composition; it has approximately 20% clay, including allophane, which has enhanced

phosphorus retention properties (Kirkman, 1976; McIntosh, 2003). Rotomahana silt loam has high natural fertility, even with a relatively low pH (4.9 - 5.1) (Cross, 1963). The pumice soils, which are typical of Rotorua catchments, have relatively low nitrogen in their natural state (Vincent, 1980; McIntosh, 2003).

### *Climate and Hydrology*

The Okaro catchment is elevated (423 m asl) with a low-permeability layer of breccia, and therefore believed unlikely to receive surface or groundwater from other catchments (Environment Bay of Plenty, 2006; Gillon, White, & Hamilton, 2009). However, modelling of groundwater has suggested that the groundwater zone and the catchment boundary in the headwaters could differ, and calculated groundwater inflows from the Tarawera and Rotokakahi zones (White et al., 2016).

It is believed that a considerable proportion of the precipitation that falls in the Okaro catchment is quickly transferred via surface and subsurface flow to channels and ponds, with a lesser proportion infiltrating deeper in to the soil to become groundwater (Environment Bay of Plenty, 2006). This is due to the lower permeability layer of Okaro breccia being extensive, which encourages quickflow over recharge. As there was approximately 15-20 years before development of the catchment began and stabilised reduction of water quality in the lake, the lag time also suggests this catchment has a relatively young groundwater age (Environment Bay of Plenty, 2006). The groundwater thus remains shallow and mostly contributes to the surface water (Environment Bay of Plenty, 2006). Modelling has suggested that there may even be limited flow between the surrounding groundwater and Lake Okaro (White et al., 2016).

There are two unnamed streams that flow in to Lake Okaro, and one stream, the Haumi stream, exits southeast of the lake to eventually flow in to Lake Rotomahana (Environment Bay of Plenty, 2006). The northern stream (also referred to as the north western or primary stream) provides the most water in to Lake Okaro, and including its tributary, has a total channel length of

3,920 m (Environment Bay of Plenty, 2006). The southern stream (also referred to as the western or secondary stream) has a total channel length of 1070 m (Environment Bay of Plenty, 2006). Baseflow in to the lake was estimated to be 35 L/s from the streams (Environment Bay of Plenty, 2006).

Geological evidence suggests that the water level of Lake Okaro was approximately 3 m higher than it is on average at present day (Hardy, 2005; Montanaro et al., 2020). In recent history, the lake has been known to vary up to 1.5 m in level in response to rainfall (Cross, 1963). There are three ponds in the catchment (0.8 – 2.8 ha) that are the result of small crater formation, with the largest (2.8 ha) pond being part of the northern stream channel (Environment Bay of Plenty, 2006).

Soil in the Bay of Plenty region receives frequent rainfall during winter but there can be large deficits in soil moisture over summer due to low rainfall and high evapotranspiration (Chappell, 2013). The region is sheltered from all but a northerly direction, so predominantly receives rainfall from northerly tropical airstreams, but the dependency of wind direction for rainfall produces considerable seasonal variation (Chappell, 2013).

Cross (1963) described the two dominant winds for the Okaro catchment as wet, warm northerlies and dry, cold southerlies. Previous rainfall calculations have estimated a mean rainfall of 1445 mm $year^{-1}$ for the catchment, with 48% being lost as evaporation, giving approximate rainfall inflow values of 189 L $s^{-1}$ and evaporative losses of 86 L $s^{-1}$ (Gillon, White, & Hamilton, 2009).

## 1.3 Research Aims and Objectives

Storm events and particular areas of landscape can contribute a disproportionate amount of nitrate to surface water, but is under-represented in the New Zealand literature. This research aims to enhance the understanding of nitrate sources and dynamics in agricultural catchments in New Zealand, and contribute to the development of tools to

manage nitrates in New Zealand's complex landscape environment. Improved resolution of the fates of nitrate will allow more effective implementation of control points for the management of nitrate leaching and its subsequent contamination of freshwater systems.

To address this, the project combined physiochemical and hydrological data with dual nitrate and water isotopes, with the following objectives:

- Investigate storm events through high resolution monitoring and sampling data collection to determine timing and source of nitrate delivery, and how this is affected by biogeochemical and hydrological processes
- Characterise baseflow or non-stormflow conditions to compare against storm events and determine seasonal trends
- Investigate spatial differences in the catchment to help infer isotopic source and transformation signals, including the effect of environmental and physiographic differences on nitrogen dynamics

## 1.4 Thesis Outline

### 1.4.1 Chapter Two: Literature Review

This chapter firstly outlines the sources, pathways and cycling of nitrate in terrestrial and aquatic environments, focusing on the coupling with hydrological processes, namely storm events. The majority of this chapter then explores the use of stable isotopes as tracers for nitrate contamination and the understanding of nitrate dynamics and attenuation in agricultural catchments, with a focus on dual nitrate and water isotopes. This is followed by the combining other information, such as physiochemical data for a more effective multi-tracer approach.

### 1.4.2 Chapter Three: Methods

This chapter firstly details the sampling and data acquisition sites, as well as describing sampling instrumentation. Procedures for sample preparation and analysis are outlined, followed by a description of data analysis performed.

### 1.4.3 Chapter Four: Results

This chapter presents data collected from the Okaro catchment during baseflow and storm events. The data consists of stable dual nitrate and water isotopes, nitrate concentration, and physiochemical and hydrological supplementary data. Firstly, an overall picture of spatial and temporal variations is provided. The data in this section is divided in to subgroups: physiochemical and hydrological, nitrate isotopes, water isotopes and an integration of parameters. Dynamics during storm events are then explored through the storm characteristics, integrated timeseries and isotope hysteresis.

### 1.4.4 Chapter Five: Discussion

This chapter links data together and discusses how variations in isotopic values under different conditions could be used to interpret nitrate signals, and implications for nitrate management. This also chapter describes limitations and considerations for nitrate management in the Okaro catchment.

### 1.4.5 Chapter Six: Conclusion

This chapter summarises the findings and implications of this research and identifies directions for future research opportunities.

# Chapter Two

# Literature Review

This his chapter introduces the concepts and processes that are pertinent to nitrogen sources, cycling, and transport, as well the mechanisms by which stable isotopes are used to trace nitrate source and transport. The chapter starts with an outline of nitrogen sources and their temporal variability, an overview of nitrogen cycling, which can affect these nitrogen sources, followed by the hydrological flow paths responsible for their delivery in to freshwater systems. The chapter then centres on stable isotopes, the mechanisms that effect their relative proportions in the environment, and their use as tracers for nitrogen sources and flow paths, with a focus on nitrate ($\delta^{15}N$, $\delta^{18}O$) and its evolution as a tracer. Lastly, an outline of water ($\delta^{2}H$, $\delta^{18}O$) isotopes and their use in this context.

## 2.1 Nitrogen Sources, Cycling and Pathways

An increase in nitrate concentrations in receiving waters have been largely credited to intensive agricultural landuse, but the full impact may be concealed by the environment's ability to attenuate nitrogen through denitrification (up to 60%) (Gruber and Galloway, 2008; Wells et al., 2016). A reduction in an environment's ability to remove part of this excess nitrogen could result in greater eutrophication of the receiving environments.

### 2.1.1 Nitrogen Sources and Cycling

***Sources***

In agricultural catchments, nitrogen contamination of surface waters is largely a result of inorganic nitrogen fertiliser application, animal excreta and other organic nitrogen sources (Kellan, 2005).

An integration of fertiliser and livestock urine form the nitrate leached from pasture (Buckthought et al., 2015; Wells et al., 2016). In New Zealand, the application of nitrogen fertiliser (generally as urea), has increased sevenfold,

with an average of 150 kg N $ha^{-1}$ $yr^{-1}$ for dairy farms (Wells et al., 2016). Inputs of nitrogen from livestock excreta have also increased as a result of higher stocking rates and increased irrigation enhancing nitrate leaching (McDowell et al., 2011). Annually, urine spots can cover approximately a quarter of a dairy paddock (Moir et al., 2011). The high excess nitrogen in urine spots (700–1000 kg $ha^{-1}$) from dairy cows contributes most of the nitrate in New Zealand groundwater (Di and Cameron, 2002; Moir et al. 2011). Unlike the concentrated and continuous nature of urine delivered to pasture, nitrogen fertiliser is applied conservatively and only when required for pasture growth, and thus contributes less direct leaching (Ledgard et al., 1999).

Of the nitrogen deposited to soil, a varying amount will subsequently discharge in to surface water, both spatially and over time (Sudduth et al., 2013; Wells et al., 2016).

***Cycling***

Changes in land use and vegetation, as well as an increase in atmospheric nitrogen deposition, alters nitrogen cycling in soils (Kellan, 2005). Plant cover in pastoral systems reduces nitrate concentrations and subsequent nitrate leaching (Rayner et al., 2019).

Denitrification requires a set of conditions to occur, which include low dissolved oxygen, electron donors (typically carbon) and denitrifying bacteria (Seitzinger et al., 2006). As these required conditions vary both temporally and spatially at different scales, quantification of denitrification and its effects on nitrogen fluxes can be problematic at catchment scales (Groffman et al., 2009; Woodward, Stenger, and Bidwell, 2013).

Declining nitrate concentrations coupled with low dissolved oxygen along a groundwater flow path can be an indication that denitrification has occurred (Clague, Stenger, & Clough, 2015). As nitrate can be removed by groundwater through denitrification, it is important to determine leaching losses, nitrate attenuation and flow paths for nitrogen loading models since

there may not be nitrate conservation between the root zone and groundwater discharging in to surface waters (Woodward, Stenger, and Bidwell, 2013).

Modelled nitrate concentrations in streams tend to be higher than what is actually measured (Woodward, Stenger, and Bidwell, 2013). These predictions are based on nitrate leached from the root zone as the source, but do not incorporate factors pertaining to the extent of nitrogen transformations, which will affect the end nitrate concentration in the surface water (Clague, Stenger, & Clough, 2015).

Monitoring can suggest that there are only temporal changes to nutrient loading in surface water on seasonal time scales, however nutrient concentrations have been shown to have the potential to change substantially on daily time scales (Lam et al., 2012; Woodward, Stenger, and Bidwell, 2013).

***Continuous Nitrate Measurement***

The progression of technology that can continuously monitor nitrate-N has provided insight into the fluctuation of nitrate-N concentrations at a variety of time scales. This continuous measurement allowed Burkitt et al. (2017) to detect nitrate trends in the Manawatu River, leading to further understanding of catchment scale influences on nitrate concentration, something poorly covered in the New Zealand literature. They noted that while discrete samples throughout the year showed the same general trends, it did not capture the first runoff event after the dry season, or concentrations during peak flows, when there can be high nitrate delivery (Burkitt et al., 2017).

High-resolution nitrate concentration data allows for better understanding of nitrate dynamics under different conditions in catchments and ability to target when nitrate is delivered to water bodies, as well as how much, allowing better estimates for nitrate load calculations (Burkitt et al., 2017).

### 2.1.2 Hydrological Flow paths

Feng, Schilling, and Chan (2013) investigated diurnal nitrate concentration fluctuations in the Racoon River (Iowa, United States) using a dynamic regression model, which suggested that 95% of variation could be explained by the combination of daily precipitation and discharge, and their complex interaction in the catchment. Different flow paths will vary in their contribution to nitrogen loading depending on the hydrological setting at the time (Woodward, Stenger, and Bidwell, 2013).

Translatory flow describes lateral throughflow due to precipitation infiltrating in to the soil and displacing water previously stored in the soil, which subsequently enters in to the stream channel (McDonnell, 2014). Brooks et al. (2010) found that soil water that was tightly held in pores during the dry season did not contribute to runoff generation in the subsequent wet season. Other studies have also found a distinct separation of water pools between that of water used by vegetation and that of mobile water participating in ground and stream flow, known as the ‘the two water worlds’ hypothesis (McDonnell, 2014). This concept is shown diagrammatically in Figure 2.1 through hypothetical water isotope cycling in a forested catchment. This is contradictory to the piston flow displacement mechanisms of translatory flow first described by Hewlett and Hibbert in 1967 (McDonnell, 2014).

Isotopic variation of stream water, groundwater and soil water is below that of the isotopic distribution of the rainfall inputs, with the lightest and heaviest fractionation being truncated (McDonnell, 2014).
In catchments with humid climates, the mobile water falls along the meteoric line (McDonnell, 2014).

Soil water found deepest in the soil profile are closest to the local meteoric line, and progressively deviates from the line with decreasing soil depth due to evaporative effects on the water isotopes (McDonnell, 2014).

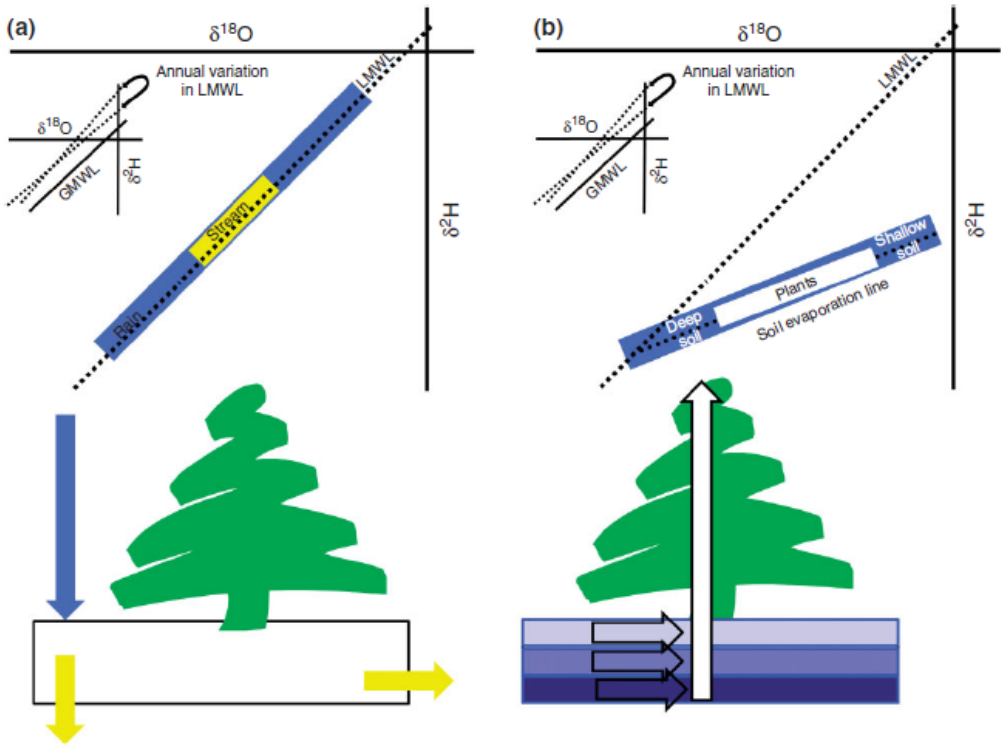


**Figure 2.1.** Separate water pools in a forested catchment according to the two water worlds hypothesis, with (a) showing mobile water that participates in flow generation, and (b) water used by vegetation demonstrating low mobility mixing (McDonnell, 2014).

As nitrate is a highly mobile anion, it is rapidly lost through the soil as leachate, which then enters the groundwater before discharging in to surface water (Pärn et al., 2012). The dominant source of nitrate to surface water in lowland catchments is through groundwater flow paths, rather than overland and channel flow (Wriedt and Rode, 2006; Lam et al., 2012; Pärn et al., 2012).

As groundwater can store large volumes and discharge at slow rates, historical inputs of nitrate may continue to discharge in to surface waters well after mitigation actions have been implemented to reduce nitrate leaching (Wriedt and Rode, 2006; Woodward, Stenger, and Bidwell, 2013).

Nitrate concentrations have been found to elevate at the start of the drainage season (May - July in New Zealand), when precipitation-induced runoff flow increases (Burkitt et al., 2017). Burkitt et al. (2017) noted that

nitrate concentrations in the Manawatu River began to decrease around October and stayed reduced over the following months.

Groundwater can attenuate nitrate through denitrification, mainly producing dintrogen gas (Woodward, Stenger, and Bidwell, 2013). In agricultural catchments, this has the potential to remove a proportion of leached nitrate before it flows in to surface water (Clague, Stenger, & Clough, 2015). Aquifers which have smaller water residence times can prove more clarity around nitrogen dynamics and delivery when monitored at high frequencies (Huebsch et al., 2015).

### *Storm Events*

Surface and subsurface flow paths are modified during storm events (Figure 2.2), which results in changes in hydrological connectivity and activation of additional source zones (Blaen et al., 2017). This enhanced connectivity, namely to riparian areas, delivers nitrogen to surface waters from areas not usually contributing nitrogen during base flow (Blaen et al., 2017).

Blaen et al. (2017) found that several select storm event hydroclimatic conditions (including antecedent) could predict the variability of nutrient loads to streams. Such dynamic nitrogen flux models can often be limited by a lack of detailed catchment information, such as biogeochemical, hydrological, physiographic and landuse data (Woodward, Stenger, and Bidwell, 2013).

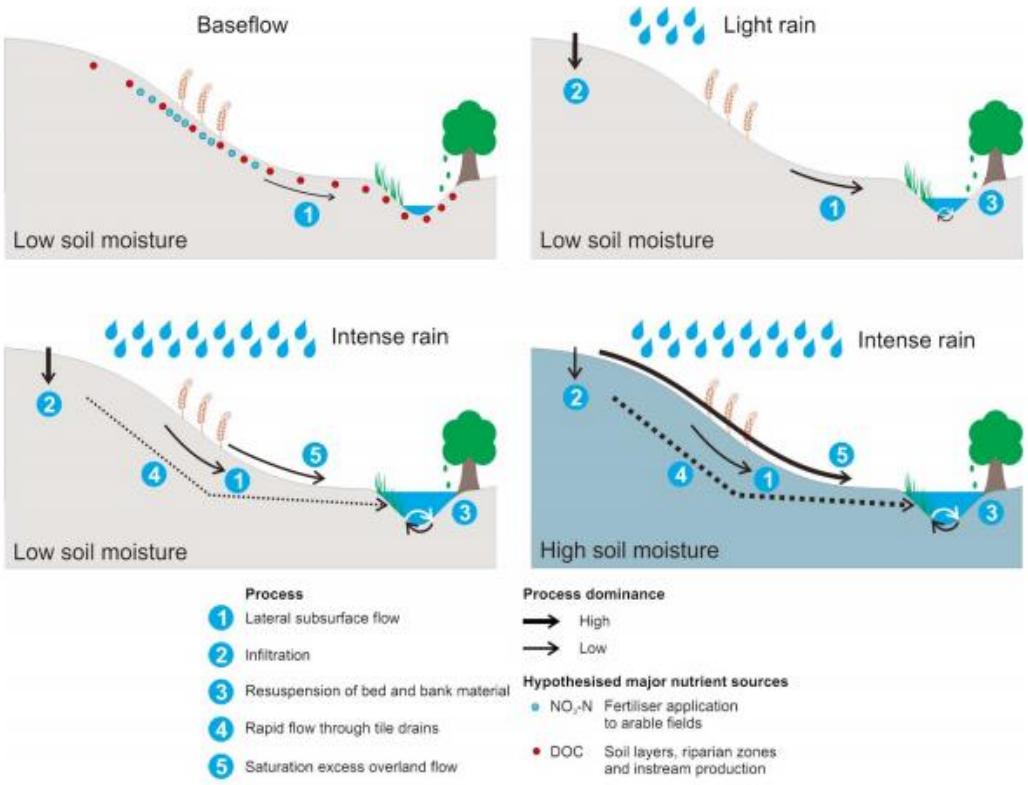


**Figure 2.2.** Conceptual model demonstrating hydrological and nutrient delivery responses to different catchment hydrological conditions (Blaen et al., 2017).

There are limited studies which assess how conditions before and during storm events affect nutrient loading and changes to source zones (Blaen et al., 2017).

Time series of stream discharge and physiochemical parameters can provide an integrated signal of catchment processes, and more likely to be available for modelling (Woodward, Stenger, and Bidwell, 2013). Physiochemical composition of stream water can reveal the changing proportions of overland flow and groundwater that are discharging in to surface water (Woodward, Stenger, and Bidwell, 2013).

***Hysteresis***

Nutrient sources and pathways in riverine catchments have been investigated through hysteretic behaviour between discharge and physiochemical parameters (Chen et al., 2012; Lloyd et al., 2016). Blaen et al. (2017) analysed nitrate and dissolved organic carbon using hysteresis

indices during storm events using normalised data for fair comparisons between events. They observed dynamic initiation of different source zones of dissolved organic carbon and nitrate that varied between events.

## 2.2 Stable Isotopes

Isotopes are variants of elements in that they have a different number of neutrons and consequently different masses. Isotopes that are non-radioactive, as they do not decay, are termed stable isotopes (Kendall and Caldwell, 1998).

Stable isotope composition (δ) is described in parts per thousands (per mil, or ‰) and is reported relative to an appropriate standard (Kendall and Caldwell, 1998). To calculate δ values is shown in Equation 1 below.

$$\delta(\text{in } ‰) = \left(\frac{R_x}{R_s} - 1\right) \times 1000 \quad (1)$$

Where *R* is the ratio of the isotope (heavy/light), and *x* and *s* denote sample and standard, respectively (Kendall and Caldwell, 1998).

The differing neutron number and thus masses between isotopes of an element give them slightly different properties, and for elements with low atomic numbers the mass difference is sufficient enough to cause fractionation during biogeochemical reactions or processes (Kendall and Caldwell, 1998). The mass difference has the potential to have a mass-dependent isotope fractionation effect; whereas neutron number difference can have a non-mass-dependent effect as it involves nuclear interaction (Kendall and Caldwell, 1998).

Isotopic fractionation (α):

$$\alpha = \frac{R_p}{R_r} \quad (2)$$

where $R_p$ and $R_r$ are the ratios of the isotope (heavy/light) for the product and the reactant, respectively.

Isotopic enrichment (ε):

$$\varepsilon_{p-r} = (\alpha - 1) \times 1000 \quad (3)$$

One of the two main isotopic fractionation mechanisms is kinetic processes. In kinetic isotope fractionation, reaction rates in forward and backward directions are not equal, and are dependent on mass ratios of the isotopes and their associated energies (Kendall and Caldwell, 1998). Isotope reactions may become unidirectional if products and reactants are no longer in contact. The reaction rates and pathways, as well as the bond energies involved in the reaction, will determine the extent of kinetic fractionation (Kendall and Caldwell, 1998).

The other main mechanism, isotope exchange reactions, can be placed under kinetic processes where equilibrium is possible, i.e. in a well-mixed closed system. In these equilibrium conditions, the heavier isotopes will tend to accumulate in the compound that has the higher oxidation state, and preferentially in the denser material or phase e.g. ratio of heavy to light isotopes is higher for a liquid than a gas (Kendall and Caldwell, 1998).
Heavier isotopes give molecules higher dissociation energy and therefore are more stable as their chemical bonds require more energy to break, so the effect is more evident the lower the temperature (Kendall and Caldwell, 1998).

Nitrogen has two stable isotopes: the more abundant and lighter $^{14}N$ isotope, and the less common heavier $^{15}N$ isotope. Isotopic composition can vary greatly due to nitrogen's wide-ranging oxidation states (-3 to +5) (Kendall, 1998).

Stable isotopes have become a useful tool for differentiating nitrogen sources and inferring nitrogen cycling in a range of environments (Cohen et al., 2012).

## 2.3 Dual Isotope Nitrate ($\delta^{15}N\text{-}NO_3^-$ and $\delta^{18}O\text{-}NO_3^-$)

Dual stable isotopes of nitrate ($\delta^{15}N\text{-}NO_3^-$ and $\delta^{18}O\text{-}NO_3^-$) are used as a prefatory indication of potential sources of the nitrate in various environments (Kendall, 1998; Zhang et al., 2018).

### 2.3.1 Nitrate Source Discrimination

While $\delta^{15}N\text{-}NO_3^-$ assists in discriminating the source of nitrate, (whether it is from atmospheric deposition, fertiliser, soil processes, animal excreta or sewage), there can be overlap of sources, and therefore critical to combine other indicators to better identify nitrate sources (Kendall, 1998). The addition of $\delta^{18}O\text{-}NO_3^-$ can support further discrimination between sources with similar $\delta^{15}N\text{-}NO_3^-$ values (Zhang et al., 2018).

#### *Signatures of Sources*

A wide range of δ15N values have been identified in a variety of sources (Figure 2.3). Values of $\delta^{15}N\text{-}NO_3^-$ are lower in chemical fertiliser (0‰ to 3‰) and precipitation (-10‰to 8‰), while higher in sewage and manure (7‰ to 20‰, or potentially higher) (Zhang et al., 2018).

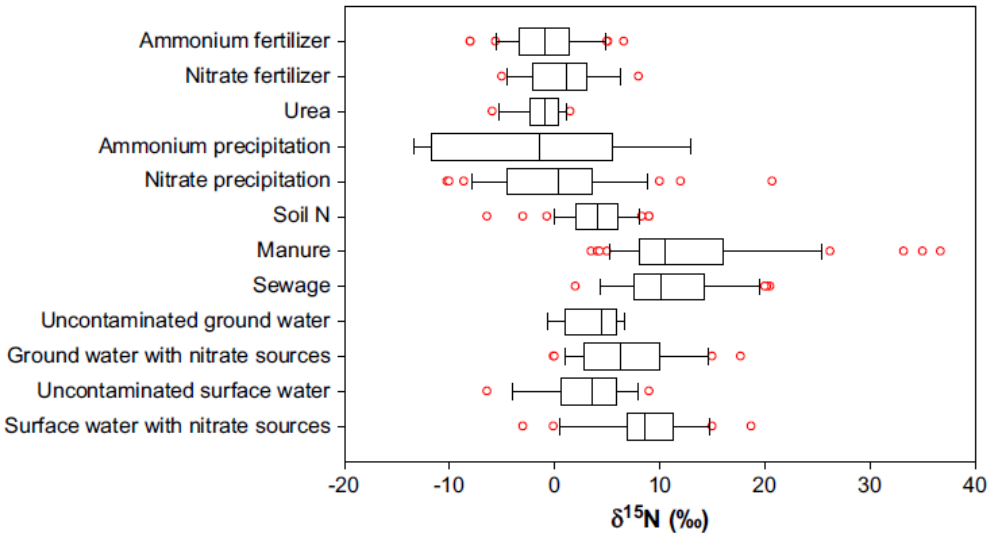


**Figure 2.3.** Range of $\delta^{15}N$ values for different nitrogen sources (Xue et al., 2009).

### *Soil*

In soil, nitrogen cycling is largely driven by biological processes, such as nitrification, denitrification and assimilation, and often result in increases and decreases of $\delta^{15}N$ in the residual and product, respectively (Kendall, 1998). Pasture soils have leachate with $\delta^{15}N\text{-}NO_3^-$ values of +0.3‰ to +6.6‰ (Wells et al., 2016).

### *Fertiliser*

Ammonium and synthetic fertiliser are derived from atmospheric N, and therefore have similar $\delta^{15}N$ values to that of precipitation (Townsend et al., 2007). The value of $\delta^{18}O\text{-}NO_3^-$ of these sources can help differentiate between the two, with $\delta^{18}O$ being high in precipitation (~+20‰ and +70‰) and lower in synthetic nitrate fertiliser (+22‰ ± 3‰) (Zhang et al., 2018). This is also contrasted to soil derived nitrate, with $\delta^{18}O\text{-}NO_3^-$ usually ranging between +0.8‰ and +5.8‰ (Durka et al. 1994). For sewage and manure, typical values of $\delta^{18}O\text{-}NO_3^-$ are less than +15‰ (Kendall, 1998). In New Zealand, $\delta^{18}O\text{-}NO_3^-$ values from atmospheric $^{18}O$ are not as high, as atmospheric N deposition and industrial inputs are minimal (Stevenson et al. 2010).

Residual effects of previous applications of fertiliser have been identified in subsequent years, as $\delta^{15}N$ remains higher in the drainage waters than that of non-fertilised pastures (Kellman, 2005). It is therefore important to take in to account previous landuse activities when interpreting sources through $\delta^{15}N$ values.

### *Animal Excreta*

The nitrogen in bovine urine is primarily in the form of urea (Selbie et al., 2015). Once in contact with the pasture soil, urea is transformed to ammonium which results in an equilibrium shift to increase ammonia (Sherlock and Goh, 1984).

Bovine urine alters isotope values over time due to the extent of denitrification (Rayner et al., 2019). Plant cover in pastures also alters isotopic values, but the effect is greatest when there is no introduction of urine (Rayner et al., 2019).

### *Factors affecting $\delta^{18}O$*

In relation to VSMOW, atmospheric $\delta^{18}O\text{-}O_2$ is consistently +23.5‰ (Kroopnick and Craig, 1972), but can be altered in the soil environment, resulting in soil $\delta^{18}O\text{-}O_2$ becoming higher due to respiration or lower with increasing depth where diffusion is dominant (lighter $^{16}O$ isotopes diffuse faster) (Spoelstra et al., 2007). Consequently, soil $\delta^{18}O\text{-}O_2$ will depend on factors that affect the respiration rate and diffusion through the soil profile, such as the temperature, moisture and structure of the soil, and the microbial community present (Spoelstra et al., 2007). Synthetic nitrate has heavier $\delta^{18}O\text{-}NO_3^-$ values, as the nitrification steps to produce it differ, resulting in only atmospheric oxygen being incorporated (Veale et al., 2019).

Rayner et al. (2019) found that the $\delta^{18}O\text{-}NO_3^-$ values in the leachate of a pastoral system did not vary temporally, or by the different plant treatments, but became higher as the rate of bovine urine application increased.

While types of sources of nitrate have characteristic isotopic compositions, some of which have been well documented, many factors can cause temporal and spatial variations to these values. These include atmospheric and climatic conditions, anthropogenic inputs, emissions, and the geology and topography of the area (Zhang et al., 2018).

### 2.3.2 Indicators of Nitrogen Transformations

Dual isotopes of nitrate ($\delta^{15}N\text{-}NO_3^-$ and $\delta^{18}O\text{-}NO_3^-$) have also been utilised for inferring nitrogen transformations, such as relative contributions through assimilatory and dissimilatory pathways, and their temporal variability (Cohen et al., 2012).

In the Taihu Lake area in China, Chen et al. (2012) found the dominant sources of nitrate vary among seasons, but sewage and manure were primary sources in both winter and summer, and $\delta^{18}O\text{-}NO_3^-$ values indicate microbial nitrification is also likely a contributor of nitrate all year. Precipitation was found to only be a significant source of nitrate in summer, and soil organic nitrogen contributed to nitrate only during winter in the study area with a lower anthropogenic influence.

Denitrification can produce seasonal variation in fractionation in response to changing discharge and temperature, with nitrogen removal being reduced at higher discharges, whereas during higher discharge and load conditions fractionation increases overall (Ruehl et al., 2007; Chen et al.,2012).

Greater variation in isotopic values can occur both seasonally but also along the longitudinal profile of a river, dependent on changes in source, internal cycling, landscape and management (Cohen et al., 2012). If fractionation processes occur between the source and the point of monitoring, this can have a confounding effect on interpretation of the source (Zhang et al., 2018). Drainage water can have $\delta^{15}N\text{-}NO_3^-$ values higher than the source $\delta^{15}N$ if fractionation processes occur along the flow path (Kellman, 2005).

In oxidised groundwater, the isotopic composition should be the same as that of the source, if no other nitrogen transformations have occurred (Kendall, 1998). If the same source of groundwater then enters a reduced state, denitrification can occur and this fractionation process results in the enrichment of both $^{15}N$ and $^{18}O$ (typically observed as a slope of 2:1) (Clague, Stenger, & Clough, 2015).

If mixing occurs between two nitrate pools this can mask an individual pool's isotopic signal, predominantly by atmospheric nitrate which can conceal fractionation in surface water, especially that of microbial processes (Wells et al., 2016). Isotopically distinct nitrate pools passing through agricultural soils have been found to have more normalised $\delta^{15}N\text{-}NO_3^-$ and $\delta^{18}O\text{-}NO_3^-$ values (-10‰ to +10‰) (Granger et al., 2008). Low nitrate availability will limit isotope fractionation, but is unlikely in areas that are well mixed (Cohen et al., 2012).

### *Denitrification*

An essential part of identifying nitrate contamination through isotopic tracing is being able to identify denitrification and the magnitude of its effects on the source's isotopic composition (Clague, Stenger, & Clough, 2015; Veale et al., 2019). Quantifying denitrification in surface waters through nitrate isotopes has been limited due to a lack of full comprehension of the mechanisms involved (Wells et al., 2019).

Earlier studies on denitrification have assumed it is occurring if in a reduced environment with decreasing nitrate concentrations, but a decrease in nitrate in groundwater could also occur to dilution with water that has lower nitrate concentrations. Determining denitrification based on the end product ($N_2$) is complicated as and requires further analysis to discriminate the excess $N_2$ from denitrification from $N_2$ originally in the groundwater from the atmosphere, as well as assuming the groundwater recharge temperature. In contrast, dual nitrate isotope composition combined with nitrate concentrations can indicate denitrification activity (Groffman et al., 2006).

Clague, Stenger, and Clough (2015), sampled shallow groundwater in an agricultural catchment in New Zealand for dual nitrate isotopes to assess where and to what degree denitrification was occurring. The rates of denitrification varied among the sites sampled, and one site also experienced seasonal fluctuations (Gley soil site where water level can near the surface). Groundwater that was sufficiently oxidised, displayed highly variable isotopic compositions, which suggested more than one source of nitrate. The combination of multiple sources, reduced groundwater with very low nitrate, and limited quantification of groundwater flow paths, constrained interpretation of denitrification in this catchment (Clague, Stenger, & Clough, 2015).

Veale et al. (2019) analysed a dataset of nitrate isotopes of groundwater in California (1200 dual-isotope results) to determine the effectiveness of using nitrate–oxygen isotope ratios for source determination. Comparison of the data to the idealised nitrification model (where nitrate consists of one oxygen atom from the atmosphere and two oxygen atoms from ambient water) had just under 80% of $\delta^{18}O\text{-}NO_3^-$ samples fall within one standard deviation of the predicted value, while 19% had substantially higher values. These higher values suggest other mechanisms such as extensive denitrification, source mixing or a preserved synthetic nitrate signature. In their analysis, Veale et al. (2019) suggested the higher $\delta^{18}O\text{-}NO_3^-$ values were distorted by different forms of N-fertiliser inputs, mixing of sources, and post-deposition nitrogen transformation in the soil, or an additive combination of mechanisms. They concluded $\delta^{18}O\text{-}NO_3^-$ values that were higher than predicted needed further investigation of oxygen isotope-fractionation processes to explain, but that coupled with related parameters such as landuse of denitrification, $\delta^{18}O\text{-}NO_3^-$ values could improve the assessment of nitrogen cycling and origin. Denitrification in riparian areas can have high fractionation, comparable to that of groundwater (Sebilo et al., 2003).

### *Nitrification*

The process of nitrification can also affect the $\delta^{15}N\text{-}NO_3^-$ to $\delta^{18}O\text{-}NO_3^-$ relationship as nitrate is synthesised from different sources of nitrogen and oxygen; the idealised oxygen contribution is one third from dissolved oxygen and two thirds from the ambient water (Spoelstra et al., 2007). Nitrification also has several reaction steps, and the degree of fractionation depends on the rate-limiting step; in agricultural systems where nitrogen is not limited, this can result in larger fractionation (Kendall, 1998).

Nitrification in soil by microorganisms gives $\delta^{15}N\text{-}NO_3^-$ values of in the range of -3‰ to +5‰, and $\delta^{18}O\text{-}NO_3^-$ values in the range of -5‰ to +5‰ (Zhang et al., 2018). Sebilo et al. (2006) found nitrification to produce $\delta^{18}O\text{-}NO_3^-$ values of -3‰.

When temperature, dissolved oxygen and pH are higher, such as during the day, nitrification tends to increase, whereas when these parameters are low, decoupling occurs (Cohen et al., 2012). Diel variation in primary production can give $\delta^{18}O$ values of -12‰ to -24‰ for nitrate, and between -4‰ and 0‰ for water; ammonium provides $\delta^{15}N$ for nitrification and results in a small degree of fractionation (Mayer et al., 2001).

### *Volatilisation*

Volatilisation is the removal of ammonia gas from the surface soil in to the atmosphere. This process involves multiple steps where fractionation can occur and thus can result in substantial enrichment in $\delta^{15}N$ values (Kendall, 1998).

### *Mineralisation*

Mineralisation is the process by which organic matter is converted to ammonium ($NH_4^+$) in the soil, with a normally low degree of fractionation of a few per mil from that of the soil organic nitrogen (Kendall, 1998).

### *Assimilation*

Assimilation is the uptake or incorporation of nitrogenous compounds in to organisms. Microorganisms in soils have been observed to produce soil nitrogen residuals of -1.6‰ to +1‰, while a much larger range of fractionation has been observed for assimilation in aquatic ecosystems (-27 to 0‰) (Kendall, 1998).

### *Fixation*

Atmospheric nitrogen ($N_2$) may be fixed by bacteria, such as cyanobacteria and those found on root nodules (e.g. legumes); this often results in organic products with values of $\delta^{15}N$ that are slightly less than 0‰ (-3 to +1‰), which is lower than other organic nitrogen producing-mechanisms and therefore considered indicative of fixation (Kendall, 1998).

### *Dual Nitrate Isotope Plots*

A useful tool for assessing nitrogen dynamics is the comparison of $\delta^{15}N$ and $\delta^{18}O$ in nitrate, specifically, indicating whether nitrogen removal has occurred due to denitrification or assimilation (as both have enrichment in the remaining nitrate pool) (Cohen et al., 2012).

If N removal is by assimilation, the regression slope will resemble a 1:1 relationship, that is, enrichment of $\delta^{15}N\text{-}NO_3^-$ will be approximately the same as $\delta^{18}O\text{-}NO_3^-$ (Granger et al., 2004). If N removal is by denitrification, the regression slope will resemble a 2:1 relationship, that is, enrichment of $\delta^{15}N\text{-}NO_3^-$ will be approximately twice that of $\delta^{18}O\text{-}NO_3^-$ (Lehmann et al., 2003). However, Granger et al. (2008) observed respiratory denitrifiers produce the 1:1 relationship in a laboratory study.

Groundwater studies have been more likely to show the 2:1 slope relationship between $\delta^{15}N\text{-}NO_3^-$ and $\delta^{18}O\text{-}NO_3^-$, but some studies have also seen this relationship in rivers (Ruehl et al., 2007; Chen et al., 2009)
Cohen et al. (2012) studied a spring-fed river that demonstrated variable isotopic composition, even with relatively consistent source water chemistry

and discharge. Both the diel and longitudinal profile sampling showed the 1:1 relationship, despite denitrification believed to be the dominant nitrogen-removing process.

### 2.3.3 Methodologies for Nitrate Isotope Analysis

Analytical techniques commonly used for the determination of nitrate and oxygen isotopic compositions are the denitrifier, ion exchange, and Cd-azide reduction methods (Zhang et al., 2018).

The ion exchange method for nitrate is broadly comprised by isolating nitrate before converting it, with many potential variations (Silva et al., 2000). The method developed by Silva et al. (2000) includes passing water samples through anion-exchange resin columns to purify and concentrate the nitrate. The concentrated nitrate is eluted with HCL and the resultant acidic eluant neutralised with $Ag_2O$. For $\delta^{15}N$ analysis, this eluant is then filtered to remove precipitate, and freeze-dried to produce solid $AgNO_3$, so it can be combusted to $N_2$ and allow for isotopic analysis (Silva et al., 2000). For proper $\delta^{18}O$ analysis, other anions that contain oxygen, as well as dissolved organic matter, must be removed from the neutralised eluant to avoid adsorption interference. Once filtered and freeze-dried, $AgNO_3$ is combusted with graphite to form $CO_2$, then subjected to cryogenic purification before isotopic analysis. Isotope ratio mass spectrometry (IRMS) is then used to determine the $^{15}N$ and $^{18}O$ values (Zhang et al., 2018).

The denitrifier method, developed by Sigman et al. (2001) and Caaciotti et al. (2002), is where nitrate is converted to nitrous oxide by denitrifying bacteria which cannot reduce the nitrous oxide. The extracted nitrous oxide is then analysed for the isotopic composition of both $^{15}N$ and $^{18}O$ (Zhang et al., 2018). This method requires less sample preparation, is applicable to samples with low nitrate concentrations, and can be processed with only a small amount of sample. Additionally, there is no interference as it is not affected by organic nitrogen and only nitrate is converted in the process.

Drawbacks of this method are that it cannot differentiate nitrate and nitrite (so requires it to be removed or corrected to avoid isotopic bias), $^{18}O$ analysis requires further correction (due to incomplete transformation in to nitrous oxide), and potential issues around bacteria cultivation (Zhang et al., 2018).

A newer method by McIlvin et al. (2005), the Cd-azide reduction method, reduces nitrate to nitrite through the addition of cadmium, then further reduction to produce nitrous oxide through the addition of azides. After further purification of nitrous oxide, it is analysed for $^{15}N$ and $^{18}O$ with IRMS. The Cd-azide reduction method's advantages include its ability to run easily prepared small sample volumes in automatic batches at reasonable costs and no interference from organics. Drawbacks include the use of toxic reagents and lack of discrimination between nitrite, which will require correction for final isotopic values (Zhang et al., 2018).

### 2.3.4 Progression as a Tracer

#### *Methodology*

The use of 15N as an indicator of nitrate sources has been used since the 1970s (Zhang et al., 2018). Nitrate source tracing methodology that has focused around isotope signatures has progressed through four general stages: inferring source from $\delta^{15}N\text{-}NO_3^-$ alone, from $\delta^{15}N\text{-}NO_3^-$ and $\delta^{18}O\text{-}NO_3^-$ combined, use of multiple isotopes or accompanied by other tracers, and use of mathematical models or similar for quantification (Zhang et al., 2018).

As nitrate isotope for source identification has progressed, there has been a move towards implementing more qualitative methodologies, rather than qualitative, and is focused mainly on source contribution ratios (Zhang et al., 2018).

Mass-balance models for mixing of nitrate sources is usually limited to three sources, but similar sources can be treated as one (Zhang et al., 2018). Other potential issues with these models are that they do not take in to account variation in source signature and fractionation processes along the flow path (Zhang et al., 2018).

The SIAR (Stable Isotope Analysis in R) package for R is a Bayesian mixing model for determining the proportional source contributions, and the probability for each potential contribution proportion (Zhang et al., 2018). This model has the advantage of being able to analyse contributions by greater than three sources and acknowledges isotopic fractionation. However, SIAR is still limited by source isotopic signature variation and can only provide contribution ranges rather than absolute values (Zhang et al., 2018).

The mass-conservation mixing model IsoSource is a linear multisource model that determines source contribution ratios using an iterative method, providing all possible source contribution ratios. However, it is not often used in surface water systems, despite having a simple user interface and no need for programming (Zhang et al., 2018).

***Pitfalls and room for improvement***

While the isotope compositions provided valuable information, they highlight the perils of inferring processes from natural isotope patterns. Tracing sources of nitrogen in the environment is made difficult by the potential for different fractionation mechanisms to occur multiple cycles of fractionation processes and to occur (Kendall, 1998).

The current extent of dual nitrate isotope studies of surface water is unevenly distributed (Zhang et al., 2018). While an increase in the number of these studies would allow for greater ease in nitrate source identification, a more diverse range of hydrological, geological and biochemical environments studied would allow for more accurate and more broadly applicable reference of source signals.

While vast improvements have been made to the overall synoptic approach of using nitrate isotopes to determine their source, further refining of the assumptions and techniques used is required. The main areas for further investigation include how source values are altered through denitrification and fractionation pathways (Veale et al., 2019).

An issue with current research is much of the analysis is qualitative, inferring fractionation processes on a broad level and not quantifying contributions of the processes themselves to the degree of fractionation (Zhang et al., 2018).

Findings in one area cannot be directly applied to another, as the fractionation processes observed are associated with that geological environment and hydrological conditions (Zhang et al., 2018).

## 2.4 Water Isotopes

The use of stable water isotopes is an effective means for deconvoluting flow paths of water and relative contributions in a catchment, especially during storm events where the rainfall isotopic values differ from the pre-event values (Genereux and Hooper, 1998).

Stewart et al. (2007) used $\delta^{18}O$ values in combination with other hydrochemical tracers to demonstrate that the Pukemanga Stream in New Zealand, had a discharge dominated by groundwater flows. Amesbury et al. (2015) observed water isotopic patterns that suggested their previously defined ombrotrophic peatland may be in fact receiving external hydrological inputs, likely overland flow or snowmelt.

### 2.4.1 Sources

Water isotopic ratios ($\delta^{2}H$ and $\delta^{18}O$) reflect the conditions associated with precipitation, such as temperature and humidity, which determine evaporation and condensation and thus the degree of fractionation (Amesbury et al., 2015).

New Zealand experiences high variability in $\delta^{2}H\text{-}H_2O$ and $\delta^{18}O\text{-}H_2O$ values in rainfall, which has been attributed to a compressed latitude and contrasting rainfall origins (subtropical from the north and sub-Antarctic from the south) that alter temperature and relative humidity (Baisden et al., 2016b). This high variability in New Zealand rainfall was well predicted through a model that included the regression of precipitation volumes, elevation and temperature, but still faced difficulties predicting individual events (Baisden et al., 2016b).

Soil water fractions have different isotopic values as a consequence of their different mobility's (Landon et al.,1999). This can have an effect on interpretation, depending on the fraction of water involved in the process of concern and the method used to collect the soil water. Wick samplers and suction lysimeters collect differing fractions of the mobile water, and tightly bound water has to be collected in the laboratory through extraction from the soil (McDonnell, 2014).

### 2.4.2 D-excess

Deuterium excess (*d*-excess) refines information on the origins of the precipitation air masses, and the conditions that have led to isotopic alterations during transit of the air masses to their precipitation endpoint (Bershaw, 2018). However, the interpretation of this second-order isotope parameter can be impeded as both changes can affect the values of *d*-excess indistinctively, especially if sources and conditions of vapour transport are long and complex.

## 2.5 Importance of Research

Identifying nitrate sources is the first step in trying to manage them. A better understanding of source signature variability and the effects of fractionation during different nitrogen transformations is necessary for accurate identification of nitrate sources in catchments, especially in New Zealand's complex environments (Xue et al. 2009).

Effectively managing nitrate losses from pastoral systems, while still maintaining sufficient production, is required to balance economic sustainability with minimised environmental impact. This requires managing nitrates at several different control points, which can only be achieved through knowledge of the dynamic processes and application.

# Chapter Three

# Methods

This chapter provides information on the sampling and data acquisition locations, sampling methodology, instrumentation, sample analysis and data analysis of the project data collection and supplementary information acquired. Firstly, location and environmental setting of the project sample sites are detailed and provide necessary context for future interpretations, as well as the Bay of Plenty monitoring sites in the catchment outlined. Field methodologies are described, including the collection, processing and storage of samples, coupled with instrumentation used in the field. This is followed by the sample analyses undertaken and the laboratory methodologies used. Finally, the processes and mechanisms for data analysis are described.

## 3.1 Monitoring Sites

The monitoring sites include sampling sites specific to this project, and monitoring sites belong to Bay of Plenty Regional Council, but whose data was utilised for this project.

### 3.1.1 Project Sample Sites

The majority of the samples are located at the bottom of the Okaro catchment, in close proximity to the wetland and inflow in to Lake Okaro (Figure 3.1). An array of sites were chosen to capture a wide range of hydrological and chemical conditions that occur in the catchment and that contribute to nitrogen dynamics. One site was chosen to undertake higher resolution temporal sampling, both during baseflow and during rain events.

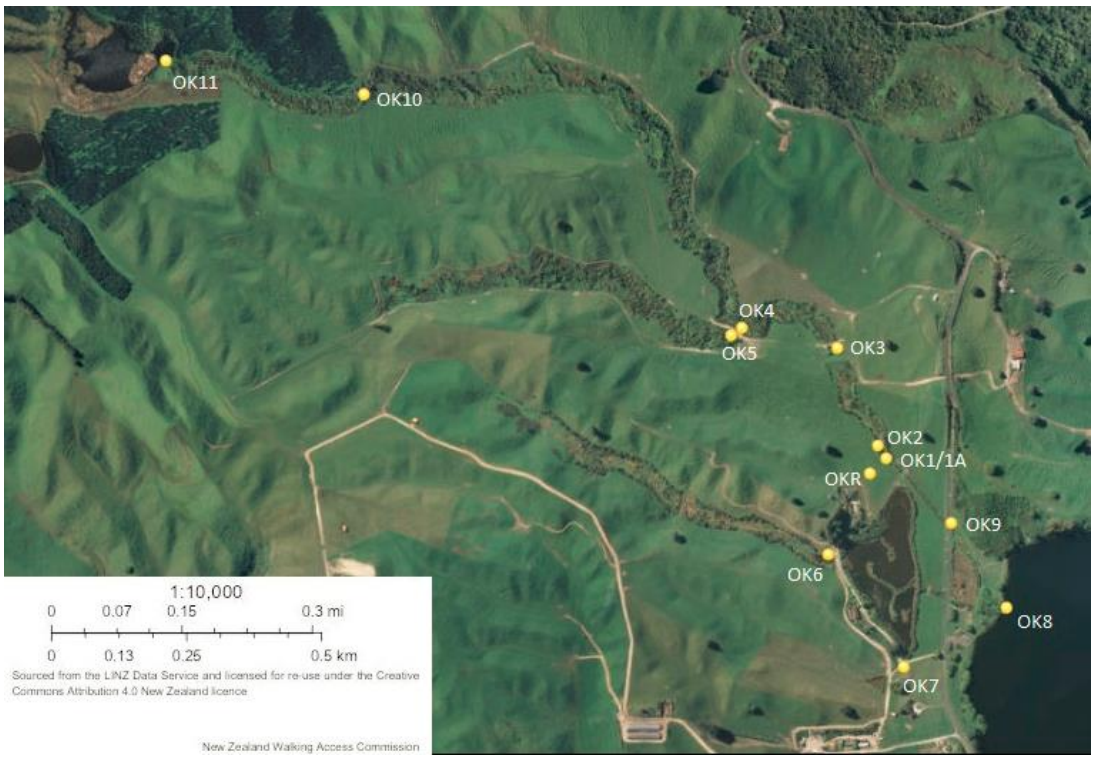


**Figure 3.1.** Overview of Okaro Catchment project sampling sites

The altered flow paths of the streams in and around the constructed wetland are shown in Figure 3.2.

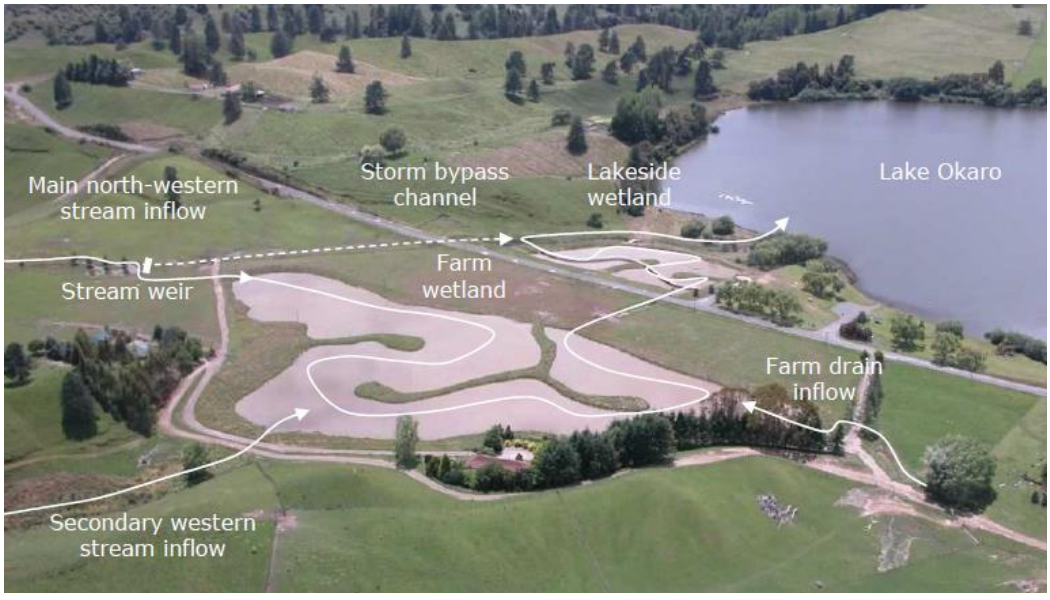


**Figure 3.2.** Wetland flow path overview, including stream inflows, bypass channel, wetland network, farm drain inflow and outflow. Photo taken after wetland construction, before wetland and riparian planting (Tanner et al., 2007).

### *OK1/1A*

The main sampling site is on the primary inflow stream, also known as the main north-western or north stream (Figure 3.3). It is at the inlet pipe to the diversion pipe which flows in to the main wetland. The wooden weir structure allowed for the autosampler and several instruments to be installed for rain event sampling and where there would be consistent flow in times of low flow for permanent structures. The site has a deep layer of fine sediment and there are submerged macrophytes.

**Figure 3.3.** Main sampling site (OK1) on the primary north-western stream in the Okaro catchment.

### *OK1P1 and OK1P2*

**Figure 3.4.** Piezometers P1 and P2 located at the OK1 site

The piezometers at OK1 are located on the stream margin, and access water in the hyporheic at different depths. Despite their close proximity (~30 cm), they drain soils with differing properties. During periods of high rainfall, the stream water level can get close to them (Figure A.17).

***OK3 and OK3P1***

The OK3 site is upstream of OK1 on the primary stream. It is just upstream of the detention bunds. The OK3 piezometer is relatively shallow on the stream margin. An empty pipe in the stream holds an additional sensor (Solinist) during storm events.

**Figure 3.5.** OK3 sample site on the primary stream.

***OK4***

The OK4 site is where the tributary is diverted through a culvert under the road, with approximately a metre drop, just before it flows in to the primary stream. There is a build up of sediment at this site.

**Figure 3.6.** OK4 site where tributary feeds in to primary stream.

***OK5***

OK5 is the sample site before the tributary flows through the culvert and then in to the primary stream. OK4 was used initially as during summer the trees are all in leaf and is difficult to access. The site is heavily shaded, especially in summer, and there is a vast amount of detritus

**Figure 3.7.** OK5 site where tributary flows through culvert

***OK6***

**Figure 3.8.** OK6 site on the secondary stream before it enters the main wetland

OK6 is located at the bottom of the secondary stream where it enters the wetland. The gradient is fairly low and could be described as a transitional area between stream and wetland.

***OK7***

**Figure 3.9.** OK7 in ephemeral drain. Red line indicates drain, with black dots indicating embankment. Sourced from LINZ Data Service.

OK7 is a grassed farm drain that is usually dry, or stagnant, but collects runoff during moderate rain. This ephemeral drain receives runoff from a lifestyle property, farm tracks and slopes around the dairy shed, which flows through a culvert in to the wetland.

***OK8***

**Figure 3.10.** OK8 site at the inlet of Lake Okaro

The OK8 site is where the original channel of the primary or ‘north’ stream entered Lake Okaro, now both streams enter the lake from this point. It receives water from the wetlands and bypass flow from the primary stream when activated.

***OK9***

**Figure 3.11.** OK9 site on bypass channel.

The OK9 site is on the bypass channel, the old channel of the primary stream before it was diverted in to the wetland. It is located just after downstream of the bridge before the wetland flows in to the channel. When there is no bypass flow the channel is a stagnant drain.

***OK10***

**Figure 3.12.** Upper site on the primary stream.

The OK10 site is further upstream on the primary stream, approximately 500 m downstream of the detention lake, with a mixture of sheep and beef and exotic forestry draining in to this section of stream. The stream is in a deeper channel and almost undetectable in dense long vegetation.

***OK11***

**Figure 3.13.** OK11 is at the access to the detention pond.

OK11 is by the access point to the detention pond. It is a large body of water with a variety of rushes and sedges. It was a crater pond that has been engineered on the outlet to reduce sediment loads and restrict high flows.

***OKR***

A rainfall collector was stationed near OK1 in a fenced area to collect rainwater over the study period. During storm events, a separate collector was placed in the adjacent paddock where there was less interference from nearby trees and shrubbery.

### 3.1.2 BOPRC Sites

***Telemetry Data***

*Okaro Wetland (Outflow G)*

**Figure 3.14.** Wetland outlet telemetered stage level

The monitoring equipment at the wetland outlet (G) records stage height (m), which then is used to calculate a discharge ($m^3/s$) based off frequently updated flow curves. Recording frequency of 5 minutes.

*Okaro at Okaro Rd*

Land-based monitoring situated at the Waionehu Farm herd-home which measures rain depth (mm), soil temperature (°C) and soil moisture as a percentage of moisture in the top 250 mm of soil. Recordings are made every 15 minutes, with rain depth recording every tip or sum over an hour. The soil moisture is also used by farmers as part of best practise effluent irrigation practises, with a ‘traffic light’ indicator system.

*Lake Okaro Monitoring Buoy*

The lake monitoring buoy records a range of water quality and meteorological data every 15 minutes. Data utilised from this site are wind direction (degrees), air temperature (°C), and barometric pressure (hPa).

### *Historical and Monitoring Data*

Monitoring data was downloaded from the Bay of Plenty Regional Council's Environmental Data Portal. The downloaded data is from the sites mentioned above. Historical data consisted of routine water quality sampling of the streams and lakes, as well as partial water quality and continuous flow data from the wetland implementation and assessment projects.

## 3.2 Sample Acquisition and Preparation for Analysis

### 3.2.1 Manual Sampling

#### *Collection*

The majority of samples were collected by drawing water directly in to a 60 mL syringe after it had been rinsed with sample water three times. Some sample sites, such as OK4, OK8 and OK9, required a sample to be first collected by a telescopic container, which was also rinsed three times with sample water. All samples were immediately processed on site, with the exception of the majority event samples, which were stored in secondary bulk bottles, and then either processed on site or stored on ice before processing in the laboratory.

#### *Rainwater*

**Figure 3.15.** Example of a rainfall collector

Rainwater collectors consist of a funnel and a collector bottle, which is housed inside an enclosed, weighted bucket. The funnel has mesh secured over the top to avoid larger material blocking the pipe. Bottles are filled with paraffin oil to a depth of at least 1 cm to inhibit evaporation. They are collected once a month but is dependent on rainfall amounts.

### 3.2.2 Autosampler

Storm event high-frequency sampling was undertaken using a Manning Model VST Sampler (Manning Environmental, Inc.), which is a portable vacuum pump autosampler that collects and stores up to 24 samples (Figure 3.16).

**Figure 3.16.** Manning VST autosampler unit (left) and sample bottles held in the suspension plate.

The Manning was used on the time interval setting, and programming depended on forecasts of rain intensities and duration. Two chamber fills were used for each sample collection, and these were deposited in to 1 L bottles, to ensure a sufficient volume of sample. These bottles sat in the bottom bottle case, which was filled with ice to help preserve the samples.

### 3.2.3 Sample Storage and Preparation

***Processing***

Samples for different analysis were processed as follows:

- Total Nitrogen –15 mL falcon tube, 14 mL unfiltered sample
- Dissolved Nitrogen –15 mL falcon tube, 14 mL filtered (0.45 µm) sample
- Water Isotopes – 15-30 mL tube, fill with no head space, filtered (0.45 µm) sample
- Nitrate Isotopes – 100 mL Stowers Astraline bottle, filtered (0.45 µm) sample

The filters used were either 0.45 µm Whatman glass microfibre filters, or disposable 0.45 µm Sartorius Minisart syringe filters.

#### *Rainwater*

Rainwater collector bottles were swapped out on site, sealed and labelled. To extract the rainwater sample, a tube was placed in the collector bottle, and then the bottle was gently squeezed to expel water. This was done initially to waste, to flush out any oil trapped in the tube, before filling a cleaned, dry beaker with sample. The sample was finally pipetted in to small glass vials (three duplicates), and intentionally overflowed to remove any oil that may be remaining.

#### *Preservation and Storage*

Nutrient samples were frozen as soon as possible, and stored in the freezer until they were analysed. Water isotope samples were stored in their original containers or subsampled in to 1.5 mL glass vials, which were stored in a fridge until analysis. Nitrate isotope samples were preserved with 1 mL sulfanilic acid and stored at room temperature.

## 3.3 Field Measurements

### 3.3.1 Discrete Measurements

Handheld meters were used for taking discrete physiochemical measurements, the units used were the YSI ProSolo, YSI Pro2030 and YSI 650MDS. Parameters measured differed between the units used, and were availability dependent. The majority of spatial measurements were taken using the YSI ProSolo. Parameters measured were dissolved oxygen, water temperature, specific conductivity, salinity, total dissolved solids, and pH when available.

### 3.3.2 High-frequency Measurements

#### *Handheld Meter*

The YSI 650MDS was set up to measure the February event at OK1, however due to an issue with the sampling settlings the memory became full after just under three hours of recording. Data was recorded at a frequency of one minute.

The YSI ProDSS was set up to measure the July event at OK1 (as well as September and December 2019), and recorded for 24 hours until the battery was empty. As it was a brand new instrument that was used for the first time in the field during this event, there had not been an opportunity to test prior to deployment. Data was recorded at a frequency of one minute.

### *Mayfly*

A Decagon CTD device connected to an EnviroDIY Mayfly Data Logger, powered by a solar panel (Figure 3.17), was deployed at OK1 for continuous measurement of measuring conductivity, temperature and depth. The 'Mayfly' was deployed 3 July 2019, the day prior to the July event peak.

**Figure 3.17.** Mayfly logger stored in orange case, inset showing CTD

Measurements are recorded on an SD card and the data is manually downloaded upon site visit, and cellular model for live monitoring is being trialled. Cleaning of the CTD is required on every site visit and a cleaning and downloading log is kept.

### *Solinist*

A Solinist level logger (LTC Levelogger Junior) was deployed at OK3 in the February 2019 and July 2019 events, and measured at frequencies of five and one minute intervals, respectively. The level logger measured water level, water temperature and conductivity. The Barologger (Gold) recorded barometric pressure at intervals of one minute during the July event.

***Trios NICO Optical Nitrate Analyser***


A TriOS NICO optical nitrate analyser was lent for high-resolution event monitoring of nitrate fluctuations. This UV photometer has four detection channels and was provided with a 50 mm path length setup. It measures nitrate and nitrate-N, absorbance and calculates a sensor quality index.

**Figure 3.18.** TriOS NICO optical nitrate analyser

## 3.4 Laboratory Analysis

### 3.4.1 Nitrate

Samples were analysed for Nitrate-N through Hills Laboratory (R J Hill Laboratories Limited) in Hamilton, using Ion Chromatography (APHA 4110 B (modified) 23rd ed. 2017). Results were reported in $g/m^3$, with a detection limit of 0.05 $g/m^3$.

Sample 41 (OK1A_NUT1D_040719_15) was noticed to have some particulate before submission, the laboratory were made aware and were requested to filter this sample before analysis, which was done using a 0.45 µm filter.

### 3.4.2 Isotopes

***Water Isotopes***

Samples were analysed for water isotopes ($\delta^{2}H$, $\delta^{18}O$) at the University of Waikato. The instrument used was the LGR Triple-Liquid Water Isotope Analyzer (T-LWIA), which provides isotope ratio measurements through high-resolution laser absorption spectroscopy.

Results are reported with respect to VSMOW, in units of per mil (‰). Measurements were normalised to internal and working LGR standards, which had been calibrated to values measured by the National Isotope Centre (GNS Science).

***Nitrate Isotopes***

Samples were analysed for dual nitrate ($\delta^{15}N$, $\delta^{18}O$) isotopes at the National Isotope Centre (GNS Science). The method employed has been modified from McIlvin and Altabet (2005), based off discussion with Mark Altabet.

The method involves converting nitrate to nitrous oxide through a series of steps of transformations and eliminations, and then being cryofocused through two traps before analysis. The nitrous oxide is then passed through a gas chromatography column and into an Isoprime IRMS, where the isotopic values of $\delta^{15}N$ and $\delta^{18}O$ in the nitrate can be determined (J. Coopers, personal communications, 18 October 2019).

The analytical precision for $\delta^{15}N$ and for $\delta^{18}O$ measurements is 0.3 ‰, with the exception of the samples below 0.1 mg/L which may be lower (J. Coopers, personal communications, 18 October 2019).

Results for $\delta^{15}N$ are reported with respect to AIR, and $\delta^{18}O$ results with respect to VSMOW, with units of per mil (‰). Measurements ($\delta^{15}N$, $\delta^{18}O$) were normalised to an internal standard, $KNO_3$b (+10.7 ‰, +11.7 ‰), and

to two international standards, USGS 34 (-1.8 ‰, -27.9 ‰) and IAEA-$NO_3$ (+4.7‰, +25.6‰) (J. Coopers, personal communications, 18 October 2019).

## 3.5 Data Analysis

Data and graphical analyses were performed in Excel® 2010 (v.14.0.6117.5003), including the use of the Analysis Toolpak addin.

### 3.5.1 Barometric Compensation

The water level readings recorded for the February 2019 event were not accompanied by the barometric pressure logger, as such barometric compensation was undertaken manually. This was completed by the manufacturer's instructions, with the following steps:

1) Retrieval of barometric pressure recorded by the Lake Okaro buoy and conversion to metres
2) Remove normalisation to sea level of barometric measurement
3) Subtract barometric pressure residual from the measured water level to produce corrected water level value

### 3.5.2 Calculations and Transformations

***Nitrification Model***

To calculate the predicted value of $\delta^{18}O\text{-}NO_3^-$ from the idealised nitrification model, the following equation was used:

$$\delta^{18}O\text{-}NO_3^- = \tfrac{1}{3}\,\delta^{18}O\text{-}O_2 + \tfrac{2}{3}\,\delta^{18}O\text{-}H_2O \qquad (4)$$

Where atmospheric $\delta^{18}O\text{-}O_2$ is consistently +23.5‰ (Kroopnick and Craig, 1972).

### *Deuterium Excess*

The following equation Dansgaard (1964) was used to calculate deuterium excess:

$$\text{d-excess} = \delta^{2}H - (8 \times \delta^{18}O) \quad (5)$$

### *Specific Conductivity*

The Solinist conductivity readings were normalised (to 25°C) for specific conductivity, with the measured temperature. The following equation was used at the manufacturer's recommendation:

$$\text{Specific Conductivity} = \text{Conductivity} / (1 + 0.02(\text{temp(C)} - 25)) \quad (6)$$

# Chapter Four

# Results

This chapter presents data collected from the sampling of the Okaro catchment in two sections, one covering base flow conditions over multiple seasons, and the second covering storm events. The first provides an overview of the spatial and temporal variation in the Okaro catchment. This begins with outlining the range of environmental conditions (meteorological, hydrological and physiochemical) experienced within the catchment during the study period. Then all stable isotope results are displayed as an overview of captured ranges, and to identify general trends in this catchment. Secondly, data acquired from storm events are investigated in detail, including possible hysteresis, and different patterns between summer and winter events identified. This section is also supplemented by the integration or inter-comparison of isotopic tracers, and the accompanying hydrological and physiochemical data, in order to further discriminate between signals and mechanisms, and identify potential contributing factors to nitrate delivery.

## 4.1 Overall Spatial and Temporal Variation

Data collected in the Okaro catchment is presented in this section to provide an overview of spatial and temporal variability in nitrate and water isotopes and the general environment conditions of the period sampled. The temporal data includes data from high-frequency sampling of the main site, OK1, during storm events, around storm events, as well as baseline monitoring over summer, autumn and winter. Spatial data includes sample data from up to 13 sample sites; some sample sites have had repeat sampling undertaken, namely in proximity to storm events, whereas others have been undertaken to ascertain the degree of variation in different hydrological settings.

### 4.1.1 Hydrological and Physiochemical

The summary of catchment environmental conditions (Table 4.1) includes only December 2018 to November 2019 to represent an annual 12-month period, and not skew averages with an extra summer month. Monthly rainfall totals in December 2018 and December 2019 were very similar (180 mm and 176 mm, respectively), and both well above historic averages. All other data is extended, where available, to provide the ability to compare more broadly among seasons.

The rainfall during this study period (1188 mm) is lightly less than the 10 year preceding average (1280 mm $yr^{-1}$). However, monthly rainfall totals were well below monthly averages until July 2019, resulting in an unusually dry autumn and an unusually wet spring.

**Table 4.1.** Summary of environmental conditions in the Okaro catchment from December 2018 to November 2019 Ranges indicate minimum to maximum values over the period, with the mean in brackets.

| | | | |
|---|---|---|---|
| **Rainfall** | | **Soil** | |
| Total (mm) | 1188 | Moisture (%) | 13.3 - 42.5 (*24.5*) |
| Monthly (mm) | 22 - 184 (*97.3*) | Temperature (°C) | 5.2 - 24.7 (*14.6*) |
| Intensity (mm/hr) | 0 - 18.2 (*0.1*) | | |
| **Discharge** | | | |
| Wetland Outlet* ($m^3/s$) | 0.20 - 0.48 (*0.25*) | | |

* Data missing between April and July 2019

The continuation of dry weather from the end of summer in to autumn resulted in extended low soil moisture conditions, with soil water content being below the permanent wilting point until it consistently began increasing at the end of May 2019 in (Figure 4.1). For most of the year, soil moisture content was below historical averages, and did not reach field capacity during any stage of the period.

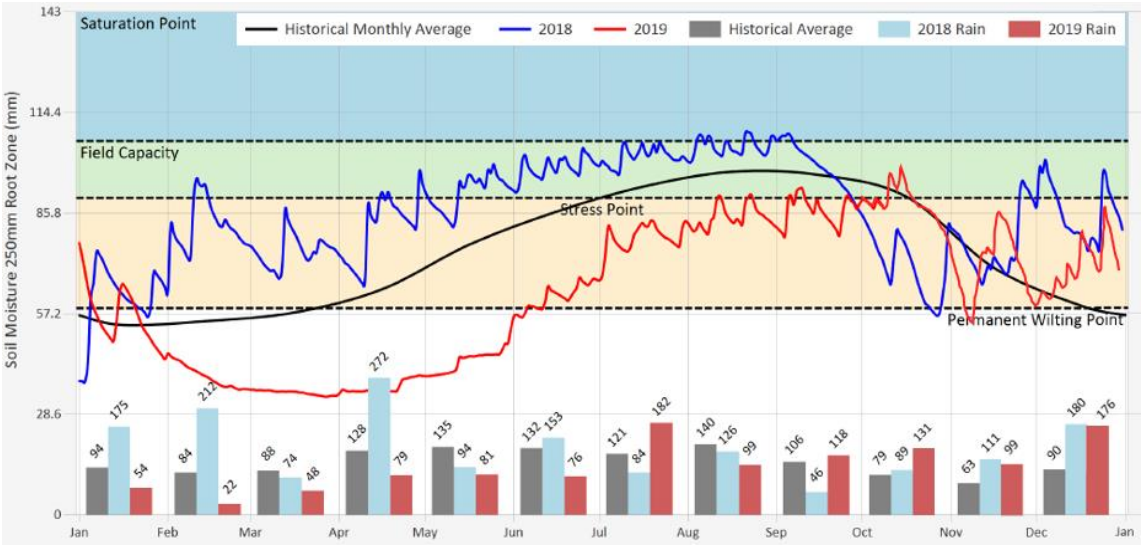


**Figure 4.1.** Graphical summary of 2018, 2019 and historical data for monthly rainfall amounts (mm) and soil moisture (mm) in the top 250 mm of soil (modified from Bay of Plenty Regional Council, 2020)

During this dry period there was limited response of soil moisture to rainfall (Figure 4.2). Higher intensity rainfall appears to have less of an effect on soil moisture compared to extended periods of lower rainfall intensities, and a similar outcome is seen at the wetland outflow, but to a lesser extent. Nitrate concentration appears to increase with soil moisture during autumn (Figure 4.2), with a stronger association in autumn and winter compared to summer, however nitrate samples for this season is limited.

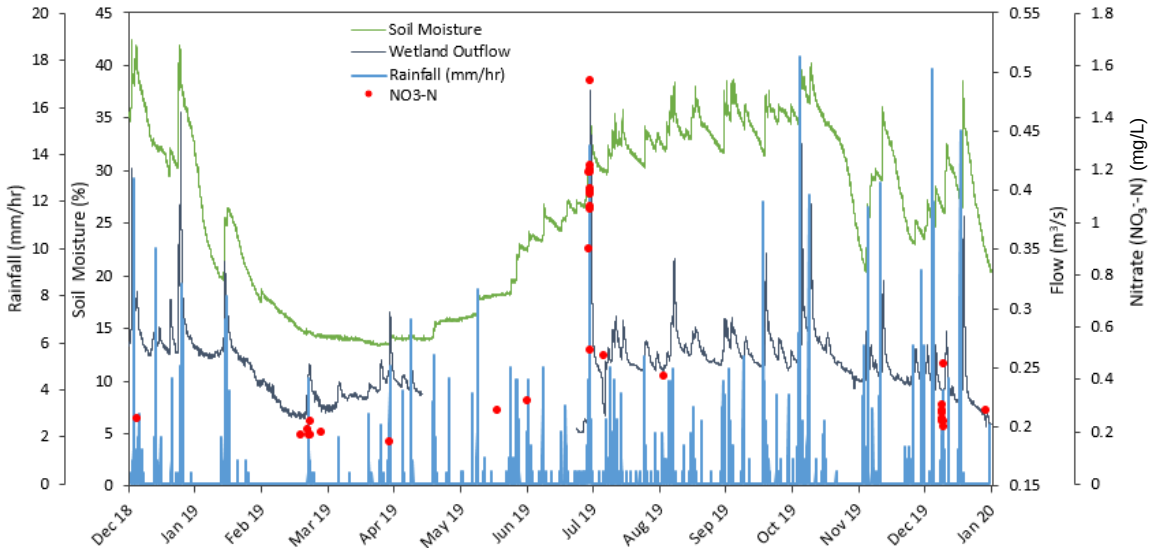


**Figure 4.2.** Time series of hydrological parameters and nitrate concentration in the Okaro catchment for the sampling period, December 2018 to the beginning of January 2020. Wetland outflow was unavailable in May and June 2019.

Changes to nitrate concentration during storm events were not solely affected by antecedent soil moisture, as the December 2019 summer event did not experience the same increase in nitrate as in the July 2019 winter event, despite similar soil moistures levels at the initiation of both events. The December 2019 summer event showed more of an increase in nitrate concentration through its duration but not to the same magnitude as the July winter event.

At the main site (OK1), the nitrate concentration during the whole period ranged from 0.16 to 1.54 mg/L, with an average of 0.74 mg/L. However, the inclusion of storm event high nitrate concentrations substantially increases the average at the main site (from 0.29 mg/L at baseflow) (Figure 4.3).

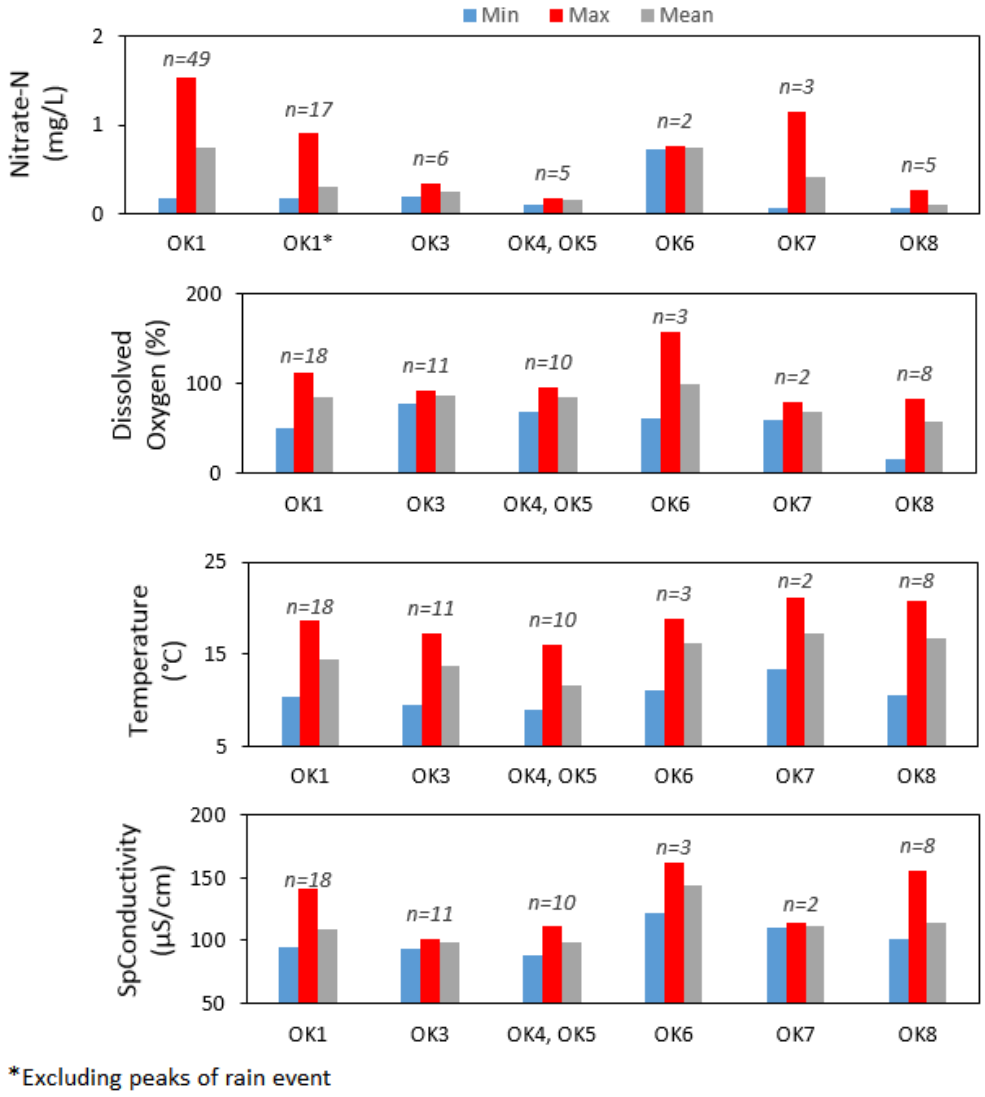


**Figure 4.3.** Physiochemical and nitrate summaries at several sampling sites in the Okaro catchment between December 2018 and December 2019.

The main site (OK1) had a similar average nitrate concentration, average dissolved oxygen content compared to the further upstream site OK3. The tributary on the main stream (OK4, OK5) had lower concentrations overall compared to the main trunk, which it would ultimately dilute upon mixing. OK4 and OK5 experiences the lowest temperatures, and higher conductivity than OK3. OK6 experiences a wide range of dissolved oxygen content, reaching over saturation, as well as the highest conductivity values.

The farm drain (OK7) had contrasting nitrate concentrations in summer and winter, with relatively warmer temperature and an ample amount of dissolved oxygen. The lake inlet (OK8) demonstrates a smaller degree of variation in nitrates, but substantial variation in dissolved oxygen. It also experiences the lowest dissolved oxygen measured, a higher conductivity and generally has a higher temperature. Other sites are excluded due to only one recorded measurement.

### 4.1.2 Dual Isotope Nitrate ($\delta^{15}N$ and $\delta^{18}O$)

Samples taken from the Okaro catchment between December 2018 and August 2019 had $\delta^{15}N\text{-}NO_3^-$ values ranging from +1.0 to +8.4 ‰, and $\delta^{18}O\text{-}NO_3^-$ values ranging from -1.4 to +6.4 ‰ (Figure 4.4) excluding an outlier with high error, which will be discussed in Section 5.3. The main site, OK1, represented by medium blue circles, has a $^{15}N$-enrichment relationship of essentially 2:1, with a reasonable fit ($R^2$=0.6021). The fit is stronger at $\delta^{15}N\text{-}NO_3^-$ values below approximately +5 ‰, after which there is more spread in the data. Sites OK4, OK5, OK6 and OK11 sit closer to the 1:1 line. The 1:1 and 2:1 slopes are based off relationships described in the literature, and are projected from a hypothetical ‘starting point’ fractionation of 0 ‰ $\delta^{15}N\text{-}NO_3^-$ and -2 ‰ $\delta^{18}O\text{-}NO_3^-$.

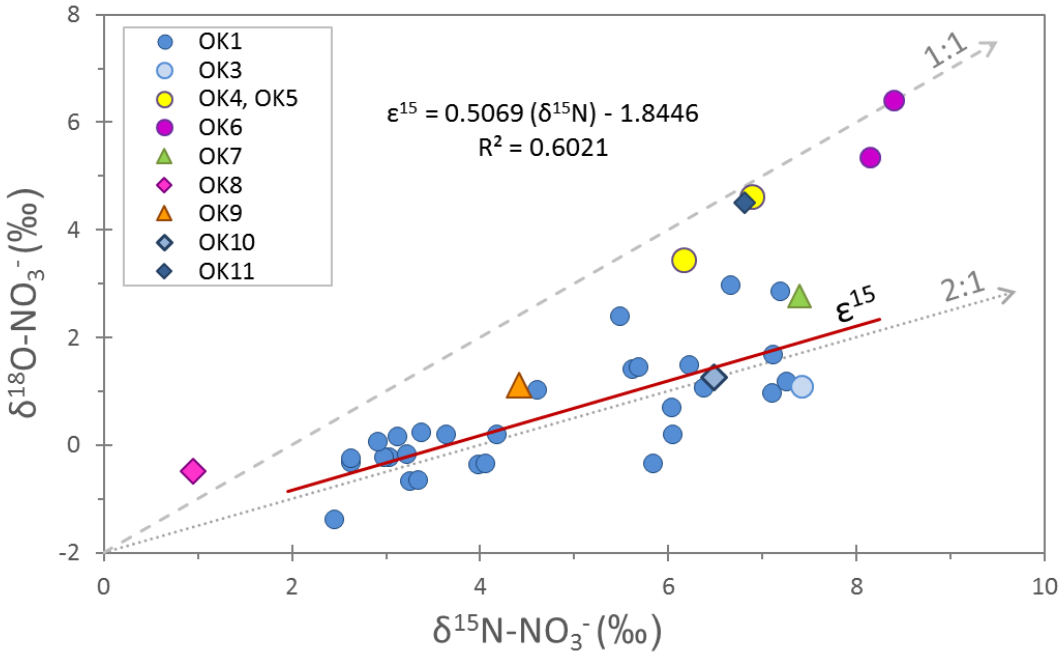


**Figure 4.4.** Dual nitrate isotope ($\delta^{15}N$ and $\delta^{18}O$) composition of a range of spatial samples in the Okaro catchment, taken between December 2018 and August 2019, and separated by site. The slopes are empirically-based indicators of the dominant nitrate behaviour in an environmental system and placed to show potential divergence from a hypothetical "starting point"; 2:1 (dotted) line suggesting denitrification, 1:1 (dashed) line suggesting assimilation or denitrification and mixing (DAM). $\varepsilon^{15}$ (red line) is the enrichment slope calculated for the OK1 site by linear regression.

All samples analysed for dual nitrate isotopes lie within the source indicator class parallelograms as defined by Baisden et al. (2016), based on research of agricultural areas in New Zealand (Figure 4.5). Samples within each indicator class lay in the approximate slope of their respective parallelograms.

The majority of samples lie in to the Soil N indicator class, with only July event samples and a lake inlet sample falling in the Ammonium Fertiliser/Urea/Urine indicator class (Figure 4.5). No samples taken over this period lie in the Nitrate Fertiliser or Effluent indicator classes, however two samples, both from OK6 (shown as purple circles in (Figure 4.4), are near the border of the Effluent indicator class.

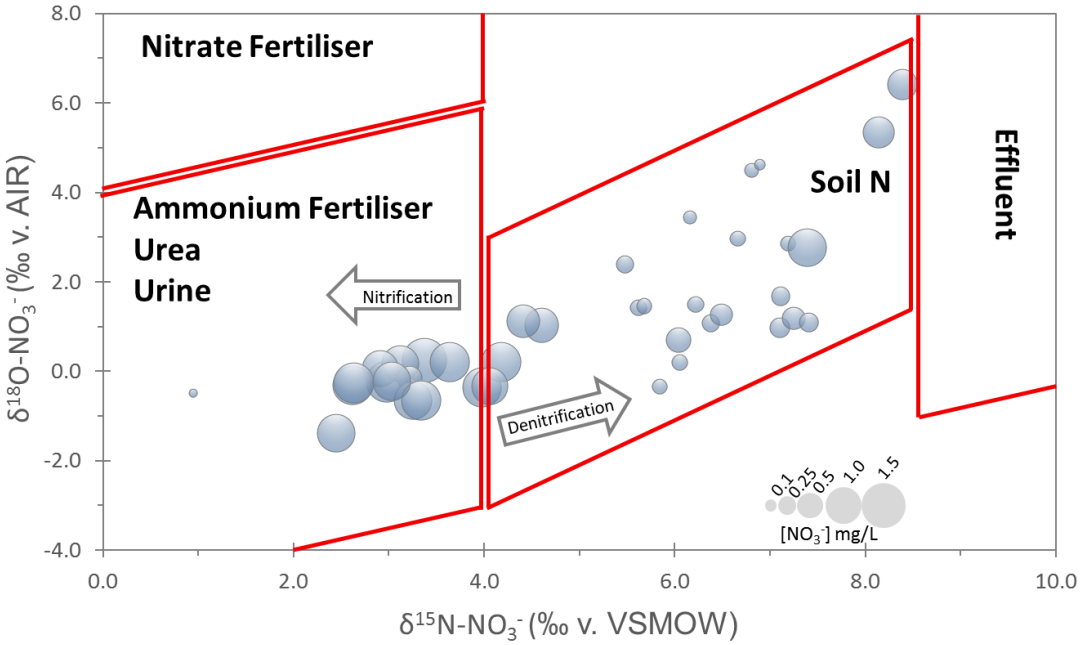


**Figure 4.5.** Dual nitrate isotope ($\delta^{15}N$ and $\delta^{18}O$) composition of a range of spatial samples in the Okaro catchment, taken between December 2018 and August 2019. Circle size denotes nitrate concentration (mg/L) per visual scale displayed. Red parallelograms represent typical values of $\delta^{15}N$ and $\delta^{18}O$ from different sources (indicator classes) based on studies by Baisden et al. (2016) of agricultural areas in New Zealand. Arrows convey theoretical fractionation directions of stated nitrogen process.

Samples with higher nitrate concentrations were predominantly in the Ammonium Fertiliser/Urea/Urine indicator class, or on the edges of the Soil N indicator class. The singular, higher-nitrate concentration sample in the Soil N indicator class is that of OK7, or the farm drain/run off sample (shown as a green triangle in Figure 4.4).

### 4.1.3 Water Isotopes ($\delta^2H$ and $\delta^{18}O$)

Samples taken from the Okaro catchment (including rainfall) between December 2018 and January 2020, sit above the Global Meteoric Water Line (GMWL) (Figure 4.6), with the exception of the February farm drain/runoff (OK7) samples, a summer lake inlet (OK8) sample, and a few of the recent December 2019 summer event stream samples from OK1.

Rainfall samples had $\delta^2H$-$H_2O$ values ranging from -4.8 to -67.9 ‰, and $\delta^{18}O$-$H_2O$ values ranging from -1.92 to -9.81 ‰, compared to the surface water samples, which lay in the approximate range of -32 ‰ to -45 ‰ $\delta^2H$-$H_2O$ and -5 ‰ to -8 ‰ $\delta^{18}O$-$H_2O$.

The July farm drain/runoff (OK7) samples sit amongst the other surface water samples, whereas the February farm drain/runoff (OK7) samples lie on the opposite side of the GMWL, and within the summer rainfall zone. Stream samples lay closer to the winter rainfall zone than the summer rainfall zone.

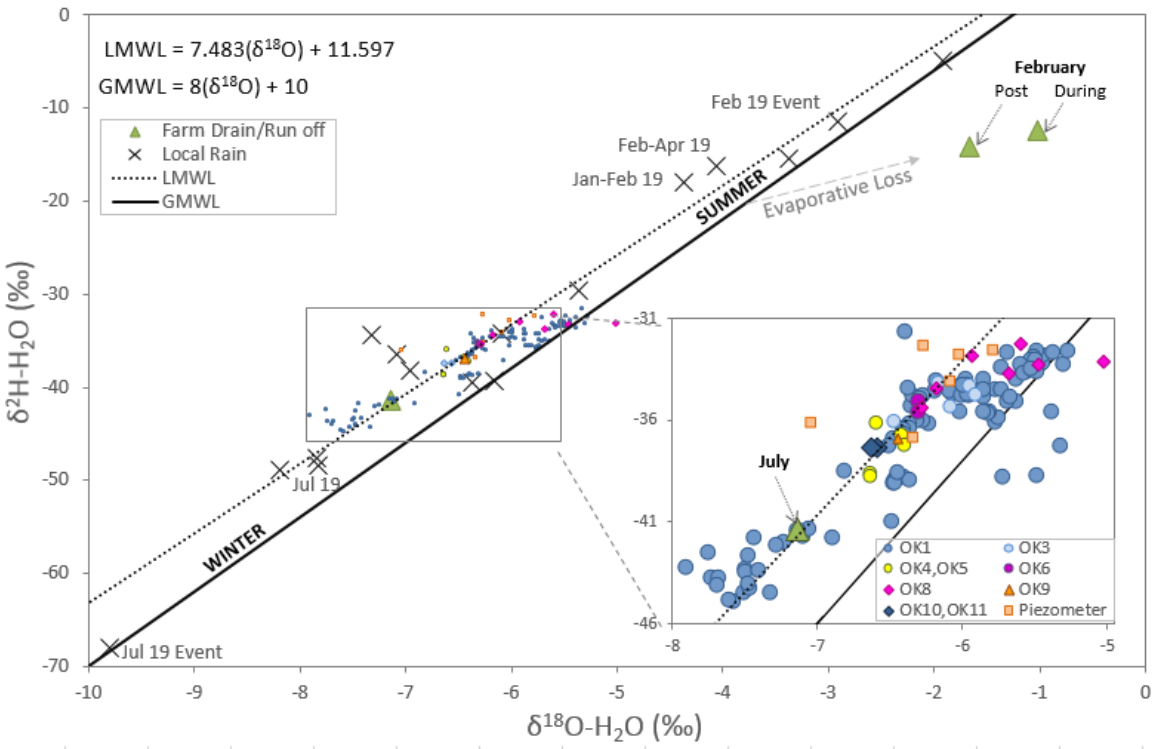


**Figure 4.6.** Dual water isotope ($\delta^2H$ and $\delta^{18}O$) composition of a range of spatial samples and collected rainfall in the Okaro catchment, taken between December 2018 and January 2020. The local meteoric water line (LMWL) is a linear fit of the rainfall samples collected over this time (represented by crosses), with only associated storm event rainfall labelled to avoid excess visual clutter. Runoff samples collected around storm events are labelled green triangles, with pre and post in reference to peak rainfall. Inset provided for enhanced visibility of sample value distributions.

The water isotopic signature ranges are mainly subdivided in to two sections, with most of the spatial samples located to the top of the graph (Figure 4.6, inset). The tributary of the main (northern) stream, represented by sites OK4 and OK5, has a consistently more negative δ values compared to that of OK3. Samples from the lake inlet (OK8), are overall less negative compared to other stream samples, and are closer in value to OKP1 samples.

Samples taken from the piezometers at OK1 were less negative than that of samples taken at OK3P1. Isotopic values of OK1 piezometers P1 and P2 samples were markedly different for $\delta^2H$ (-35.4 ‰ and -32.6 ‰, respectively), considering they were taken at the same time and they are in close proximity.

The deuterium excess (D-excess) of OK1 samples fluctuate, and appear to have a seasonal aspect to them, which is highlighted by the qualitative red dashed line (Figure 4.7). During winter the OK1 stream samples have a greater D-excess, with the lowest D-excess in summer, and stream D-excess values only reducing late spring.

During the summer event (February 2019), the D-excess of samples taken during the storm all had higher D-excess values than what was observed before and after the event, as portrayed by the black arrow (Figure 4.7). Most also had a D-excess greater than that of the rain collected during the event. Stream samples from a December 2019 event showed an overall decreasing D-excess, opposite to that of the collected rain.

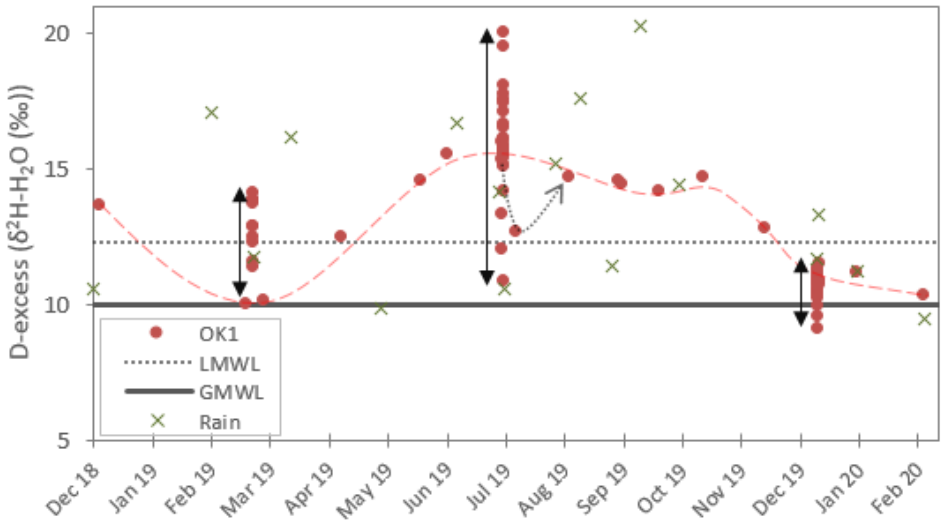


**Figure 4.7.** Time series of deuterium excess of samples taken at the main site (OK1) between December 2018 to February 2020, including both storm event and monitoring samples. The local meteoric water line (LMWL) is a linear fit of the rainfall samples collected (represented by crosses) over this time in the Okaro catchment. The red dashed line is a qualitative indication of OK1 monitoring sample D-excess pattern.

During the winter event (July 2019), the D-excess of samples taken during the storm had both higher and lower D-excess values than what was observed before the event. Approximately a week after the winter event the stream D-excess value was lower than before the storm, but approximately a month after the storm event the stream return to a more seasonally typical D-excess value, as demonstrated by the block dotted arrow. The rain D-excess for this event was lower than the stream seasonal values

Due to the lack of sufficient data for seasonal means to calculate D-excess anomaly, collected rainfall D-excess have also been included for general, non-robust qualitative analysis of D-excess anomaly.

### 4.1.4 Integration and Inter-comparison

The theoretical line represents the predicted or idealised nitrification model where one oxygen from the atmosphere and two from the ambient water make up the nitrate. Samples taken at OK1 are all below this line, and lie along the one negative standard deviation from the theoretical or predicted line (Figure 4.8), both above and below. These samples appear to follow general trend/slope of the theoretical line.

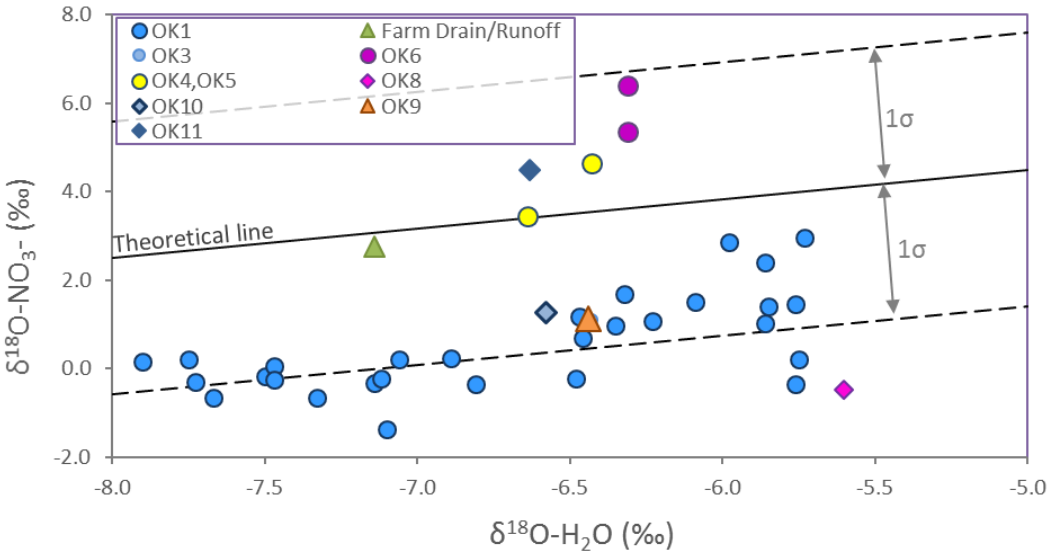


**Figure 4.8.** Comparison of $\delta^{18}O\text{-}NO_3^-$ and $\delta^{18}O\text{-}H_2O$ composition of a range of spatial samples in the Okaro catchment, taken between December 2018 and August 2019. The 'Theoretical line" (solid line) represents the idealised nitrification model (Equation 1), with the dashed lines being one positive or negative standard deviation from the predicted values.

Samples from sites OK4, OK5, OK6 and OK11 lie between the theoretical or predicted line, and one positive standard deviation from this line. No samples were above one positive standard deviation, but samples from OK6 (southern secondary stream) were the closest. The farm runoff/drain (OK7) sits sample is approximately on the theoretical line.

## 4.2 Storm Events

Storm events that occurred in February 2019 (summer event) and July 2019 (winter event) are covered in detail here. A summer event was captured in December 2019 as part of another study, and will not be covered in detail in this section.

### 4.2.1 Storm Characteristics

The winter event had both a significantly higher amount and intensity of rainfall compared to that of the summer event ( Table 4.2). Note that there was additional rainfall around the summer event but it was limited in volume and duration, and have been excluded from the totals considering is scattered nature.

**Table 4.2.** Comparison of meteorological and environmental conditions between the Summer (February 2019) and Winter (July 2019) storm events at Okaro. Ranges indicate minimum to maximum, with the mean in brackets; single values are totals.

| | Summer Event | Winter Event |
|---|---|---|
| Total Rainfall Amount (mm) | 5.7 | 89 |
| Rainfall Intensity (mm/hr) | 0 - 0.8 (*0.2*) | 0 - 12.5 (*2.5*) |
| Event Duration (hours) | 22 | 34 |
| Soil Moisture (%) | 14.5 - 14.8 (*14.7*) | 29.4 - 34.9 (*32.3*) |
| Relative Humidity (%) | 75.5 - 91.3 (*86.1*) | 83.3 - 92.1 (*89.4*) |
| Air Temperature (°C) | 16.8 - 19.9 (*18.1*) | 5.9 - 14.7 (*12.2*) |
| Wind Speed (m/s) | 0.5 - 4.9 (*2.6*) | 1.1 - 8 (*3.9*) |
| Predominant Wind Directions | N-NW | N-NW then S-SE |

Humidity for both events were on average quite similar, but the summer event reached a lower humidity. The air temperature for the summer event was relatively low for February. Both storm events had prolonged north-to-north westerly wind directions, but the winter event had a change to southerly to south-easterly winds after the initiation of the main part of the event.

Soil moisture during the summer event did not vary much (0.3%), and the winter event experienced a slight variation in comparison (approximately 5%). Soil moisture levels during the summer event were below the 'Permanent Wilting Point' (refer to Figure 4.1). During the winter event, soil moisture was in the 'irrigate with caution' band, and still considerably below the field capacity of 51%.

### 4.2.2 Storm Event Integration and Inter-comparison

***Summer Event***

There was some initial rainfall before monitoring could begin, which saw the main increase in soil moisture occur (Figure 4.9). As main event rainfall begins, there is a drop in $\delta^{18}O\text{-}H_2O$, and conductivity begins to rise (Point A). The greatest rainfall intensity causes another drop in $\delta^{18}O\text{-}H_2O$, followed by an increase in $\delta^{2}H\text{-}H_2O$, an increase in nitrate isotope values, and a decrease in nitrate (Point B). There is another increase in $\delta^{2}H\text{-}H_2O$ after a preceding decrease, which occurs at highest measured nitrate result, but not coupled with any physiochemical or hydrological changes (Point C). At the start of the spike in depth, salinity decreases and there is another increase in $\delta^{2}H\text{-}H_2O$ after preceding decrease (Point D). At peak stream depth there is a dip in conductivity (Point E). As stream depth stabilises, the conductivity starts to decrease (Point F).

***Winter Event***

Rain occurred before the monitoring could begin but captured the very beginning of the main part of the event. As a period of heavy rain begins, the soil moisture jumps up (Figure 4.10), the conductivity starts to drops, and the pH and dissolved oxygen (%) increase (Point A). An increase in depth but no increase in soil moisture occurs, sensor interference indicates spike in turbidity (Point B). Nitrate concentrations increase and all isotopic values begin to decrease. The pH and dissolved oxygen (%) hit their event peak and begin to fall, as does salinity.

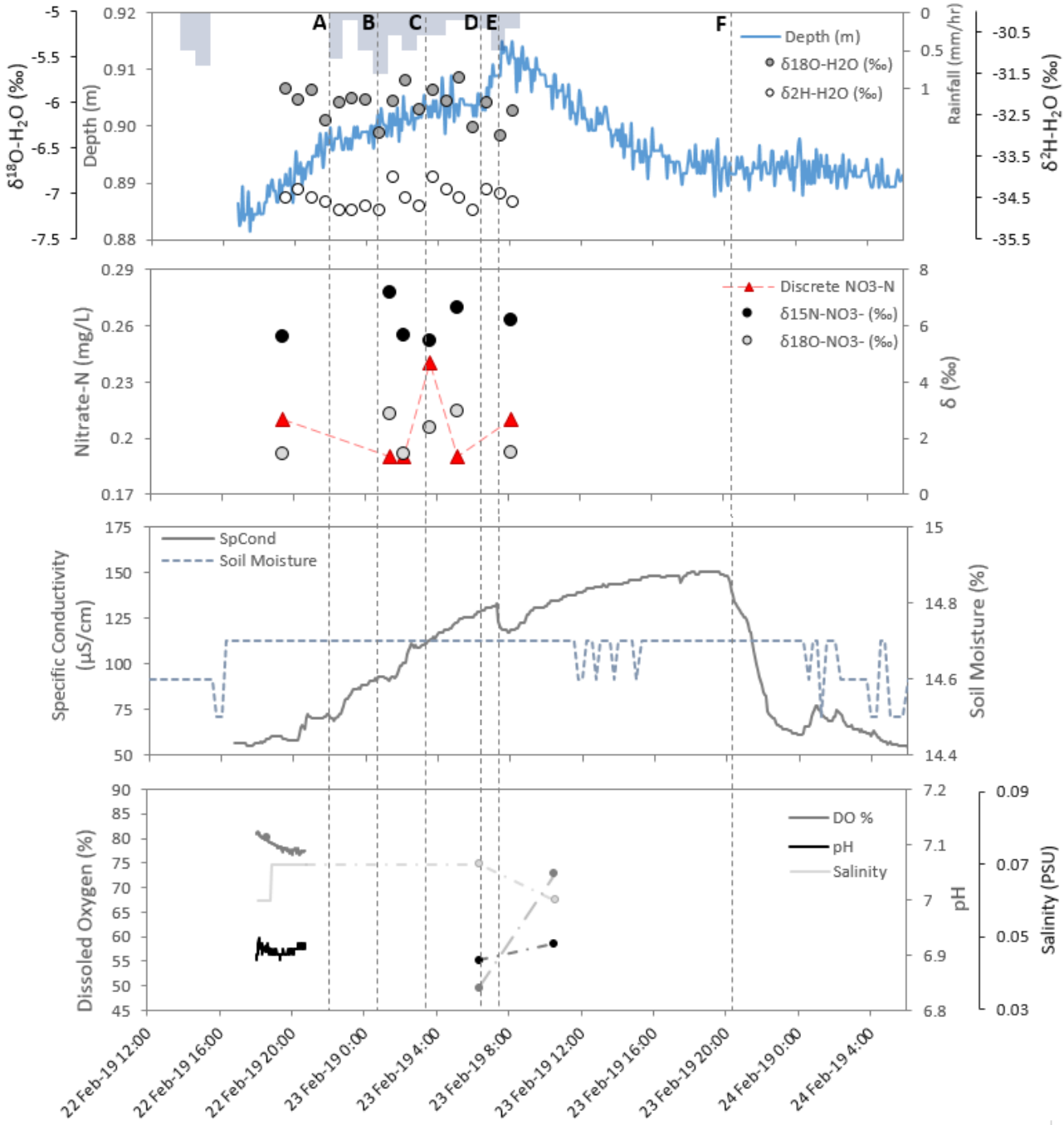


**Figure 4.9.** Time series of the isotopic, hydrological and physiochemical data at OK1 around a summer event (February 2019). Vertical dashed lines are labelled with letters to compare time points of particular interest.

During the highest intensity rainfall there is a peak in nitrate concentrations (Point C). As the depth begins to decrease there is a dip in nitrate concentration before slowly increasing (Point D). There is another smaller amount of rain that falls, and the soil moisture is more responsive to rainfall (Point E). This rain also corresponds to a slight dip in nitrate concentration before general lowering trend in concentration for discrete samples, and similarly a drop in $\delta^{15}N\text{-}NO_3^-$, $\delta^{18}O\text{-}NO_3^-$ and $\delta^{18}O\text{-}H_2O$ before an overall increase in values. Most parameters then move towards stabilising.

Conductivity responded differently to the two events. In the summer event, conductivity began to increase with rain, and continued to increase after the rainfall had ceased, and then decreased once the water depth had stabilised (point F). During the winter event, conductivity remained consistent until the rainfall began to intensify, then a decrease was observed until the rain intensity decreased, at which point the conductivity started to increase to pre-event values and did not continue to rise.

A similar opposing trend was seen in salinity but there is limited data for the summer event. Despite the limited data for the summer event for physiochemical parameters, it can be observed that in the summer event, the DO dropped to much lower saturation levels than what occurred in the well monitoring winter event.

In the summer event, the changes in $\delta^{15}N\text{-}NO_3^-$ and $\delta^{18}O\text{-}NO_3^-$ were more mostly paired responses, whereas in the winter event there was a lag or differing responses.

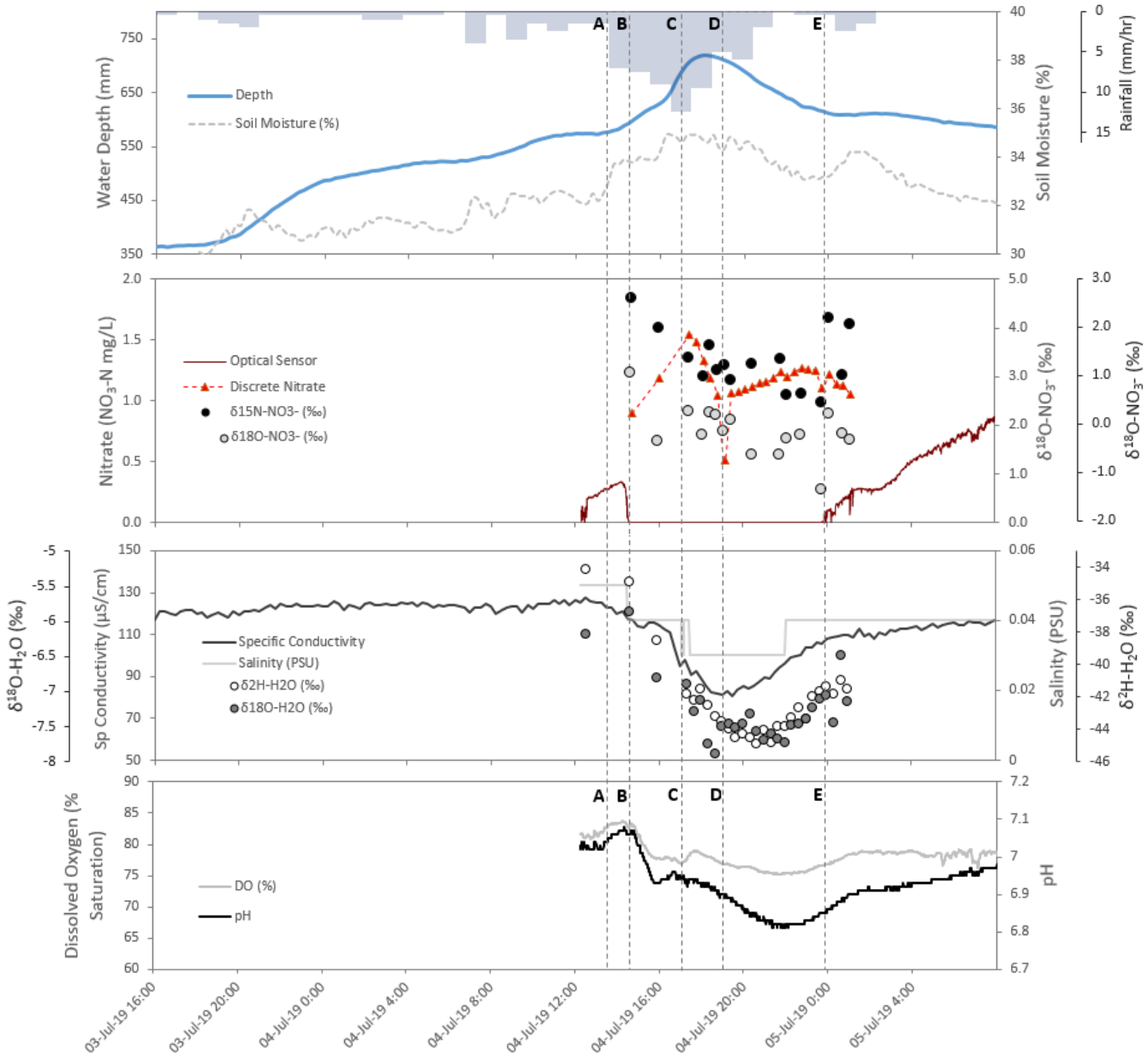


**Figure 4.10.** Time series of the isotopic, hydrological and physiochemical data at OK1 around a winter event (July 2019). Vertical dashed lines are labelled with letters to compare time points of particular interest.

### 4.2.3 Nitrate Isotopes and Nitrate Concentrations

***Nitrate Isotope Hysteresis***

Dual nitrate isotopes ($\delta^{15}N$ and $\delta^{18}O$) displayed overall hysteresis-type behaviour during the summer (February 2019) and winter event (July 2019) in the Okaro catchment (Figure 4.11). The winter event demonstrated a anti-clockwise, elongated, elliptical loop, with both $\delta^{15}N$ and $\delta^{18}O$ values decreasing before increasing. In comparison, the summer event behaved oppositely, demonstrating an overall clockwise, elliptical loop, with $\delta^{18}O$ increasing before $\delta^{15}N$ increased, followed by both decreasing. This pattern was interrupted by a shift to the opposite side of the loop, before the isotopic value return to that of the previous sample.

The winter event also showed 'flip' behaviour, with some consecutive samples having isotopic values typical of the opposite curve of the loop. These changes are larger than the analytical precision of 0.3‰.

The biggest shift in isotopic values during the winter event was for $\delta^{15}N$ values. Values of $\delta^{18}O$ showed a more gradual decrease, but remained lower on the falling curve compared to the rising curve. The second sample in the winter event has very similar isotopic values to the last sample in the event.

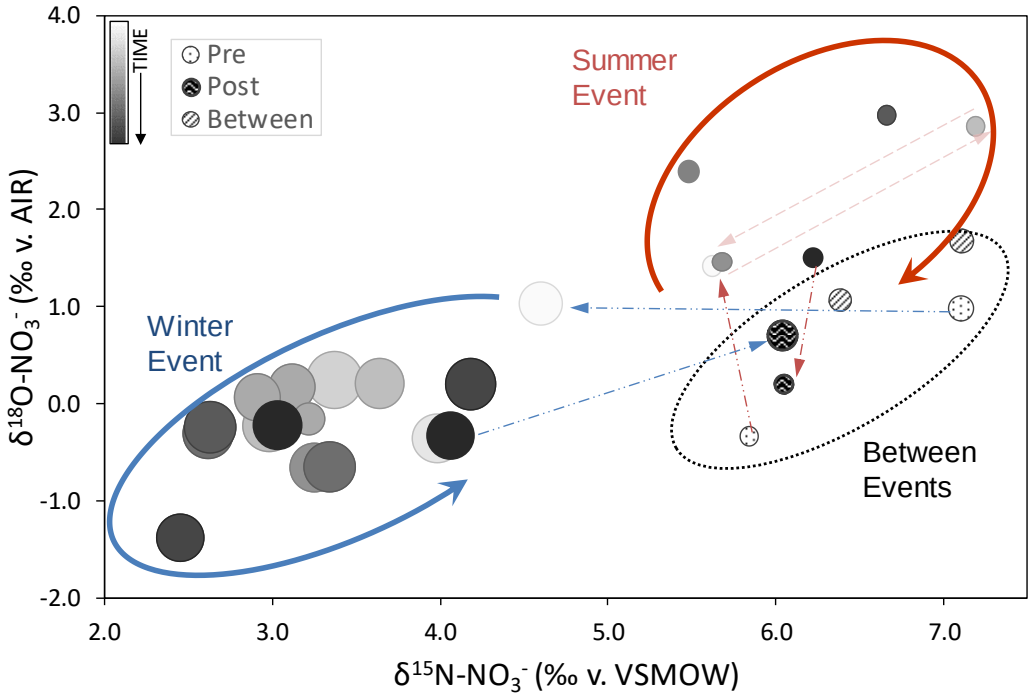


**Figure 4.11.** Time series of dual nitrate isotopes ($\delta^{15}N$ and $\delta^{18}O$) displaying hysteresis behaviour, for a summer (February 2019) and winter event (July 2019) in the Okaro catchment. Scale of light to dark grey signifies relative time during storm event of the sample, and the bubble size relative to its nitrate concentration. Monitoring samples before, after and between events have been included for comparison (patterned circles). The solid red and blue arrows denote the general direction of hysteresis loop for the summer and winter event respectively. Dash dot lines show direction of isotopic change from pre and to post. Red dashed line shows inter-event composition interchange.

Samples from before and after (pre and post) the event are in a similar range (denote by the black dotted ellipse), with the between event samples (also referred to as monitoring samples), which notably is also elliptical in shape. Compared to the non-event samples, the winter event showed a greater change in $\delta^{15}N$ values, where the summer event values stayed similar. The summer event $\delta^{18}O$ values had a slightly greater range than the winter despite having less samples.

The summer event showed an overall enrichment in both $\delta^{15}N$ and $\delta^{18}O$, whereas the winter event showed overall depletion in both isotopic values (Figure 4.12). Both $\delta^{15}N$ and $\delta^{18}O$ have more positive δ values winter, and less positive δ in winter. Post event samples for both the events appear to have some signs of residual effects from the preceding storm event, as they are closer to the storm event values compared to the pre samples.

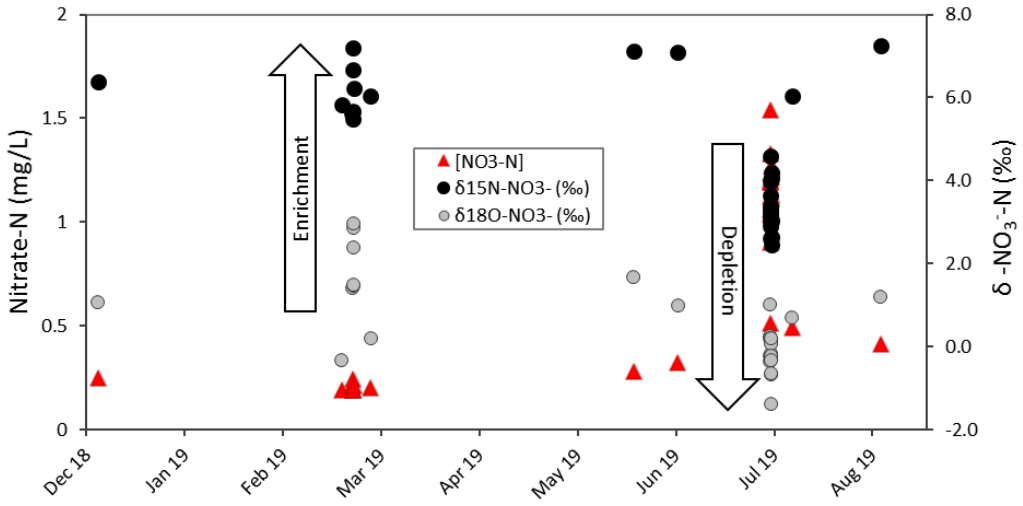


**Figure 4.12.** Comparison of nitrate isotope ($\delta^{15}N$ and $\delta^{18}O$) values at OK1 in the Okaro catchment, between December 2018 and August 2019, showing direction of fractionation during storm events and seasonal differences

### 4.2.4 Water Isotopes

***Water Isotope Hysteresis***

A hysteresis pattern was not strongly evident in the February summer event (Figure 4.13). The February event samples had limited shift in $\delta^{2}H$ values, and it was $\delta^{18}O$ values that predominantly shifted, resulting in a shift along a 'horizontal' plane (refer to Figure A.2, for detailed order). The before and after (labelled as pre and post) for the February summer event are very similar, and sit at a more negative $\delta^{2}H$ value compared to the event, and have $\delta^{18}O$ values similar to the right extent of the event $\delta^{18}O$ range. The December 2019 summer event samples overall shift in parallel to the LMWL,

with some limited ‘horizontal’ sift as seen in February. The overall isotopic signature of the water becomes less depleted (see Figure A.12 for detail).

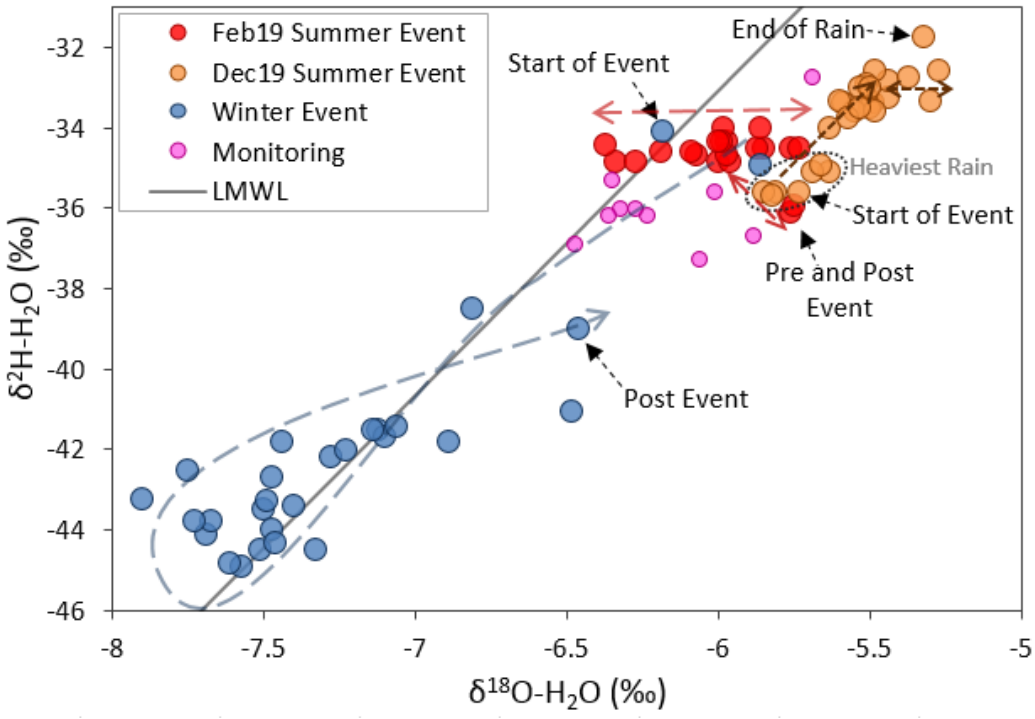


**Figure 4.13.** Time series of dual water isotopes ($\delta^2H$ and $\delta^{18}O$) displaying some hysteresis behaviour, for two summer (February 2019, December 2019) and a winter event (July 2019) at the OK1 site in the Okaro catchment. Monitoring samples (pink circles) have been included for comparison. The dashed arrows denote the general direction of isotopic shift and hysteresis loop. Dotted circle indicates period of heaviest rain in December 2019 event.

The winter event samples had shift in both δ2H and δ18O values, and of a greater magnitude compared to the summer event. A hysteresis loop was more evident in this event, with an overall pattern of an anti-clockwise eight-shaped loop. The event began with δ2H and δ18O values becoming increasingly negative, and following roughly along the LMWL. Isotopic values of the falling curve overall were higher above the LMWL, and δ2H and δ18O values becoming less negative. The start of the winter event (first and second sample) had similar isotopic values to those of the summer event. The post event sample and the second to last sample had more similar isotopic values (Figure A.3).

The monitoring samples (pink circles) in general stay close to the LMWL, with the November and April 2019 monitoring samples being the furthest away. The monitoring isotopic values lie between the majority of the winter, and summer event samples, although are much closer to the summer event samples. The November monitoring sample lies above the summer event samples.

# Chapter Five

# Discussion

This chapter begins with the synthesis of isotopic, hydrological and physiochemical data for the different study sites in the catchment and discusses the spatial and temporal variability. Secondly, the synthesis of the main site temporal data is discussed, focusing on seasonal and inter and intra storm variation. The chapter then proceeds by fully discussing limitations and uncertainties in the datasets that were briefly mentioned or not addressed in previous chapters. Finally, inferences from results are provided, along with their implications for both the Okaro catchment and for New Zealand, before recommendations are provided.

## 5.1 Spatial and Temporal Variation in the Catchment

This section covers the spatial variation, and any captured temporal variations within the spatial sites.

### 5.1.1 Upper Catchment (OK10 and OK11)

The primary stream sample from the upper catchment (OK10) had $\delta^{15}N\text{-}NO_3^-$ and $\delta^{18}O\text{-}NO_3^-$ values similar to other sites' baseflow samples taken. Approximately 500 m upstream at the detention pond (OK11), the $\delta^{15}N\text{-}NO_3^-$ value was similar, but the $\delta^{18}O\text{-}NO_3^-$ value was about 3.2 ‰ higher. The detention pond (OK11) had a nitrate concentration that was less than half of the downstream (OK10) concentration (0.16 mg/L and 0.39 mg/L, respectively). Dissolved oxygen was much higher at the detention pond (121.0%) than downstream at OK10 (86.8%). Considering the high oxygen and the environmental setting of the detention lake, respiration is likely responsible for this. There is likely to be denitrification in the sediment bed reducing nitrates and there will also be nitrate uptake from macrophytes.

The water isotopic compositions of these samples are approximately the same. The values are low in the observed water isotopic range (more depleted), but only one set was taken in winter (which experiences more depleted values) and so is likely a function of this.

### 5.1.2 Tributary (OK4 and OK5)

Samples from the primary stream tributary (OK4, OK5) have more depleted $\delta^{2}H\text{-}H_2O$ and $\delta^{18}O\text{-}H_2O$ values, consistently sitting low in the range of observed values, through summer and winter. This is likely a function of being a short, shaded tributary, and shares similar water isotope ratios of sites higher up in the catchment.

Between the sample taken December 2018 to the sample taken February 2019, an increase in $\delta^{15}N\text{-}NO_3^-$ and $\delta^{18}O\text{-}NO_3^-$ values, and a reduction in nitrate concentration, was observed. The tributary consistently had lower nitrate and dissolved oxygen concentrations than in the main trunk of the primary river (OK3, OK1). There is likely a mixture of microbial processes cycling nitrogen at this site.

### 5.1.3 Secondary Stream (OK6)

Samples from the secondary stream (OK6) were only taken around the February event and so limited assumptions can be made about its isotopic "profile". The water isotopic values were slightly more depleted than those of OK1 samples taken around the same time. These samples had the nitrate isotopic values that are most close to the ranges of effluent (Figure 4.5), which is fairly likely considering OK6's close proximity to the dairy shed. The secondary stream (OK6) samples were taken a day a part (during and post February event), with the day after sample having lower isotopic values but a higher nitrate concentration. Of the samples taken around the February summer event, only the secondary stream had substantial nitrate concentrations, however, it also did not experience a significant increase in nitrate-N (0.72 – 76 mg/L). This site had the highest dissolved oxygen (156.7%) and specific conductivity (161.6 µS/cm) concentrations recorded in the catchment.

Considering the site is almost a wetland by point of sampling and implications of this on parameters, as well as limited data for the site, it is difficult to ascertain how much of the observed characteristics can be

attributed to dairy. Land contours and riparian margins, as well as being a central part of the dairy farm, made access to a more representative site difficult, and thus the limited collection of data.

### 5.1.4 Bypass Channel (OK9)

The sample from OK9 (bypass/old stream channel) was taken during the July event, and as this bypass was activated during the event it is unsurprising that the $\delta^{15}N\text{-}NO_3^-$ and $\delta^{18}O\text{-}NO_3^-$ values are similar to that from the OK1 site at this time. At first glance, it appears that the water isotopes do not follow the same relationship as the nitrate isotopes. However, the bypass stream (OK9) sample was taken in the very early stages of the event, when the stream samples isotopic values had just begun to deplete with the event. It shared similar dissolved oxygen and nitrate concentrations as the earliest OK1 sample, so most likely by this time, the usually stagnant drain water in this channel had been flushed out to the lake.

### 5.1.5 Lake Inlet (OK8)

The OK8 (lake inlet) sample has the lowest $\delta^{15}N\text{-}NO_3^-$ value of all samples (+0.95 ‰). This sample was taken the day after the February event, with the sample taken the day of the event having a nitrate concentration below the detection limit of 0.05 mg/L and could not be analysed for $\delta^{15}N\text{-}NO_3^-$. The nitrate concentration of this sample was low (0.06 mg/L). Samples taken pre (3 days prior) and post (5 days after) event were also below nitrate detection limits. There was not a sample for the July event for nitrate, but Bay of Plenty Regional Council routine monitoring at the lake outlet (site ‘H’) since 2018 had a mean nitrate+nitrite N concentration of 0.305 ± 0.258 mg/L. These confirm relatively variable concentrations at this site. More recent data taken from OK8 shows the change in relative fractions of nitrogen at OK8 during the event December 2019 and two months after at baseflow (Figure 5.1).

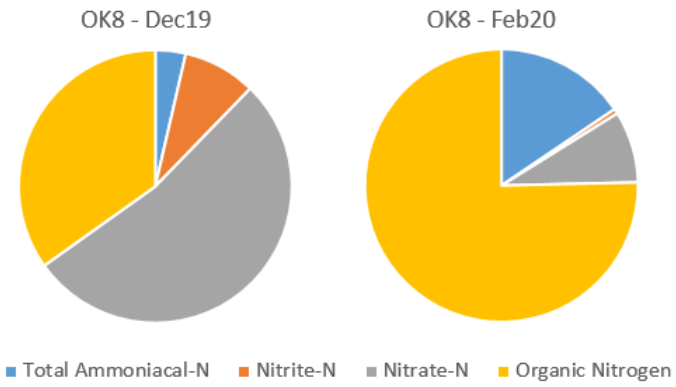


**Figure 5.1.** Lake inlet (OK8) fractions of nitrogen during a storm event in December 2019 compared to a baseflow sample in February 2020.

During the December 2019 event, nitrate was the dominant fraction of total nitrogen at OK8. In contrast, during baseflow monitoring in February 2020 the dominant fraction was organic nitrogen. Dissolved oxygen measured at this site is highly variable, with summer measurements usually below 60% saturation.

All other samples with $\delta^{15}N\text{-}NO_3^-$ values below +5 ‰ were associated with the July event. Due to a low $\delta^{15}N\text{-}NO_3^-$ value combined with a low $\delta^{18}O\text{-}NO_3^-$ value (-0.48 ‰), a low nitrate concentration and the site receiving water from the wetland, this nitrate is believed to be from nitrification.

Water isotope values for the lake inlet (OK8) generally sit within a relatively narrow band of $\delta^{2}H\text{-}H_2O$ values of -34 ‰ to -32 ‰, with the majority of variability being within $\delta^{18}O\text{-}H_2O$ values (approximately -6.3 ‰ to -5.0 ‰). The exception to this pattern is two samples that are more depleted for both water isotopes; one from the July storm event and the other being the post February event sample (approximately four days after). There is potential at this site for backflow and mixing with lake waters.

### 5.1.6 Farm Drain/Runoff (OK7)

The runoff/farm drain sample (OK7) for July had $\delta^{15}N\text{-}NO_3^-$ and $\delta^{18}O\text{-}NO_3^-$ values most similar to those observed in the February event for the primary stream (OK1), but nitrate concentrations similar to the July event stream

samples from the primary stream (OK1). The $\delta^{15}N\text{-}NO_3^-$ and $\delta^{18}O\text{-}NO_3^-$ values are also relatively close to that of OK6, and have nitrate values that are similar as well. Their close proximity then further suggests some shared nitrate sources, such as a potential effluent signature as described prior.It should be noted that the samples were taken in different seasons. The runoff/farm drain sample taken during the February event had a nitrate concentration below the detection limit so could not be analysed. This low nitrate concentration was probably due to plant uptake from the soil reserves, but without more detailed physiochemical data and $\delta^{15}N\text{-}NO_3^-$ and $\delta^{18}O\text{-}NO_3^-$ values, denitrification cannot be ruled out completely.

As the July event water isotopic values from OK1 match that of the farm drain (OK7) during the event, and the uniqueness of the values, indicate that this water is predominantly from the same origin, which appears to be the rainwater. However, the $\delta^{15}N\text{-}NO_3^-$ and $\delta^{18}O\text{-}NO_3^-$ values between the farm drain/runoff sample and OK1 stream samples for the July event are substantially different, although some variation is expected due to the nature of the waters they reside in.

The February event farm drain/runoff $\delta^{2}H\text{-}H_2O$ and $\delta^{18}O\text{-}O_2$ values signify the water source has undergone evaporation. If the two samples taken a day a part are reasonable representation of the evaporative vector during the event, the source is potentially a mix of soil water and rain. As the drain is ephemeral there is no ability for a pre-event sample in most conditions but there will be a window for a post rainfall sample. More samples during the progression of the storm may indicate temporal variability of source of the water. Caution has to be applied comparing a single reference value to a greater temporal frequency data set, especially as the drain is in a different part of the catchment where landuse and physiographic conditions differ.

### 5.1.7 Piezometers (OK1P1, OK1P2 and OK3P1)

The marked difference in $\delta^{2}H\text{-}H_2O$ values (~3‰) of OK1 piezometers P1 and P2, is likely due to the depth of each individual well, as they intersect

different groundwater flow paths, as a difference of . Piezometer P2's well casing is deeper in the soil than P1. During augering, P2 required more excavation of soil material until water was located, despite its close proximity to the stream. The soil material excavated from P2 was different in comparison to P1, it appeared more gley-like and had a dark horizon. Due to the depth of the well and limited available water for sample, another piezometer (P1) was excavated, and despite being approximately 30 cm away, had a much high water table.

The piezometers at OK1 have consistently less depleted water isotopic values compared to the overall range, and in a similar band as the lake inlet (OK8) but closer to and above the LMWL (compared to more below at OK8). Samples from the piezometer further upstream at OK3 have notably more depleted values.

The OK1P2 sample had a nitrate concentration of 0.05 mg/L, just at the detection limit, and thus was the only piezometer sample that could be analysed for nitrate isotopes as the other two piezometer samples had below detectable nitrate concentrations (<0.05 mg/L). The piezometers have characteristics positively associated with reducing conditions, such as this low nitrate concentration (0.05 mg/L), low DO (<2.5 mg/L) and the presence of (presumably) dissolved organic matter to act as an electron donor. McMahon and Böhlke (1996) found the hyporheic zone of the Platte River, USA, underwent denitrification to a substantial degree, more so than the riparian margin. The $\delta^{18}O\text{-}NO_3^-$ value reported for the OK1P2 sample had an unusually high value of 20‰, but had a high error margin as was close to the laboratory blank, and therefore was excluded from analysis. The $\delta^{15}N\text{-}NO_3^-$ value was +3.7‰.

The deepest well (4.7 m) at the Morrinsville site in the Toenepi catchment study site (Clague, Stenger, & Clough, 2015) had a value very similar to this, with the site reported as having the most isotopic variability despite relatively constant DO and nitrate concentration. The authors attributed to increased measurement uncertainties at low nitrate concentrations. While

the piezometer sample had the lowest reported nitrate concentration of samples above the threshold (0.05 mg/L), the OK8 sample had a similarly low nitrate concentration of 0.06 mg/L. Considering all other values observed, unless this a very large margin of uncertainty, the result may be real, and complex multi-step fractionations have occurred. Another potential reason, is that there was interference in the analysis method from dissolved organic carbon, discussed further in Section 5.3.2.

## 5.2 Main Site (OK1) Variation

### 5.2.1 Baseflow and Seasonal Variation

#### *Nitrate Concentrations*

The lowest nitrate concentrations were observed during summer, with increasing concentration from late autumn (May), reaching the highest values in July and August (Figure 4.2). It is believed nitrate concentrations began to decrease slowly from August over spring (nitrate analyser correction regression estimate of 0.39 mg/L from September 2019, see Section 5.3.4 for details) until the next result available in December 2019, of 0.24 mg/L.

Burkitt et al. (2017) reported higher nitrate concentrations at the start of the drainage season (May, June and July) in the Manawatu River, New Zealand, as discharge increased. Nitrate concentrations began to decrease from spring and remained low for the rest of spring and summer, even during increases in discharge (Figure 5.2).

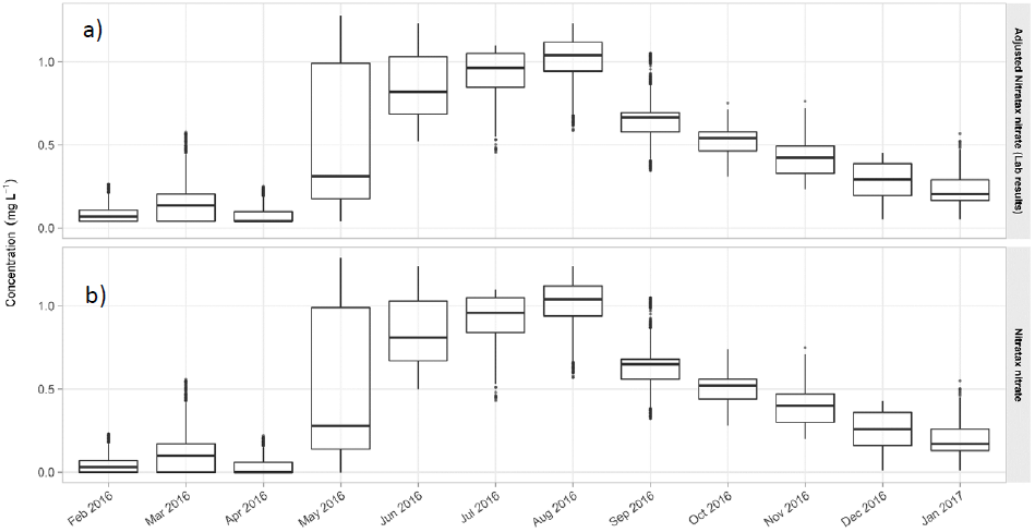


**Figure 5.2.** Monthly nitrate concentration ranges in the Manawatu River in 2016 (Burkitt et al., 2017)

Burkitt et al. (2017) postulated that this decrease in nitrate may be due to nitrate loss through surface runoff rather than drainage, which has been observed to lose less nitrate. This could explain why the February event at Okaro had very low nitrate increases. The extremely dry soil would have facilitated dominantly overland flow, and would explain the very limited increase in soil moisture content over the period. Another factor that could explain the lower nitrate concentrations over the late spring to summer is the increasing temperatures enhancing denitrification in the soil. However, baseflow $\delta^{15}N\text{-}NO_3^-$ and $\delta^{18}O\text{-}NO_3^-$ values were in a similar range during all seasons, with the February event samples having the same range of $\delta^{15}N\text{-}NO_3^-$ values, but more enriched $\delta^{18}O\text{-}NO_3^-$ values.

Clague, Stenger, and Clough (2015) observed higher nitrate concentrations in soil water at all depths during early winter, but lower nitrate concentrations during late winter to early spring. They postulated that this was a result of the accumulation of nitrate in the topsoil over summer, which then leached when water was available to mobilise it, subsequently diminishing the nitrate stored in the root zone. Dry conditions in summer restrict plant nutrient uptake, and water availability to mobilise the nitrate (i.e. leaching) resulting in this nitrate being stored in the root zone over this period.

Warming temperatures in spring could also increase denitrification, lowering nitrate concentrations. The change in nitrate concentrations also coincided with a change in isotopic values, with the late winter/early spring samples generally being more enriched in $^{15}N$ and $^{18}O$ (Clague, Stenger, & Clough, 2015).

Variation in nitrate concentrations at OK1 did occur seasonally, but the most pronounced increases in nitrate were observed in storm events, namely the July 2019 winter event (Figure 5.3). Inclusion of storm event nitrate concentrations skews mean nitrate concentration (0.74 mg/L) compared to nitrate concentrations at baseflow/monitoring conditions (0.29 mg/L). The higher nitrate concentrations, plus greater resolution during these events, over-imprints on the catchment nitrate statistics. However, this also highlights the dangers of not incorporating storm event nitrate concentrations, especially in calculations of nutrient loading. Blaen et al. (2017) observed that the events studied contributed 42% of the nitrate loads, even though the events only accounted for 31% of the time.

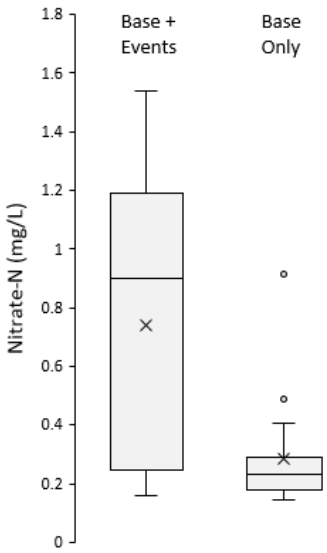


**Figure 5.3.** Nitrate-N concentrations at the OK1 site on the primary stream in the Okaro catchment. Samples collected December 2018 to February 2020

During the development and assessment of the wetland, nitrate-N was measured in the range of approximately 0.08 to 0.68 mg/L at the primary stream diversion (OK1), and approximately 0.02 to 0.92 mg/L at the

secondary stream (OK6), both with similar median nitrate concentrations of 0.39 mg/L (Hudson et al., 2009). These ranges are similar to those measured during routine monitoring prior to 2008; however, during this period the maximum concentrations recorded were approximately 0.2 mg/L higher and the secondary stream median was lower than that of the primary stream. The secondary stream experiences a larger fluctuation in nitrate concentrations.

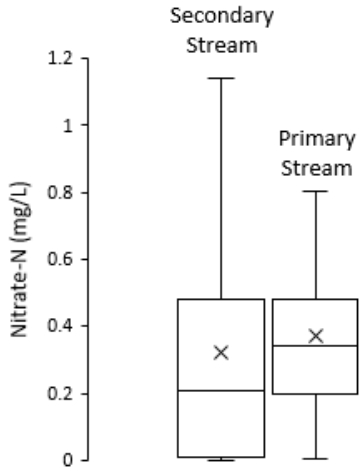


**Figure 5.4.** BOPRC routine monitoring of nitrate-N in the primary ('north') and secondary ('south') stream in the Okaro catchment from 2003 to 2007.

Diurnal fluctuations in nitrate concentrations must be considered. Monitoring of baseline samples generally occurred around the middle of the day or early afternoon, which would assist in reducing some of the diurnal variation effects. Seasonal biological processing of nitrate in streams also needs to be taken in to account. Nitrate utilisation by periphyton is poorly studied in New Zealand, but believed to be the cause of diurnal fluctuations in nitrate concentrations observed over autumn in the Manawatu River (Burkitt et al., 2017).

### *Isotopes*

Routine monitoring of nitrate isotope ratios at the main site demonstrated an apparent $\delta^{15}N\text{-}NO_3^-$ and $\delta^{18}O\text{-}NO_3^-$ 'baseline' range of approximately +5.8 ‰ to +7.3 ‰, and -0.5 ‰ to +1.7 ‰, respectively. These ranges are typical of soil nitrogen in agricultural systems in New Zealand (Baisden et al., 2016). At base flow, Burns et al. (2009) identified the dominant source

of nitrate as that derived from nitrification in the soil, however these were both forested catchments.

Dual nitrate isotope ratios from the OK1 site for the entire period plot along a 2:1 enrichment slope (ε15). However, if samples are separated in to subgroups, other relationships are evident (Figure 5.5). The July event samples also had a 2:1 enrichment slope; however, this is not surprising considering the samples from this event contribute over half of the samples for the main site, and thus a disproportionate amount of weight to the linear regression. The February event samples had an enrichment slope of 1.4:1, whereas baseline samples had a steeper enrichment slope of 1.1:1.

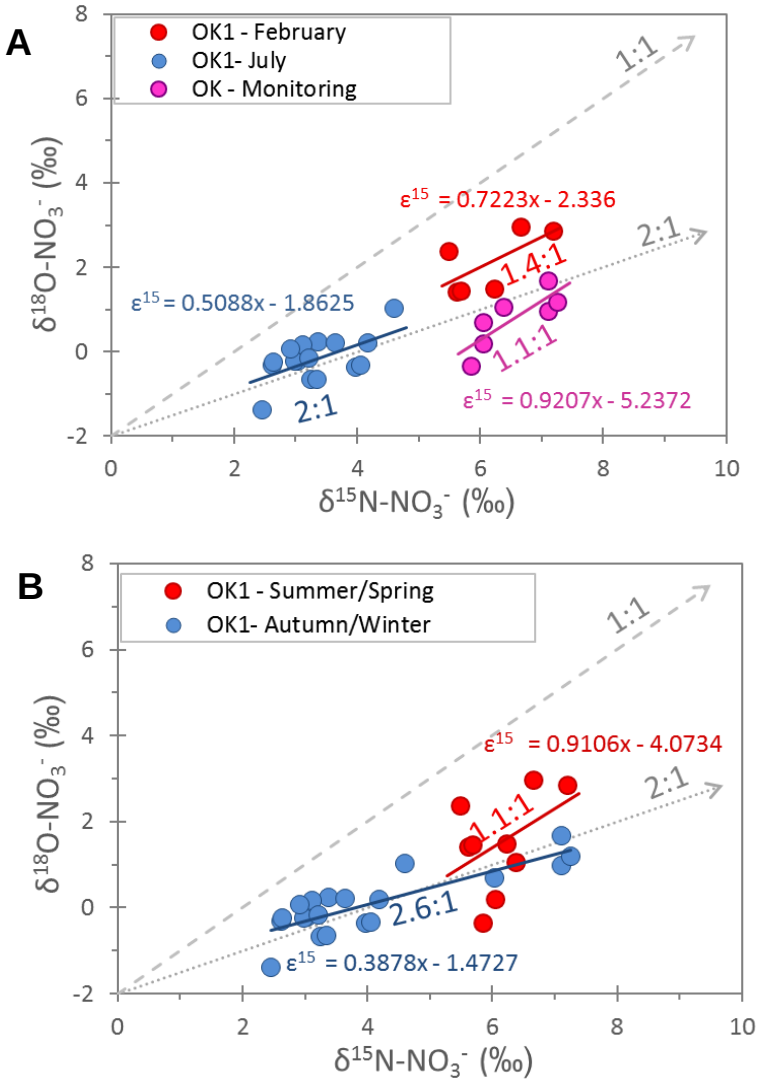


**Figure 5.5.** Enrichment slopes ($\varepsilon^{15}$) of OK1 samples separated by events and baseflow (A), and seasonally (B).

When divided by seasons, the two groups, summer/spring and autumn/winter, had quite different enrichments slopes (1.1:1 and 2.6:1, respectively) (Figure 5.5, B). The summer/spring slope may even be steeper than this, but this regression isn't as strong due to a much smaller number of samples and a weak fit ($R^2 = 0.20$). When applying an enrichment to the entire period, these relationships are concealed.

A wide range of slopes have indicated denitrification, from 2.1:1 to 1.3:1 (Chen et al., 2009). Clague, Stenger, and Clough (2015) observed an enrichment slope ($^{15}N:^{18}O$) of 1.4:1 at their groundwater study site in an agricultural catchment in the Waikato region.

There appears a slight disconnect in samples at approximate $\delta^{15}N\text{-}NO_3^-$ values of +5 ‰ (Figure 4.4). All samples below this value from the OK1 are from the July event (covered in Section 5.2.1); the only other samples are from OK8 and OK9. A similar disconnect in the nitrate isotope data is seen in the water isotope data, with a split in isotopic values at an approximate isotopic composition of -40 ‰ $\delta^2H\text{-}H_2O$ and -7 ‰ $\delta^{18}O\text{-}H_2O$. Samples with more depleted water isotopic values were that of the July 2019 storm event stream samples and runoff sample. All other samples in both time and space, besides rainfall samples, were less depleted than this. This will be further discussed in Section 5.2.2.

Investigation of relationships between nitrate concentration and $\delta^{15}N\text{-}NO_3^-$ values at the main site yielded nothing conclusive. A linear line was produced for $\delta^{15}N\text{-}NO_3^-$ against $1/[NO_3^-]$, which is suggestive of endmember mixing (Figure 5.6**,** A). However, a linear line was also produced when $\delta^{15}N\text{-}NO_3^-$ was plotted against $\ln[NO_3^-]$, a relationship which suggests kinetic fractionation (Figure 5.6, B).

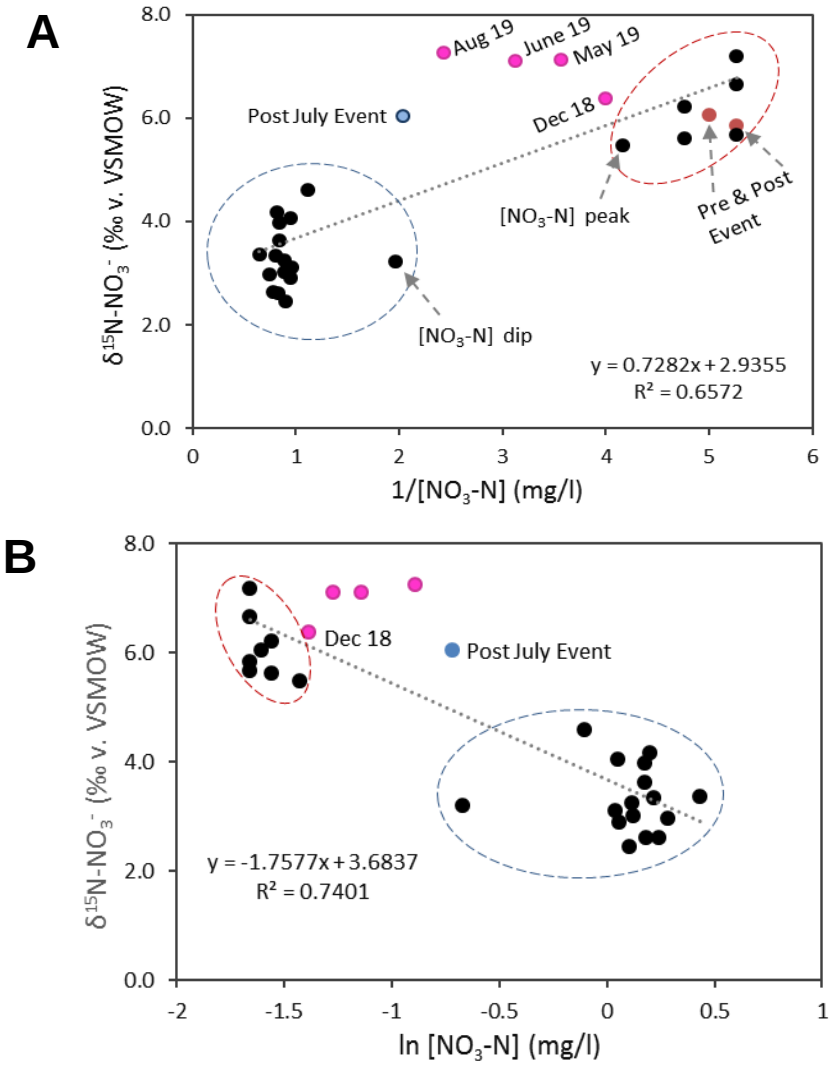


**Figure 5.6.** Exploring relationships described in the literature between $\delta^{15}N$ and nitrate concentration once transformed by the inverse (A) and natural log (B), to signify if fractionation or mixing has occurred. Linear regression fit based on all samples.

Despite fair $R^2$ values, the linear regression relationships are not strong, and are disproportionately weighted by the large amount of sampling in the July event. Relationships within storms had linear regressions with low $R^2$ values, but the potential dilution effect of the rainwater on nitrate concentrations would further complicate identifying relationships. Cey et al. (1999) observed a lack of relationship to support their hypothesis that denitrification was occurring, however, managed to determine it was the controlling mechanism through the additional use of $\delta^{18}O\text{-}NO_3^-$ values, oxygen and redox potential.

Water isotope ratios at OK1 displayed limited seasonal variation in the baseflow $\delta^{2}H\text{-}H_2O$ and $\delta^{18}O\text{-}H_2O$ values, besides the horizontal shift in $\delta^{18}O\text{-}H_2O$ values in summer, presumably due to enhanced evaporation of water in the stream baseflow. D-excess was lowest and closest to the GMWL in summer, with the opposite being true in winter (Figure 4.7), which is consistent with what is generally observed for locations who experience wet winters (Bershaw, 2018).

### 5.2.2 Storm Events

#### *February 2019 – Summer Event*

Conductivity increased during the summer event with a brief drop occurring at approximately peak depth, suggesting a short period of dilution. Conductivity actually began increasing before the main period of rain, in combination with the depth, indicating some slow movement of water from rain prior. After the rain had ceased, conductivity gradually increased and dropped quickly as water depth stabilised, indicating stormflow was contributing the increase in conductivity. Generally, a decrease in $\delta^{18}O\text{-}H_2O$ values occurred with the higher intensity rainfall periods, with a lag in the increase in $\delta^{2}H\text{-}H_2O$ before gradually decreasing. This behaviour suggests pulses in the relative contributions of water sources with rain. Nitrate isotope ratio samples were more sparse and did not capture any obvious patterns, changes in nitrate concentration did not appear to correlate with $\delta^{15}N\text{-}NO_3^-$ and $\delta^{18}O\text{-}NO_3^-$. When the pre-event sample is compared to the first recorded event sample, there is minimal difference in $\delta^{15}N\text{-}NO_3^-$, but a difference in $\delta^{18}O\text{-}NO_3^-$ values of 1.7‰. The summer event changes in DO and pH are likely a function of aquatic respiration as the changes occurred during the transition in to sunlight hours.

#### *December 2019 – Summer Event*

This event is covered briefly, as only limited preliminary data was available at the time. Water isotope sampling is covered in the comparison of events, but saw a shift in source during the event. Preliminary total nitrogen fractions have been measured during and after the event (Figure 5.7. **Total nitrogen**

**concentrations at OK1, separated in to nitrate + nitrite, and total Kjeldahl nitrogen. Samples taken during the December 2019 storm event and two monitoring samples in 2020, separated by dashed lines.**

and indicate that Total Kjeldahl Nitrogen (TKN) varies more than nitrate and nitrite.

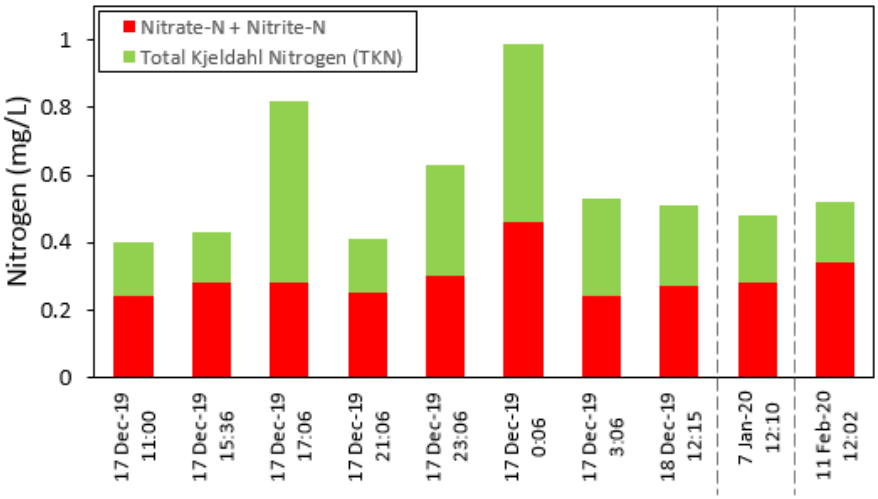


**Figure 5.7.** Total nitrogen concentrations at OK1, separated in to nitrate + nitrite, and total Kjeldahl nitrogen. Samples taken during the December 2019 storm event and two monitoring samples in 2020, separated by dashed lines.

While these results do not affect interpretation of the nitrate concentrations reported, it demonstrates the opportunity to gain insight on storm event nitrogen sources and their consequential downstream effects, where nitrogen cycling can change their relative proportions. Ammoniacal-N concentrations were analysed for the January and February 2020 baseflow monitoring and allows for separation of ammoniacal-N and organic nitrogen from total TKN. Results showed the approximate proportions of TKN as a third ammoniacal-N and two thirds organic nitrogen.

### *July – Winter Event*

The July 2019 event changes in OK1 water isotopic values can largely be explained by the change in wind direction. The scattered rain that began later on 3 July 2019 was from the north to northwest, and progressed to a northerly and north-easterly when the main rain event began, before changing to predominantly a south to south-easterly wind (Figure 5.8).

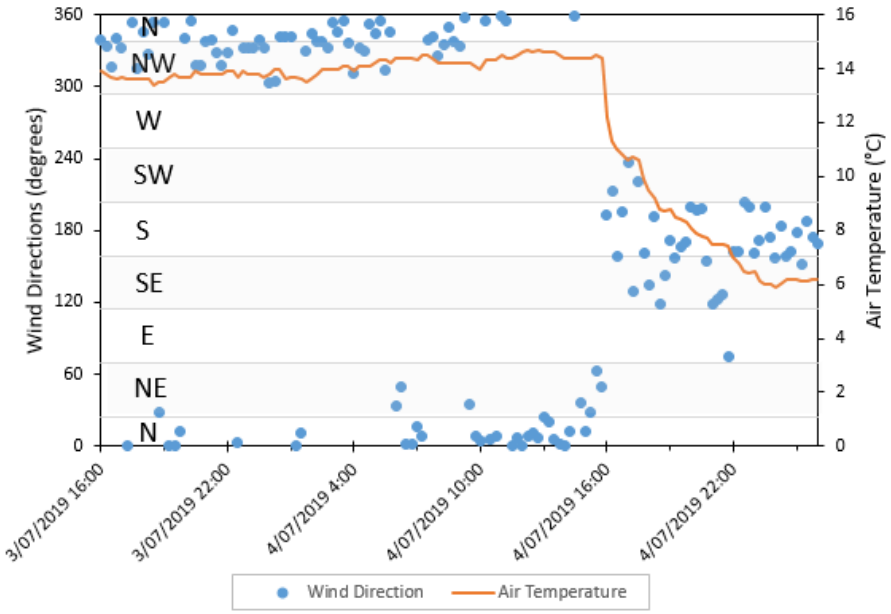


**Figure 5.8.** Wind direction and air temperature during the July 2019 winter event.

These winds from the south brought cold air, which saw a sudden and continuous reduction in air temperature. This cold southerly brought isotopically depleted rain, which dominated the event rainfall collection sample, giving rain $\delta^{2}H\text{-}H_2O$ and $\delta^{18}O\text{-}H_2O$ values of -67.9 ‰ and -9.81 ‰, respectively. As a consequence, the majority of the OK1 stream samples during this event have a substantially more depleted isotopic signature than all other event and baseline stream samples. The reduction in conductivity is further confirmation of dilution of stream water from the rainwater.

On the falling limb of the hydrograph there is a relatively brief period where several parameters shift (Figure 4.10. Time series of the isotopic, hydrological and physiochemical data at OK1 around a winter event (July 2019). Vertical dashed lines are labelled with letters to compare time points of particular interest., Point E). Despite limited rainfall at the time and no increase in depth, an increase in soil moisture begins and a slight dip in the otherwise fairly continuous nitrate concentrations occurs, as well as the optical nitrate sensor begins recording values again, in combination with a shift in nitrate isotopic ratios. This sample is seen as visually separate from the other samples in Figure 4.12 and Figure 5.6. Following this is a change in $\delta^{18}O\text{-}H_2O$ values. This series of conditions suggests another source and

mechanism of transport occurred briefly before a shifting towards pre-event conditions.

### *Comparison of Storm Events*

*Hysteresis*

The February 2019 summer event experienced predominantly a 'horizontal' shift in $\delta^{18}O\text{-}H_2O$ values, with relatively little shift in δ2H-H2O values (Figure 4.12). Considering the range of δ2H-H2O values, it is unlikely this pattern is entirely the result of instrument error or precision. This narrow band of storm values is less depleted than the pre and post event samples, only shifting slightly towards the much less depleted event rainwater.

The December 2019 summer event had the heaviest rain near the beginning of the event, with limited shifting in the $\delta^{2}H\text{-}H_2O$ and $\delta^{18}O\text{-}H_2O$ values, before shifting towards the less depleted values of the rainwater. This pattern suggests that at the beginning of the event, groundwater was still the main contributor to stream flow, before rainwater began to contribute more to stream flow. Near the end of the rain, the 'horizontal' shift in $\delta^{18}O\text{-}H_2O$ values were observed, similar to what was seen through the entire February event, but to a lesser degree. This period coincides with the final rise to peak depth and conductivity rising again after the initial spike and decrease. Upon the conductivity and depth decreasing, this horizontal shift ceased. The 'End of Rain' sample was taken the following day when the rainfall had ended and the stream was on the falling limb section of the hydrograph, suggesting event water was contributing more to stream discharge than during the event.

The summer events have very similar pre event $\delta^{2}H\text{-}H_2O$ and $\delta^{18}O\text{-}H_2O$ values. This suggests that these $\delta^{2}H\text{-}H_2O$ and $\delta^{18}O\text{-}H_2O$ values describe summer baseflow. The December 2019 event stream water discharge had a greater contribution from rainwater. Events with substantial contributions of rainwater have stream samples that move in 'enriched' or 'depleted' directions along the LWML. The December event's samples' parallel

placement to the LWML is indicative of the evaporative nature of a summer event. While both in summer, these events occurred at the start and end of summer and had differing antecedent conditions.

The July 2019 winter event started with a ‘horizontal’ shift before stream $\delta^{2}H\text{-}H_2O$ and $\delta^{18}O\text{-}H_2O$ values became more depleted, shifting towards the depleted $\delta^{2}H\text{-}H_2O$ and $\delta^{18}O\text{-}H_2O$ values of the collected rainwater. This suggests that there was an initial flush of groundwater before the rainwater dominated the stream flow, increasing and then decreasing relative amounts of flow contribution.

It is unknown what causes this ‘horizontal’ shift in $\delta^{18}O\text{-}H_2O$. A similar range and pattern of $\delta^{18}O\text{-}H_2O$ shift is observed in the OK1 piezometer $\delta^{18}O\text{-}H_2O$ values (Figure 5.9), as well as in OK8, suggesting that this could be connected to soil water surrounding the wetland. Another potential explanation is the effect of evaporation. The horizontal shift in $\delta^{18}O\text{-}H_2O$ could be the changing relative contributions of more evaporated stream water and less evaporated groundwater in the case of the February event, or between the more evaporated baseflow (thus largely groundwater) and the less evaporated rainwater in the case of the December event. The monitoring stream samples, including the circled pre and post rainfall samples (Figure 5.9), mostly sitting on a horizontal plane. OK8 receives this same water, either directly through the bypass, or once through the wetland (where evaporation is more enhanced), or a mixture of these two, which would explain the similarities.

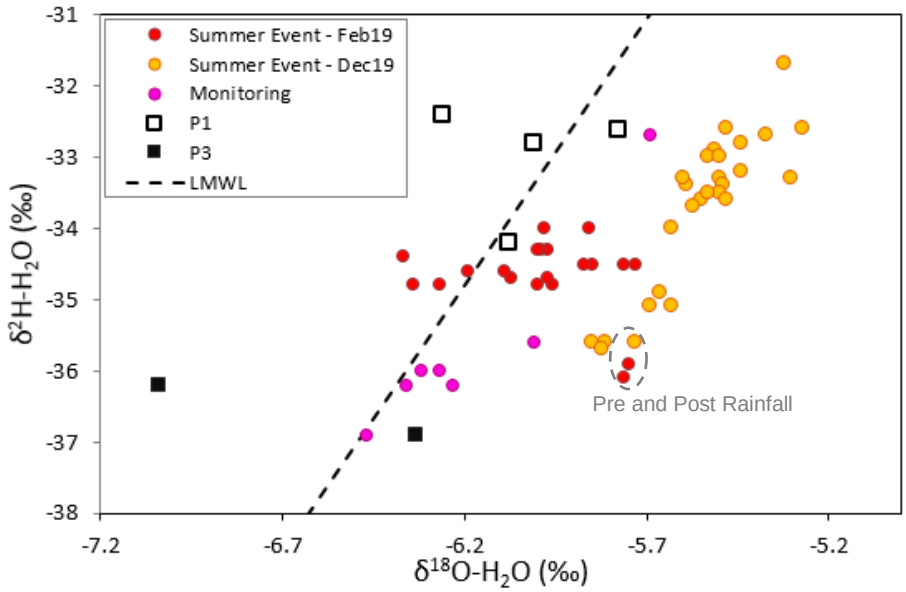


**Figure 5.9.** Water isotopic ratios of summer event stream water and baseflow for OK1, and piezometers at OK1 (P1) and OK3 (P3).

Considering most of the stream samples are below the local meteoric water line (LMWL) (viewed as 'to the right' on Figure 5.9) and the piezometers also traverse the LMWL, the interaction of the soil water causing this horizontal shift appears more likely.

Nitrate isotope ratios during the individual events displayed an overall hysteresis-like pattern, which were quite similar to that of the water isotopes (Figure 4.11). The winter event demonstrated an overall anti-clockwise loop, with both $\delta^{15}N$ and $\delta^{18}O$ values decreasing before increasing, whereas the February 2019 summer event demonstrated a clockwise loop with $\delta^{18}O$ increasing before $\delta^{15}N$ increased, followed by both decreasing. The February event saw a mid-event 'swap', suggesting there was a pulse of another source of nitrate that would become more dominant later. However, this could also be an artefact of a mislabelled sample.

Overall the February summer event enrichment in both δ15N and δ18O, whereas the winter event showed overall depletion in both isotopic values (Figure 4.12).

*D-excess*

Each storm event had a different D-excess response (Figure 4.7). The February 2019 summer event stream water moved towards a greater *d*-excess, and away from the pre-event stream *d*-excess value. The event rainwater had a lower *d*-excess than the majority of the stream samples, This suggests that there was a greater contribution of groundwater in this event, as the stream samples moved towards a more 'typical' rainwater *d* -excess, reflected by the higher *d*–excess in winter which predominantly recharges the groundwater.

The December 2019 summer event *d*-excess also shifted overall in the opposite direction of the rainfall *d*-excess, but in this case to a smaller *d*-excess. This could be another source such as partially evaporated soil water or a function of changing conditions, such as unsaturated conditions during precipitation that leads to evaporation (Bershaw, 2018).

The July 2019 winter event had *d*-excess values that shifted in both directions from the stream D-excess at the time, and away from the *d*-excess of the rainwater samples. This could be related to the change in moisture source from subtropical northerlies to sub-Antarctic southerlies.

### *Catchment Responses to Rainfall*

Higher intensity rainfall appeared to have less of an effect on soil moisture compared to extended periods of lower rainfall intensities. The February 2019 event had marginal increases in soil moisture and minimal increases in nitrate concentration in the stream samples. Despite similar antecedent soil moisture conditions, the July 2019 and December 2019 experienced significantly different stream nitrate concentrations.

The low soil moisture experienced in late summer and into autumn (below the permanent wilting point) would have substantially diminished plant uptake of nitrate in the soil, as their growth would be limited by the lack of water, in addition to cooler temperatures in autumn. As a consequence, less

nitrate would be removed in the root zone by plants before the nitrate would be mobilised with increased rain, resulting in more nitrate available for leaching.

Burkitt et al. (2017) found that nitrate concentrations were at their highest within 24 hours of discharge peaks in the Manawatu River, New Zealand, which could be captured through the use of high-resolution optical nitrate sensors. While storm events resulted in higher nitrate concentrations over all, the stormwater runoff contribution resulted in dilution of stream nitrate by the low-nitrate rainwater, resulting in periods of lower nitrate concentration during the storm event. This dilution effect has been seen in other studies during storm events (Feng, Schilling, and Chan, 2013; Paul et al., 2015; Burkitt et al., 2017). Paul et al. (2015) observed three storm events dominated by rainwater dilution, but one storm event demonstrated a different dominant water origin, that of groundwater inputs and subsurface flows. Subsurface flows have been observed to contain a greater proportion of event water than expected (Genereux and Hooper, 1998).

While the effect of dilution has been seen during the storm events in Okaro, it did not appear to experience much of the post-event nitrate increases seen in other studies (Feng, Schilling, and Chan, 2013), as streamflow can have higher discharge contributions from tile drainage, interflow and groundwater (if high in nitrate). Piezometer data showed very low nitrate concentrations so this may not be applicable, but this water is more representative of the hyporheic zone than water in the vadose or saturated groundwater zones.

The correct functioning of the nitrate sensor would have allowed for the better observation of this. During wetland assessment, an optical nitrate analyser was used on the inlet during a small winter storm, which showed a sudden drop in nitrate concentrations with a rapid increase in discharge (Figure 5.10). It was suggested that this drop in nitrate concentration over six minutes was the result of low nitrate groundwater entering the stream (NIWA, 2010).

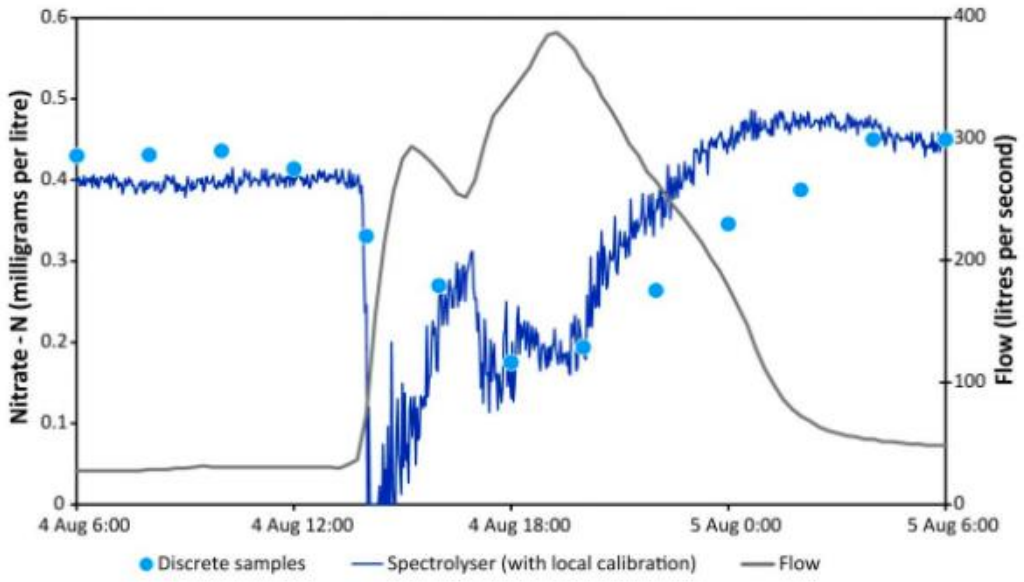


**Figure 5.10.** Comparison of continuous optical nitrate measurements with discrete laboratory nitrate concentrations, and stream discharge on the primary stream during a small storm event in August 2010 (NIWA, 2010).

The laboratory nitrate concentrations fit relatively well but the sensor quality metrics are unknown, so between the discrete samples there may have been a legitimate drop in nitrate concentration or perhaps interference from particulate mobile on the initiation of sudden heavy rain, such as what has been observed in this study. If a true representation, then temporal frequency of water sampling for storm events will have to be further scaled to capture this sort of rapid response.

## 5.3 Limitations

Issues that reduced the reliability and/or potential effectiveness of the data collected or presented are addressed here.

### 5.3.1 Physical

***Weather***

Rain event sampling was predominantly manual, and relied upon the accuracies of forecasts and short-notice availability of participants and equipment. Reliance on forecasts caused one of two problems, missing the beginning of an event (which happened in the February and July events) or the rainfall not eventuating or being later than predicted.

When setting the autosampler, both under-sampling and oversampling periods of the rainfall occurred. The use of triggers for the autosampler was explored but presented several potential issues. The use of a threshold variable would require this value to be low enough to capture the start of the event, but would then undoubtedly result in small increases causing a 'false' triggering and would require travel to site to empty and clean the collection bottles. A set time interval may not capture what samples are needed from an event. A number of set trigger levels (such as certain water levels or discharges) would be most ideal, but again the issue arises of having to travel to the site to empty and clean bottles after 'false' triggering.

This nature of sampling creates a bias for larger systems that are more easily predicted, than localised downpours, or summer convective rain that occurs fairly frequently in the inland areas of the Bay of Plenty (Chappell, 2013). A prolonged period of dry weather in the summer and autumn of 2019 resulted in limited rainfall data, with the February event being relatively small.

### 5.3.2 Sample Preparation and Analysis

***Isotopes***

Despite filtering the samples with 0.45 µm filters, particulate had settled/precipitated out in some samples, most notably the piezometers (Figure 5.11). Some samples were coloured, believed to be coloured dissolved organic matter (cDOM), which may have interfered with instrumentation or altered the sample to produce skewed results.

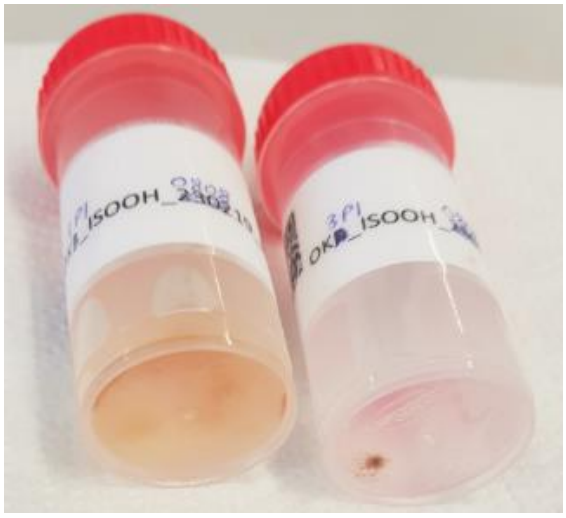

**Figure 5.11.** Piezometer samples from OK1 and OK3 showing dissolved and particulate matter.

Consequently, assuming dissolved organic carbon (DOC) is responsible for the decolouration of samples, the laboratory analysis of nitrate isotopes at Okaro may have varying degrees of unreliability. Interference of nitrate adsorption on the resins can be caused by high concentrations of other anions present in the sample, with the potential to cause fractionation of the nitrate isotopes (Silva et al., 2000). DOC retention on resins vary substantially due to the wide range of organic compounds it can incorporate, and known to be retained by resin on average 50% (Silva et al., 2000). DOC may also add nitrogen to the sample, as it contains up to 2% nitrogen, but its interference is largely unknown (Silva et al., 2000). DOC can also affect $\delta^{18}O\text{-}NO_3^-$ analysis, as substances that contain oxygen (for DOC this is 30-50%) provide a source of contamination and preparation complications, which reduce accuracy (Silva et al., 2000).

Samples analysed for water isotopes may had had interference with DOC or particulates, and potentially deposit residue in the injector block and affect the subsequent samples. Rainwater samples were not filtered, and algae particles have been observed in summer collectors, as they can sit for prolonged periods between rain events in warm conditions.

The discolouration of samples were most evident in the OK1 piezometers, in OK1 and OK9 samples during the storm events (see Figure 5.12), OK8, and in OK7. In the case of OK7, it is likely that the discolouration of the sample is not from the same compounds, as this water source is generated rapidly by rainfall runoff.

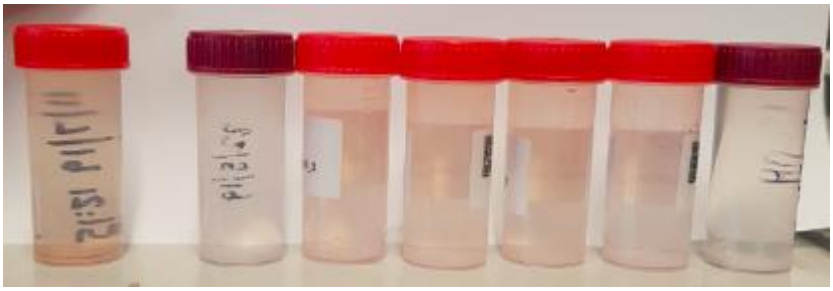

**Figure 5.12.** Samples at OK1 demonstrating discolouration of water. Sample on the far left is an OK1 piezometer, remaining samples are at various points during the July storm event, in chronological order from left to right, demonstrating discolouration variation through the event.

As nitrate values for some samples were below detection level (0.05), they were not analysed for dual nitrate isotopes, which resulted in less dual nitrate isotope data for analysis and excluded samples or sample sites with low nitrate concentrations. The farm drain/runoff (OK7) detectable nitrate in the July event but not in the summer event, and thus would only represent nitrate isotopic values during winter. A similar issue was experienced with the lake inlet (OK8) sample, which had detectable nitrate after the February event but not prior, and would represent isotopic value after rainfall and not at normal conditions in summer as well.

OK8, OK4 and OK3 had water and nitrate isotope subsamples prepared but nutrient samples could not be located at the time of their analysis. This has resulted in interpretation of $\delta^{15}N\text{-}NO_3^-$ and $\delta^{18}O\text{-}NO_3^-$ values purely based off one season's result, and as seen by other sites in the catchment, there can be substantial seasonal effects.

### 5.3.3 Monitoring Data

***Physiochemical***

Dissolved oxygen and pH are important parameters to measure as redox reactions have a significant influence on isotope fractionation (Kendall,1998). While dissolved oxygen was measure by all meter units, pH could only be measured with the YSI 650MDS and YSI ProDSS. These meters are bulky to transport around multiple sites, and not always available.

The use of different instrumentation can potentially cause bias in results, as they have different accuracies and thresholds. This was seen with salinity data, as the salinity would be below the threshold of the 650MDS, creating a bias for a higher mean.

***Hydrological***

After the wetland outlet G telemetry site was back online in July 2019, maintenance was carried out on the weir. Discharge data prior to this would have greater inaccuracies due to an improperly functioning weir, namely that it was leaking. Care also needs to be taken with the use of the wetland outlet discharge data for broader application as this does not take in to account bypass flow which now occurs more frequently, enhanced evaporation from the slower-moving, shallow wetland most also be taken in to consideration.

### 5.3.4 Optical Nitrate Analyser

Continuous nitrate concentration data from the NICO optical sensor (presented in Figure 4.10) is not believed to be reliable, and the increasing trend in nitrate after the storm is not an accurate representation of concentrations post storm.

A gradual increase in nitrate after a rainfall event has been commonly noted in other studies as mentioned previously, but further examination of the metadata suggests this trend is likely an artefact (Figure 5.13).

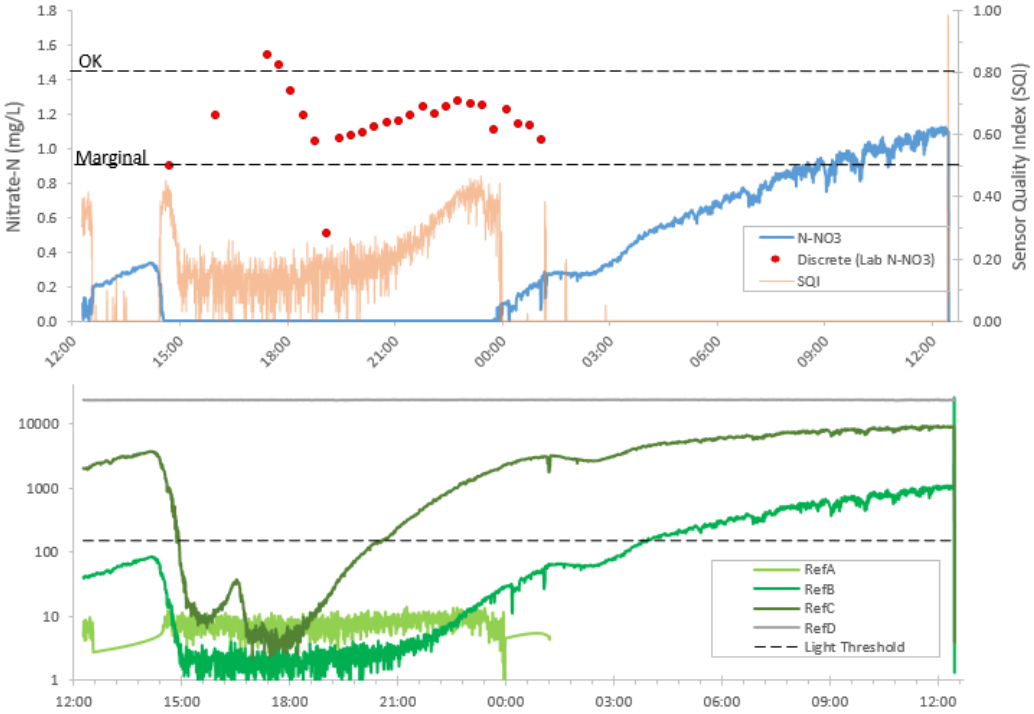


**Figure 5.13.** Nitrate data compared between the optical sensor and discrete samples, and absorbance metadata, for the July 2019 event.

Correction factors are usually applied to produce final results, as when compared to standard laboratory analysis method, the raw data show a bias Burkitt et al. (2017) found the OPUS sensor (version up from the NICO that was used in this study) to be positively biased compared to the laboratory values of the same sample. A similar technique was used to compare the sensor and laboratory data for this study, and a correlative factor was apparent when taking in to account the SQI, or signal quality index, but this relationship dissolved for SQIs of below 0.5 (Figure 5.14).

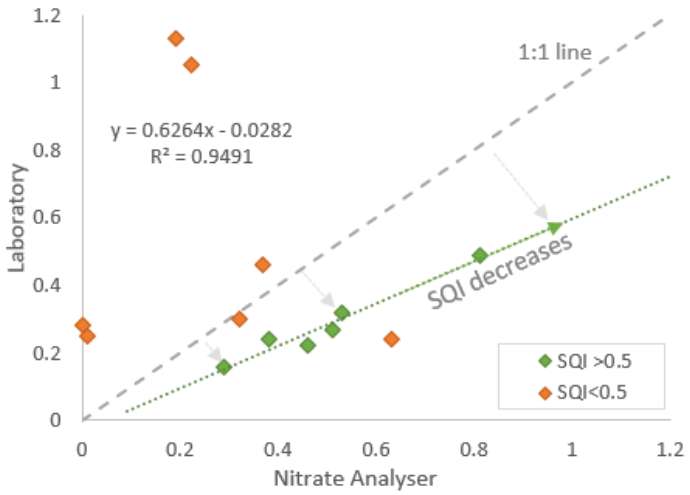


**Figure 5.14.** Comparison of sensor and laboratory nitrate concentrations, showing a predictable correlation is dependent on a sufficient signal quality index (SQI).

Path length was highlighted in several studies as an important consideration, as it determines the range of nitrate that can be detected, the change sensitivity and the susceptibility to detection interference (Huebsch et al., 2015; Snyder, Potter, & McDowell, 2018). The shorter the path length the greater the range in nitrate detection, but at the sacrifice of sensitivity.

The nitrate sensor should be calibrated in-situ, or with water from the field site, as the water matrix of the study site may be quite different to that of what the sensor was calibrated with Huebsch et al., 2015). Certain additional substances in the water composition (such as turbidity, organic matter) can cause inaccuracies (Huebsch et al., 2015).

Huebsch et al. (2015) achieved the most accurate results when onsite calibration was undertaken with a second order polynomial function. Similarly, Snyder, Potter, and McDowell (2018), found that applying corrections that were site specific produced the most accurate data. However, the water matrix can vary through time, which would affect the precision of the sensor, especially during high flows when the matrix is likely to be more different to that of the water it was calibrated to.

Multiple wavelength spectrophotometers calculate $NO_3$-N concentrations with the assistance of derivative methods, compared to double wavelength spectrophotometers which calculate $NO_3$-N by taking the difference in absorbance between the two wavelengths (Huebsch et al., 2015). The method for double wavelength spectrophotometers in theory should take into account the superposition of absorbance from interfering substances but this has not been the case in some studies (Huebsch et al., 2015).

Ions that have considerable absorbance at similar wavelengths as nitrate interfere with the optical nitrate measurements, and include nitrite ($NO_2^-$), chloride ($Cl^-$), bisulfide ($HS^-$), bromide ($Br^-$), bicarbonate ($HCO_3^-$) (Meyer et al., 2018).

Coloured dissolved organic matter, or CDOM, are soluble fractions of biogenic material that absorbs light, and can impart a yellow to brown colour on waters when concentrations are sufficient (Gholizadeh, 2016; IOCCG Protocol Series, 2018). The primary source of CDOM is allochthonous, such as decayed vegetation that has been transported by terrestrial runoff, or from riparian wetland vegetation; an autochthonous source is phytoplankton or algae (Steinberg, 2004; IOCCG Protocol Series, 2018). Elevated CDOM affects light detection in the blue-green range of the spectrum, in particular below 500 nm, and as wavelength decreases, the absorbance by CDOM increases exponentially (Gholizadeh, 2016).

Absorbance measured by the instrument for each wavelength is therefore a superposition of any species present that absorb at that particular wavelength (Meyer et al., 2018). The individual spectra signals need to be separated out for all species involved if reasonably accurate concentrations of nitrate are to be obtained (Meyer et al., 2018). CDOM is a broad grouping of humic substances with variable compositions, so its interference cannot be resolved in the same manner and different approaches have been used (IOCCG Protocol Series, 2018).

A common approach is using a mathematical function (such as linear or quadratic) to correct for absorbance by CDOM (reference). Meyer et al. (2018) added a group to account for light scattering absorbance for their multiple linear regression, and it is believed that absorption fractions of CDOM were accounted for in this group due to the high polynomial coefficients, high surface contribution and inverse relationship to salinity.

Snyder, Potter, and McDowell (2018) demonstrated that the magnitude and direction of sensor bias varied depending on the form of dissolved organic carbon (DOC), and that specified accuracy of the sensor was exceeded when the concentration of the leachate used reached 8 mg C/L. They highlighted the requirement for site specific adjustments depending on the forms of DOC present, and that sites with high DOC and low nitrate need particular consideration.

During storm events, high sediment loads obstructs the flow path of the analyser, leading to no or low quality data (Burkitt et al., 2017). Significant interference can occur in waters with inorganic sediments and detritus as they scatter light and can absorb a substantial amount of light in the blue and ultraviolet spectrum, and the extent will depend on the particle size an characteristics(Mamane, 2006; Saraceno et al., 2009). This alters the observed value as light is either not detected (through absorption or redirection) or the photon's optical path is lengthened, resulting in an underestimation (Saraceno et al., 2009).

While filtration would reduce particle interference, it would require a self-cleaning mechanism or the filter would block quickly during a storm event. The standard filtration for our discrete samples was 0.45 µm, and even at this size some of our samples still had particulates, demonstrating the presence of tiny colloidal clays or humic substances (IOCCG Protocol Series, 2018). Several studies have highlighted the requirement for a lens cleaner (Burkitt et al., 2017)

## 5.4 Inferences and Implications

### 5.4.1 Synthesis

Considering the very different summer and winter storm events sufficiently monitored in this study, it is difficult to ascertain if these are representative of storms in their respective seasons, especially with the unusually prolonged soil moisture deficit until the start of winter. The December event, while not extensively analysed in this study, provided further insight in to catchment responses, and in many respects provided an “in between” event of the two extremely different storm events.

The February 2019 summer event experienced pulses in differing water sources. Variation in the nitrate isotope ratios between baseflow and February event samples appears to occur predominantly in the oxygen ratios ($\delta^{15}O\text{-}NO_3^-$ and $\delta^{18}O\text{-}H_2O$), whereas in the July event, all isotope ratios shifted. This could suggest that the February event sources of nitrogen are alterations of the dominant nitrate contributor to the stream, rather than a separate source which appears to be the case for July. An explanation for this, that relates to the quick response of water isotopes to rainfall in February, is the flush of water in the riparian margins.

Rainwater was the dominant contributor to stream flow in the July 2019 event, as determined by the stream $\delta^2H\text{-}H_2O$ and $\delta^{18}O\text{-}H_2O$ values towards the characteristically depleted rainfall values, and further supported by low conductivity measurements. However, the suggested nitrate source in the drain of the purely dairy catchment is of a different origin, potentially a mix of effluent and soil nitrogen, but was also delivered by water that was predominantly event-based.

The Okaro catchment responded relatively quickly to the initiation of rainfall, due to its small catchment size, rolling to steep hills, well-drained soils and shallow depth to impermeable layer. Preferential flow is another mechanism by which the stream is likely receiving relatively rapid inputs of water. These pathways include that of the historic Tarawera rills and gullies, rills

developing on farm races and tracks (Figure A.18), surface cracks in dry conditions, overland flow by the easily compacted Rotomahana mud and potentially through areas of more permeable pumice sand areas, where there is no layer of low permeability Rotomahana mud, as identified by Tanner et al. (2007) during excavation of test pits for wetland construction. Fast movement through the catchment reduces retention time, and limits the ability of the landscape to attenuate or alter nutrients.

High spatial complexity is especially observable in these volcanic areas. The piezometers at the main sample site provide an example of potentially very complex flow paths. With only approximately half a metre between the piezometers, there was an observed change in water table depth, soil textures, water hydraulic conductivity and water quality parameters, as well as the deeper piezometer (P2) having the only nitrate result above the detection limit for piezometer samples and a lower $\delta^2H$-$H_2O$ value (by approximately 3‰).

While the effects of increased connectivity during storm events was not directly monitored, stagnant water in the old channel drains were measured for physiochemical parameters, which indicated depleted dissolved oxygen and elevated conductivity. These channels become connected with the streams during events and this low-quality water flushes to the lake. Variable source areas need to be considered when studying catchment responses, and the sources and dynamics of nutrients. An increase in stream depth also increases the wetted margin of the stream, potentially mobilising nutrients in the riparian margins. Increases in cDOM in the stream samples during events may be a function of flushing of this hyporheic area or from displacement of water stored in riparian margins upstream.

The effectiveness of riparian zones to buffer the nitrate inputs of agricultural systems will depend on the flowpaths, as well as the biogeochemical environment in which they transit, and therefore knowledge of this is necessary to determine their nitrate attenuation capability (Kendall, 1998).

Unfortunately, complexity of a groundwater system, such as many sources of nitrate or the lack of hydrological flow path understanding, can produce isotopic signals that are too convoluted to resolve (Clague, Stenger, & Clough, 2015). Results from this study suggest that groundwater is not the main contributor of nitrate, at least to the primary Okaro stream. However, there appears to be interactions with the hyporheic zone and wetland at this site. The visually higher cDOM concentrations in the OK1 piezometers provide further indication of a wetland connection.

Samples from OK4, OK5, OK6, OK8 and OK11 have nitrate isotopic values that sit closest to the projected 1:1 line (Figure 4.4). The primary stream tributary (OK4, OK5) and secondary stream (OK6) samples appear to have an enrichment slope that would be closer to 1:1, but as there are only two samples of each nothing robust can be drawn from this. These same sample sites also demonstrated higher than expected $\delta^{18}O\text{-}NO_3^-$ values when compared to the theoretical predicted values for nitrification (Figure 4.8), with the exception of OK8. The significantly lower nitrate isotope ratios for OK8 and the opposite relation to predicted values ($\delta^{18}O\text{-}H_2O$ higher than predicted, instead of $\delta^{18}O\text{-}NO_3$) compared to the other sites, suggests different fractionation drivers. These elevated $\delta^{18}O\text{-}NO_3^-$ values have been observed in other studies, who suggested an array of potential explanations, generally describing mechanisms that would provide $\delta^{18}O\text{-}NO_3^-$, $\delta^{18}O\text{-}H_2O$, and $\delta^{18}O\text{-}O_2$ values that were higher or lower than expected.

The aforementioned sample sites share some similarities, namely in the riparian vegetation types or the riparian environment (Figure 3.8, **Figure A.7**, Figure 3.13). This vegetation includes sedges, rushes and flaxes, such as swamp sedge (pūrei) and NZ flax (harakeke). These organic-rich environments can reduce nitrate through denitrification and plant assimilation, and provide environments for complex nitrogen fractionation. This finding in these type of environments could potentially be explained by limited or isolated denitrification, or nitrate formed with enriched $^{18}O$ due to oxygen consumption during respiration (Kendall, 1998). However, the mechanisms behind higher-than-predicted $\delta^{18}O$ caused by fractionation

cannot be adequately explained by present knowledge of the processes involved (Veale et al., 2019).

### 5.4.2 Implications

***Okaro Catchment***

The high-resolution sampling of storm events in the Okaro catchment reiterate the insight gained previously from the wetland assessment; that is, storm events contribute disproportionate amounts of nitrate loading to Lake Okaro.

The inlet and bypass weir on the main stream were designed so once the inflow in to the wetland was exceeded (184 L/s), stream flow would accumulate until it started being diverted through the bypass weir and down the old stream channel (Hudson et al., 2009; Hudson and Nagels, 2011). Although designed to omit these high flows from the wetland to prevent scouring and overloading, these flows consequently avoid the wetland and discharging directly in to the lake untreated (Hudson et al., 2009). As can be seen from Figure 4.3, the concentrations of nitrate are higher during storm events, during which the largest proportion of stream flow is bypassing the wetlands.

Hudson et al. (2009) determined that although bypass flow was infrequent (<3% of the time), it accounted for about 35% of the flow from the primary stream, and 35% of the nitrate load, in that period of monitoring (December 2007 – November 2008). In contrast, between 2008 and 2010, bypass flow occurred 1.6% of the time, but compromised 3-7% of primary stream inflow and between 2 and 7% of the total nitrate load (Hudson and Nagels, 2011).

During the July event, water was flowing completely over the weir structure (Figure A.15). It has been observed that bypass flow occurs even when storm events are not in progress, and was also the case before a storm event initiated in December 2019. In this case, it was noted that there was limited flow in to the inlet pipe. While vegetation ingress had been noted

earlier and some removed, further blockages had occurred (which have since been remedied). This process would have slowly reduced the inflow pipe capacity and increased the incidence of bypass flow. Additionally, there appears to be a substantial amount of sedimentation, and this impoundment behind the weir will be reducing the volume of stream flow that can be held before bypass flow initiates.

The consequences of these alterations to the flow dynamics means a much higher portion of primary stream inflow is bypassing the wetland, increasing the nutrient load inputs in to the lake. Based off flow and water quality characteristics recorded over the wetland assessment period, a hypothetical new pipe discharge limit (i.e. partially blocked pipe limit) was applied to the recorded discharges during this period. The estimate was derived from the median discharge and average nitrate concentrations in September during the assessment period, and based off the observation that during September 2019 baseflow, when the water was just beginning to overtop the weir.

Calculations suggested an increase in bypass flow of approximately 20%, and additional nitrate loading of approximately 150 kg/year. While these are very rough estimates, they highlight the effect bypass flow could be having on the lake water quality, which has seen an increase in TLI. However, routine monitoring by BOPRC has demonstrated an increasing concentration of nitrate + nitrate-N at both the lake inlet and the wetland outlet so bypass flow is clearly not the main driver of increasing nitrate inflow in to the lake (Figure 5.15).

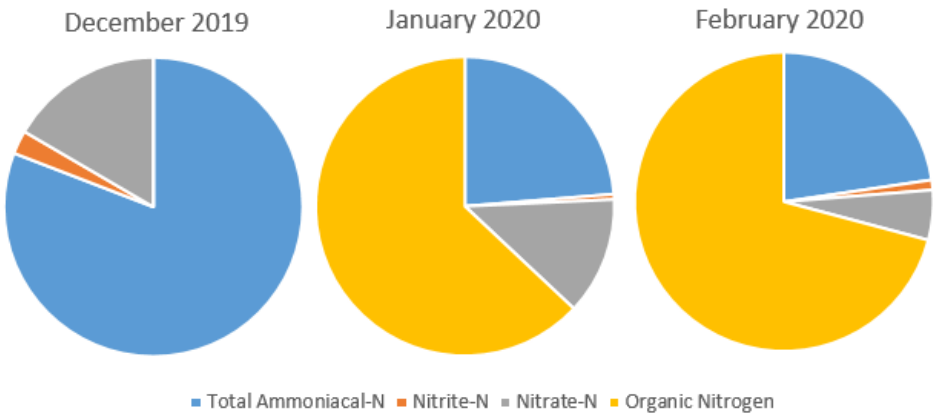


**Figure 5.15.** Wetland Outlet (G) fractions of nitrogen during a storm event in December 2019 compared to a baseflow samples in January and February 2020.

***New Zealand***

To fully understand the rainfall event contribution, a higher resolution of rainwater samples needs to be taken during an event, rather than a bulk sample, which mixes with or conceals more minor contributions. For example, the July event consisted of rainfall that originated from two opposite air masses, firstly subtropical north-northwesterlies and then sub-Antarctic south-southeasterlies, the latter 'overpowering' the rainfall isotopic ratios. There was a large degree of variation in regards to events; between seasons, in seasons and even observed within events. This high variability in New Zealand rainfall has been well predicted through a climatic and geological regressed model, but the model still faced difficulties predicting the isotopic characteristics at or below the scale of individual rain events, thus highlighting the need for finer resolution sampling during storm events (Baisden et al., 2016b).

### 5.4.3 Recommendations

The measurement of discharge would be highly beneficial for standardising physiochemical parameters with flow, allowing more accurate analysis of trends, as the data suggests that the catchment does not respond uniformly with discharge. The extensive riparian margin and in-stream vegetation and combination of ill-defined stream channel can make measuring discharge

difficult. Measurement at OK1 would require both the inlet pipe discharge being measured, as well as the bypass flow. The best option for discharge monitoring would be the outlet of the detention structures at OK3, as it has a pipe and therefore fixed area. It currently has some sediment build up and overgrowth that would need to be removed prior (Figure A.14). This site would not be able to capture the highest discharges as its purpose is high flow-restriction, but this is the same issue at OK1.

Other useful metrics for further investigation of catchment rainfall responses would be a precipitation index, to quantify antecedent rainfall. This could enhance the use of soil moisture metrics to model catchment responses, as soil moisture alone does not indicate the potential for soil runoff e.g. at the same given low soil moisture content, the runoff generated will differ if the soil has not received rain in two weeks compared to if the topsoil has been recently wetted. Various timescales for the index could be used investigated to determine if there is a connection between accumulated rainfall and isotope or water quality responses.

Rainwater collection during rain events should include multiple individual samples rather than a bulk rainwater composite sample, as discussed in Section 5.4.2. This higher resolution $\delta^{2}H$ and $\delta^{18}O$ data should be combined with rainfall yield to calculate relative contributions of rainfall and the impact on stream $\delta^{2}H$ and $\delta^{18}O$ values, so this can be discerned from other potential water sources, whose contributions are harder to quantify. The same is suggested for drainage water. Soil water and leachate should be measured, with careful consideration of the method used as they collect different fractions of the soil water.

It is suggested that piezometer samples lower in this catchment, and potentially samples in close proximity to the wetland, use smaller micron filtration (such as 0.22 µm) on the filtrate before analysis. Further investigation should be undertaken to ascertain the effect the dissolved carbon has on isotope results, and if pre-analysis ‘stripping’ of carbon would improve the results and not compromise them.

Dredging of the sediments that have been impounded behind the bypass weir will help reduce the occurrence of bypass flow, and re-suspension during events to minimise inflows of phosphorus in to the wetland and lake. Laboratory analysis should include all forms of nitrogen, to better assess nitrogen cycling, especially for the likes of the upstream detention pond and the wetland. An assessment of the wetland should be undertaken to determine the current nutrient and flow dynamics, and ascertain what maintenance needs to be carried out, such as desludging if flow short-circuiting is occurring and reducing retention time, and removing vegetation to replant to enhance assimilation, as well as additions of a carbon source for enhancing denitrification.

# Chapter Six

# Conclusion

This chapter summarises findings from the synthesis of data from spatial and temporal monitoring, and outlines the implications for this site, and the significance of the findings for nitrate management at the catchment scale. Finally, it identifies potential opportunities for further research.

## 6.1. Okaro Catchment Responses and Nitrate Dynamics

Nitrate contributions were much lower in summer relative to autumn and winter during baseflow or non-storm flow. Storm events contributed a disproportionate amount of nitrate, but the effect was most notable in winter. Despite similar antecedent soil moisture and substantial event water proportions, the primary streamflow in the December summer event experienced less of an increase in nitrate concentrations compared to the winter event, suggesting nitrate inputs during storms in this catchment are strongly linked to seasonal nitrate availability in water flow paths.

During baseflow or non-stormflow in the main inflow stream in the Lake Okaro catchment, nitrate had $\delta^{15}N$ and $\delta^{18}O$ values in the range of +5.8 ‰ to +7.3 ‰, and -0.5 ‰ to +1.7 ‰, respectively. In New Zealand pastoral systems, these ranges of values indicate a nitrogen source pertaining to normal soil nitrogen retention. In contrast, during a winter event (July 2019), the stream $\delta^{15}N\text{-}NO_3^-$ and $\delta^{18}O\text{-}NO_3^-$ values shifted to more depleted values, suggesting a change in source to that of bovine urine, while an ephemeral drain in a purely dairy landuse section had values that appeared to be of a mixed source, one of which is likely to be dairy effluent. Despite the difference in nitrate sources, the common factor was their transport vector of event water, as demonstrated by characteristic $\delta^2H$ and $\delta^{18}O$ rainwater values, which would have delivered nitrate through surface or sub-surface flow. There was an interesting pulse during the latter stages of the event that resulted in a distinct $\delta^{15}N\text{-}NO_3^-$ and $\delta^{18}O\text{-}NO_3^-$ values and a in a dip in nitrate concentration that was coupled with other physiochemical and

hydrological changes. This suggests that there may have been a pulse in a different source of water and nitrate, but the processes are unclear.

During the small summer event (February 2019), both nitrate and water isotope ratios only had a shift in $\delta^{18}O$ values, becoming more enriched than the baseflow or non-storm event isotopic ratios. This may to be a result of fractionation of the baseline isotopic signatures in isolated areas which are then connected during the event, or interaction with the hyporheic zone. Water isotopes suggest the main source of water was that of groundwater but that there appeared to be pulsed shifts in isotopic ratios related to rain, indicating changes in relative source mixing ratios. During this event, the farm drain had below detectable nitrate concentrations, further supporting a link to nitrate availability in the soil as driver of nitrate contributions to surface water, even with different surficial nitrate sources.

The December summer event saw a mix of water sources, which appear to suggest groundwater as the initial dominant flow source before shifting to a higher proportion of event water. Nitrate isotopes were not available but total nitrogen analyses showed that the total Kjeldahl nitrogen fraction was the dominant fraction changing during the rain event, which would further support the hypothesis of enhanced interactions with riparian zones during events.

## 6.2. Spatial Variability

The Okaro catchment exemplifies New Zealand's complex physiographic landscape. There were insufficient samples from the spatial sampling to reliably determine the individual site's nitrate or water sources and flow dynamics. While the intention of the spatial sampling was mainly to aid the inference of patterns seen at the main site, the results from the spatial sites often observed additional temporal variability, and generally demonstrated quite different patterns and thus making comparability difficult. However, it did indicate characteristic fractionation processes for sites of similar environments, likely due to enhanced plant and microbial processing of carbon and nitrogen.

## 6.3. Implications of the Research

Results from high-resolution monitoring of streamflow during storm events demonstrates the potential to capture dynamic shifts in distinct water sources, but can be limited by insufficient monitoring of ancillary parameters, or a lack of pre-event characterisation of streamflow. For a more robust identification of water sources contributing to streamflow during events, it is necessary to obtain a better resolution of event rainwater, and drainage water or other flow source that is being investigated. It is essential to cater the resolution of sampling to the individual catchment, which depends on the responsiveness to hydrological inputs, or important source shifts and processes may be missed. The use of multiple tracers, physiochemical and hydrological parameters allowed for enhanced interpretation of results, which would have otherwise remained ambiguous.

The spatial sampling demonstrates that even in small catchments, there may be a significant degree of heterogeneity in water and nitrate flows, in both space and time. While the construction of the wetland has helped reduce nitrogen and was tailored to consider timing and broad nitrogen dynamics, it relies heavily on geoengineering and its maintenance, and minimal alteration to the system it was designed for. To effectively address nitrogen management requirements at a catchment scale, sub-catchment units should be divided by their physiographic properties and partitioned in to management units based off their characteristic flow and nitrate properties at a finer scale, and then apply necessary control points relevant to the site rather than just broad management techniques.

## 6.4. Future Research Opportunities

Patterns observed in temporal and spatial data collected require more investigation around potential reasons or mechanisms of fractionation. Fractionation mechanisms for the higher-than-predicted $\delta^{18}O\text{-}NO_3^-$ values observed for similar organic-rich sites should be determined. Similarly, potential mechanisms to explain the $\delta^{18}O$ values shifting at the primary site

during the summer events, as observed in both water and nitrate isotope ratios when streamflows were more dominated by groundwater.

Further refinement of the Okaro catchment flows and cycling of nitrogen will help create more catered management techniques. Particular areas that need further investigation are groundwater flow paths, as well as to ascertain the groundwater nitrate and water isotope signatures, the displacement of riparian water and associated nutrients and sediment during storm events, the interaction of the wetland with the surrounding surface waters and hyporheic zone.

# References


Baisden, W., Rissman, C., Ellis, T., Rayner, S., Clough, T. J., Moore, C., Killick, M., Rodway, E., Horton, T. W., Clark, M. (2016a). *Informing policy and management in New Zealand agricultural regions using nitrogen and oxygen isotopes to quantify hot spots and hot moments of nitrate loss*. American Geophysical Union, Fall Meeting.

Baisden, W. T., Keller E. D., Van Hale, R., Frew, R. D., Wassenaar, L. I. (2016b). Precipitation isoscapes for New Zealand: enhanced temporal detail using precipitation-weighted daily climatology. *Isotopes in Environmental and Health Studies, 52*(4-5), 343-52.

BFEA. (2003). Balance Farm Environment awards - 2013 Bay Of Plenty. Retrieved from http://www.nzfeatrust.org.nz/vdb/document/37

Blaen, P. J., Khamis, K., Lloyd, C., Comer-Warner, S., Ciocca, F., Thomas, R. M., ... Krause, S. (2017). High-frequency monitoring of catchment nutrient exports reveals highly variable storm event responses and dynamic source zone activation. *Journal of Geophysical Research: Biogeosciences, 122*(9), 2265-2281. https://doi.org/10.1002 /2017JG003904

Buckthought, L. E., Clough, T. J, Cameron, K. C., Di, H. J., Shepherd, M. A. (2016). Plant N uptake in the periphery of a bovine urine patch: determining the 'effective area', *New Zealand Journal of Agricultural Research, 59*(2), 122-140, DOI: 10.1080/00288233.2015.1134589

Burkitt, L.L, Jordan, P., Singh, R., and Elwan, A. (2017). High resolution monitoring of river nitrate in agricultural catchments – a case on the Manawatu River, New Zealand. An Envirolink report (MAUX1604 / 1720-HZLC135) prepared for Horizons Regional Council, 19 pages.

Burns, D., Boyer, E., Elliott, E., and Kendall, C. (2009). Sources and Transformations of Nitrate from Streams Draining Varying Land Uses: Evidence From Dual Isotope Analysis. *Journal of environmental quality, 38*, 1149-59. 10.2134/jeq2008.0371.

Brooks, R., Barnard, R., Coulombe, R., McDonnell, J.J. (2010). Ecohydrologic separation of water between trees and streams in a Mediterranean climate. *Nat Geosci, 3*, 100–104. doi: 10.1038/NGEO722.

Chappell, P. R. (2013). *The Climate and Weather of Bay Of Plenty* (3rd ed). NIWA Science and Technology Series, Number 62

Chappell, N., Jones, T., & Tych, W. (2017). Sampling frequency for water quality variables in streams: Systems analysis to quantify minimum monitoring rates. *Water Research*. 123. 10.1016/j.watres.2017.06.047.

Chen, Z. X., Liu, G., Liu, W. G., & Lam, M., Liu, G.J., & Yin, X.B. (2012). Identification of nitrate sources in Taihu Lake and its major inflow rivers in China, using δ15N-NO3- and δ18O-NO3- values. *Water science and technology: a journal of the International Association on Water Pollution Research*. 66. 536-42. 10.2166/wst.2012.193.

Clague, J., Stenger, R., Clough, T. (2015). Evaluation of the stable isotope signatures of nitrate to detect denitrification in a shallow groundwater system in New Zealand. Agriculture, Ecosystems & Environment, 202, 10.1016/j.agee.2015.01.011.

Close, M., E., Abraham, P., Humphries, B., Lilburne, L., Cuthill., T, Wilson S. (2016). Predicting groundwater redox status on a regional scale using linear discriminant analysis. *Journal of Contaminant Hydrology, 191*,19–32.

Cohen, M., Heffernan, J., Albertin, A., Martin, J. (2012). Inference of riverine nitrogen processing from longitudinal and diel variation in dual nitrate isotopes. *Journal of Geophysical Research, 117,* G0121. 10.1029/2011JG001715.

Di, H. J., Cameron, K. C., Silva, R. G., Russell J. M., Barnett, J. W. (2002) A lysimeter study of the fate of 15N ‑ labelled nitrogen in cow urine with or without farm dairy effluent in a grazed dairy pasture soil under flood irrigation, *New Zealand Journal of Agricultural Research, 45*(4), 235-244, DOI: 10.1080/00288233.2002.9513514

Durka, W., Ernst Detlef, S., Gebauer, G., Voerkelius, S. (1994). Effects of forest decline on uptake and leaching of deposited nitrate determined from 15N and 18O measurements. Nature, 372, 765-767. 10.1038/372765a0.

Environment Bay of Plenty (2006). Lake Ōkaro action plan. Environment Bay of Plenty Publication 2006/03.53 pp

Feng, Z., Schilling, K.E. Chan, K.S. (2013). Dynamic regression modeling of daily nitrate-nitrogen concentrations in a large agricultural

watershed. *Environmental Monitoring Assessment, 185,* 4605. https://doi.org/10.1007/s10661-012-2891-7

Forsyth, D. J., Dryden, S. J., James, M. R. & Vincent, W. F. (1988). The Lake Okaro ecosystem 1. Background limnology, New Zealand *Journal of Marine and Freshwater Research, 22*(1), 17-27

Gruber, N., Galloway, J. (2008). An Earth-system perspective of the global nitrogen cycle. *Nature, 451*, 293–296 https://doi.org/10.1038/nature06592

Galloway J.,N., Townsend, A., R., Erisman J. W., Bekunda, M., Cai Z, Freney J., R., Martinelli, L., A., Seitzinger S., P., Sutton M., A. (2008). Transformation of the nitrogen cycle: recent trends, questions, and potential solutions. *Science, 320*(5878), 889-92.

Genereux and Hooper (1998). Tracing nitrogen sources and cycling in catchments. In C. Kendall and J.J. McDonnell (Eds). *Isotope tracers in catchment hydrology*. Oxford: Elsevier; p. 519–576.

Gibbs, M. M, Dudli, S., Vopel, K., Hickey, C., Wilson, P., Özkundakci, D. (2007). P- inactivation efficacy of Z2G1 as a capping agent on Lake Okaro sediment. *NIWA Client Report: HAM2007* –12 July 2007. Collaboration/NIWA project: BOP 07215.

Gillon, N., White, P., Hamilton, D. (2009). Groundwater in the Okataina caldera: model of future nitrogen loads to Lake Tarawera. CBER Report 94. Centre for Biodiversity and Ecology Research, Department of Biological Sciences, School of Science and Engineering, University of Waikato.

Gholizadeh, M. H., Melesse, A. M., Reddi, L. (2016). A Comprehensive Review on Water Quality Parameters Estimation Using Remote Sensing Techniques. Sensors (Basel, Switzerland), *16*(8), 1298. doi:10.3390/s16081298

Wriedt, G., Rode, M (2006). Modelling nitrate transport and turnover in a lowland catchment system, *Journal of Hydrology, 328*(1–2), 157-176

Groffman, P.M., Altabet, M.A., Böhlke, J.K., Butterbach-Bahl, K., David, M.B., Firestone, M.K., Giblin, A.E., Kana, T.M., Nielsen, L.P., Voytek, M.A. (2006). Methods for measuring denitrification: diverse approaches to a difficult problem. *Ecological Applications, 16*, 2091–2122.

Groffman, P.M., Butterbach-Bahl, K., Fulweiler, R.W., Gold, A.J., Morse, J.L., Stander, E.K., Tague, C., Tonitto, C., Vidon, P. (2009). Challenges to incorporating spatially and temporally explicit phenomena (hotspots and hot moments) in denitrification model. *Biogeochemistry, 93*, 49–77.

Mamane, H., Ducoste, J. J., Linden, K. G. (2006). Effect of particles on ultraviolet light penetration in natural and engineered systems. *Applied Optics*, *45*, 1844-1856.

Hardy, L. (2005). Lake Okaro: Explosions and Erosion (Honours thesis, University of Otago, Dunedin, New Zealand). Retrieved from http://www.boprc.govt.nz/media/34368/TechReports-050101-LakeOkaroExplosionsandErosion.pdf

Hudson, N., Ballantine, D., Nagels. J., Rutherford, J. (2009). Assessing the nutrient removal performance of the Lake Okaro constructed wetland. NIWA Client Report for Environment Bay of Plenty HAM 2009-114. NIWA Project BOP08215

Hudson, N., Nagels, J. (2011). Assessing the performance of the Lake Okaro constructed wetland. NIWA Client Report NO HAM2011-120. NIWA, Hamilton, New Zealand.

Huebsch, M., Grimmeisen, F., Zemann, M., Fenton, O., Richards, K.G., Jordan, P., Sawarieh, A., Blum, P., Goldscheider, N. (2015). Technical Note: Field experiences using UV/VIS sensors for high-resolution monitoring of nitrate in groundwater. *Hydrological Earth System Science, 19,* 1589–1598

IOCCG Protocol Series (2018). Inherent Optical Property Measurements and Protocols:Absorption Coefficient. In A. R. Neeley and A. Mannino, (Eds.), *IOCCG Ocean Optics and Biogeochemistry Protocols for Satellite Ocean Colour Sensor Validation, Volume 1.0*, IOCCG, Dartmouth, NS, Canada.

Kellman, L.M. (2005). A study of tile drain nitrate- 15N values as a tool for assessing nitrate sources in an agricultural region. *Nutrient Cycling in Agroecosystems, 71*, 131–137.

Kendall C. (1998). Tracing nitrogen sources and cycling in catchments. In C. Kendall and J.J. McDonnell (Eds). *Isotope tracers in catchment hydrology*. Oxford: Elsevier; p. 519–576.

Kendall, C., Caldwell, E. A. (1998). Fundamentals of Isotope Geochemistry. In C. Kendall and J.J. McDonnell (Eds). *Isotope tracers in catchment hydrology. Oxford: Elsevier*; p. 51–86.

Kerr, T., Srinivasan, M. S., Rutherford, J. (2015). Stable water isotopes across a transect of the Southern Alps, New Zealand. *Journal of Hydrometeorology, 16*(2), 702-715. doi:http://dx.doi.org.ezproxy.waikato.ac.nz/10.1175/JHM-D-13-0141.1

Kirchner, J., W., Feng, X., Neal, C., Robson, A., J. (2004). The fine structure of water‐quality dynamics: the (high‐frequency) wave of the future. *Hydrological Processes, 18*, 1353-1359. doi:10.1002/hyp.5537

Kirkman, J., H. (1975). Clay mineralogy of some tephra beds of the Rotorua area, North Island, New Zealand. *Clay Minerals, 10,* 437-449.

Kroopnick, P., Craig, H. (1972). Atmospheric Oxygen: Isotopic Composition and Solubility Fractionation. *Science*, *175*(4017), 54-55 DOI: 10.1126/science.175.4017.54

Lam, Q.D., Schmalz, B., Fohrer, N., (2012). Assessing the spatial and temporal variations of water quality in lowland areas, Northern Germany. *Journal of Hydrology, 438–439*, 137–147. http://dx.doi.org/10.1016/j.jhydrol.2012.03.011.

Landcorp Farming Limited. (2017). Annual Report 2017. Retrieved from https://pamu-au.s3.amazonaws.com/corporate/images/Landcorp-Farming-Limited-Annual-Report-2017.pdf?mtime=20180309132600

Landon M, Delin G, Komor S, Regan C. (1999). Comparison of the stable-isotopic composition of soil water collected from suction lysimeters, wick samplers, and cores in a sandy unsaturated zone. *Journal of Hydrology*, 224:45–54.

LAWA. (2020). *Lake Okaro*. Retrieved from https://www.lawa.org.nz/explore-data/bay-of-plenty-region/lakes/lake-okaro/

Lehmann, M. F., Reichert, P., Bernasconi, S. M., Barbieri, A., & McKenzie, J. A. (2003). Modelling nitrogen and oxygen isotope fractionation during denitrification in a lacustrine redox-transition zone. *Geochimica*

*et Cosmochimica Acta*, *67*(14), 2529-2542. https://doi.org/10.1016/S0016-7037(03)00085-1

Li, S., Cong-Qiang, L., Li, J., Xue, Z., Jin, G., Yunchao, L., Hu, D., Li, L. (2012). Evaluation of nitrate source in surface water of southwestern China based on stable isotopes. *Environmental Earth Sciences*, *68*. 10.1007/s12665-012-1733-9.

Lloyd, E., F. (1959). The Hot Springs and Hydrothermal Eruptions of Waiotapu. *New Zealand Journal of Geology and Geophysics, 2*, 141-176

Lloyd, C. Freer, J.E., Johnes, P., Collins, A. (2016). Using hysteresis analysis of high-resolution water quality monitoring data, including uncertainty, to infer controls on nutrient and sediment transfer in catchments. Science of The Total Environment. 543, Part A. 388 - 404. 10.1016/j.scitotenv.2015.11.028.

Mayer, B., Bollwek, S. M., Mansfeldt, T. Hütter, B. Veizer, J. (2001). The oxygen isotope composition of nitrate generated by nitrification in acid forest floors, *Geochimica et Cosmochimica Acta*, 65, 2743–2756. doi:10.1016/S0016-7037(01)00612-3.

McIlvin, M. R., Altabet, M. A. (2005). Chemical Conversion of Nitrate and Nitrite to Nitrous Oxide for Nitrogen and Oxygen Isotopic Analysis in Freshwater and Seawater. *Analytical Chemistry*, 77 (17), 5589–5595

Ministry for the Environment. (2019). *Environment Aotearoa 2019*. Wellington, NZ: Author

McDonnell, J. (2014). The two water worlds hypothesis: Ecohydrological separation of water between streams and trees? *Wiley Interdisciplinary Reviews: Water, 1.* 10.1002/wat2.1027.

McDowell, R. W., Ton Snelder, Roger Littlejohn, Matt Hickey, Neil Cox, Doug J. Booker (2011). State and potential management to improve water quality in an agricultural catchment relative to a natural baseline. *Agriculture, Ecosystems & Environment, 144*, 188-200

Meyer, D., Prien, R. D., Rautmann, L., Pallentin, M., Waniek, J. J., Schulz-Bull, D. E. (2018). In situ Determination of Nitrate and Hydrogen Sulfide

in the Baltic Sea Using an Ultraviolet Spectrophotometer. *Frontiers in Marine Science*, *5*. doi: 10.3389/fmars.2018.00431

Moir, J., Cameron, K., Di, H., Fertsak, U. (2011). The spatial coverage of dairy cattle urine patches in an intensively grazed pasture system. *The Journal of Agricultural Science, 149(*4), 473-485. doi:10.1017/S0021859610001012

Montanaro, C., Cronin, S., Scheu, B., Kennedy, B., Scott, B. (2020). Complex crater fields formed by steam-driven eruptions: Lake Okaro, New Zealand. GSA Bulletin. 10.1130/B35276.1.

NIWA. (2010). Investing in real-time water quality monitoring. Retrieved from https://niwa.co.nz/freshwater-and-estuaries/freshwater-and-estuaries-update/freshwater-update-38-october-2010/investing-in-real-time-water-quality

Özkundakci, D., Hamilton, D. P., Scholes, P. (2010). Effect of intensive catchment and in-lake restoration procedures on phosphorus concentrations in a eutrophic lake*. Ecological Engineering, 36*, 396-405. doi:10.1016/j.ecoleng.2009.11.006

Paul, A., Moussa, I., Payre-Suc, V., Probst, A., Probst, J. (2015). Flood survey of nitrate behaviour using nitrogen isotope tracing in the critical zone of a French agricultural catchment. *Comptes Rendus Geoscience, 347*, 10.1016/j.crte.2015.06.002.

Pärn, J., Pinay, G., Mander, U. (2012). Indictors of nutrients transport from agricultural catchments under temperate climate: a review. *Ecological Indicators 22*, 4–15.

Rayner, S., Clough, T., Baisden, T., Moir, J. (2019). Can ruminant urine-N rate and plants affect nitrate leaching and its isotopic composition?. *New Zealand Journal of Agricultural Research*. 1-19. 10.1080/00288233.2019.1648302.

Rissmann, C., Pearson, L., Lindsay, J., Beyer, M., Marapara, T., Badenhop, A.,Martin, A. (2018). Integrated landscape mapping of water quality controls for farm planning – applying a high resolution physiographic approach to the Waituna Catchment, Southland. In L. D. Currie and C.L. Christensen (Eds). *Farm environmental planning – Science, policy and practice*. http:flrc.massey.ac.nz/publications.html.

Occasional Report No. 31. Fertilizer and Lime Research Centre, Massey University, Palmerston North, New Zealand. 19 pages.

Ruehl, C. R., Fisher, A. T., Los Huertos, M., Wankel, S. D. Wheat, C. G. Kendall, C. Hatch, C. E. Shennan, C. (2007). Nitrate dynamics within the Pajaro River, a nutrient-rich, losing stream, *J. N. Am. Benthol. Soc., 26*, 191–206, doi:10.1899/0887-3593(2007)26[191:NDWTPR]2.0.CO;2.

Saraceno, J. F., Pellerin, B. A., Downing, B. D., Boss, E., Bachand, P.A., Bergamaschi, B. A. (2009). High-frequency in situ optical measurements during a storm event: Assessing relationships between dissolved organic matter, sediment concentrations, and hydrologic processes. *Journal of Geophysical Research, 114*, 2015

Sebilo, M., Billen, G. Mayer, B. Billou, D. Gably, M. Garnier, J. Mariotti, A.(2006), Assessing nitrification and denitrification in the Seine River and estuary using chemical and isotopic techniques, *Ecosystems, 9*, 564–577, doi:10.1007/s10021-006-0151-9.

Seitzinger, S., Harrison, J., Bohlke, J. Bouwman, A. Lowrance, R., Peterson, B.,Tobias, C., Drecht, G. (2007). Denitrification Across Landscapes and Waterscapes: A Synthesis. *Ecological applications : a publication of the Ecological Society of America, 16,* 2064-90. 10.1890/1051-0761(2006)016[2064:DALAWA]2.0.CO;2.

Selbie, D. R., Buckthought, L .E., Shepherd, M. A. (2015). The challenge of the urine patch for managing nitrogen in grazed pasture systems. *Advances in Agronomy, 129*, 229-292.

Scholes, P. (2009). Rotorua Lakes Water Quality Report 2009, Environment Bay of PlentyEnvironmental Publication 2009/12

Sherlock, R., Goh, K. (1985). Dynamics of ammonia volatilization from simulated urine patches and aqueous urea applied to pasture. II. Theoretical derivation of a simplified model. *Fertilizer Research, 6*, 3–22 https://doi.org/10.1007/BF01058161

Silva, S. R., Kendall, C., Wilkison, D.H., Ziegler, A.C., Chang, C.C.Y., Avanzino, R.J. (2000). A new method for collection of nitrate from fresh water and the analysis of nitrogen and oxygen isotope ratios. *Journal of Hydrology, 228*, 22–36.

Spoelstra, J., Schiff, S., Hazlett, P.W., Jeffries, D., Semkin, R. (2007). The isotopic composition of nitrate produced from nitrification in a

hardwood forest floor. *Geochimica et Cosmochimica Acta, 71,* 3757-3771. 10.1016/j.gca.2007.05.021.

Stark, C., Richards, K. (2008). The continuing challenge of agricultural nitrogen loss to the environment in the context of global change and advancing research. *Dynamic Soil, Dynamic Plant, 2*. 1-12.

Stevenson, B.A., Parfitt, R.L., Schipper, L.A., Baisden, W.T., Mudge, P. (2010). Relationship between soil δ15N, C/N and N losses across land uses in New Zealand, Agriculture, Ecosystems & Environment, 139(4), 736-741, https://doi.org/10.1016/j.agee.2010.10.020.

Stewart, M. K., Mehlhorn, J., Elliott, S. (2007). Hydrometric and natural tracer ($^{18}O$, silica, $^{3}H$ and $SF_6$) evidence for a dominant groundwater contribution to Pukemanga Stream, New Zealand. *Hydrological Processes, 21*, 3340–3356

Sudduth, E. B., Perakis, S. S., Bernhardt, E. S. (2013). Nitrate in watersheds: Straight from soils to streams? J*ournal of Geophysical Research: Biogeosciences, 118*, 291–302, doi:10.1002/jgrg.20030.

Snyder, L., Potter, J. D., McDowell, W. H. (2018). An evaluation of nitrate, fDOM, and turbidity sensors in New Hampshire Streams. *Water Resources Research, 54*, 2466–2479. https://doi.org/10.1002/2017WR020678

Tanner, C.C.; Caldwell, K.; Ray, D.; McIntosh, J. (2007). Constructing wetlands to treat nutrient-rich inflows to Lake Okaro, Rotorua. Presented at 5th South Pacific Stormwater Conference, Auckland, NZ, 16-18 May, 2007

Thériault, R., Rivard, C., Savard, M.M., Lefebvre, R. (2013). Nitrate sources and factors controlling its distribution in agricultural lands and groundwater in two small catchments in southern Quebec, Canada. GéoMontréal 2013 Conference Paper?

Townsend-Small, A., McCarthy, M.J., Brandes, J.A., Yang, L., Zhang, L., Gardner, W.S. (2007). Stable isotopic composition of nitrate in Lake Taihu, China, and major inflow rivers. *Hydrobiologia*, *581*, 135–140.

Turner, K., Edwards, T., Wolfe, B. (2014). Characterising Runoff Generation Processes in a Lake‐Rich Thermokarst Landscape (Old Crow Flats, Yukon, Canada) using $\delta^{18}O$, $\delta^{2}H$ and d‐excess Measurements*. Permafrost and Periglacial Processes*, *25*(1), 53-59.

Veale, N., Visser, A., Esser, B., Singleton, M.J., Moran, J.E. (2019). Nitrogen Cycle Dynamics Revealed Through δ18O-NO3− Analysis in California Groundwater. *Geosciences*, *9*, 95

Vincent, W. F. (1980). Biological transformations of nitrogen in New Zealand freshwaters. In P. W. Gandar (Ed), *Nitrogen Balances in NZ Ecosystems*. Palmerston North, NZ: DSIR

Vitousek, P. M., Aber, J. D., Howarth, R. W., Likens, G. E., Matson, P. A., Schindler, D. W., Schlesinger, W. H., Tilman, D. G. (1997). Human alteration of the global nitrogen cycle: sources and consequences. *Ecological Applications, 7*, 737-750. doi:10.1890/1051-0761(1997)007[0737:HAOTGN]2.0.CO;2

Wells, N. S., Baisden, W. T., Horton, T., Clough T. J. (2016), Spatial and temporal variations in nitrogen export from a New Zealand pastoral catchment revealed by stream water nitrate isotopic composition. *Water Resour. Res*., 52, 2840–2854, doi:10.1002/2015WR017642.

Wells, N. S., Clough, T. J., Johnson-Beebout, S. E., Elberling, B., Baisden, W.T. (2019). Effects of denitrification and transport on the isotopic composition of nitrate (δ18O, δ15N) in freshwater systems. *Science of The Total Environment*, *651*(2), 2228-2234

White, P., Toews, M., Tschritter, C., Lovett, A. (2016). Nitrogen discharge from the groundwater system to lakes and streams in the greater Lake Tarawera catchment, GNS Science Consultancy Report, 2015/108, 88 p.

Woodward, S., Stenger, R., Bidwell, V. (2013). Dynamic analysis of stream flow and water chemistry to infer subsurface water and nitrate fluxes in a lowland dairying catchment. *Journal of Hydrology*. 505. 299-311. 10.1016/j.jhydrol.2013.07.044.

Xue, D., Botte, J., De Baets, B., Accoe, F. Oertel née Nestler, A., Taylor, P., Cleemput, O., Berglund, M., & Boeckx, P. (2009). Present Limitations and Future Prospects of Stable Isotope Methods for Nitrate Source Identification in Surface and Groundwater. Water research. 43. 1159-70. 10.1016/j.watres.2008.12.048.

Zhang, Y., Peng. S., Jinxi, S., Qi, L. (2018). Application of Nitrogen and Oxygen Isotopes for Source and Fate Identification of Nitrate Pollution in Surface Water: A Review. *Applied Sciences, 9*, 18. 10.3390/app9010018.

# Appendix

## A.1 Supplementary Figures


**Figure A.1.** TLI with trends of factors (Total Nitrogen (TN), Total Phosphorous (TP), chlorophyll-a (Chla) and Secchi depth) used to determine TLI.

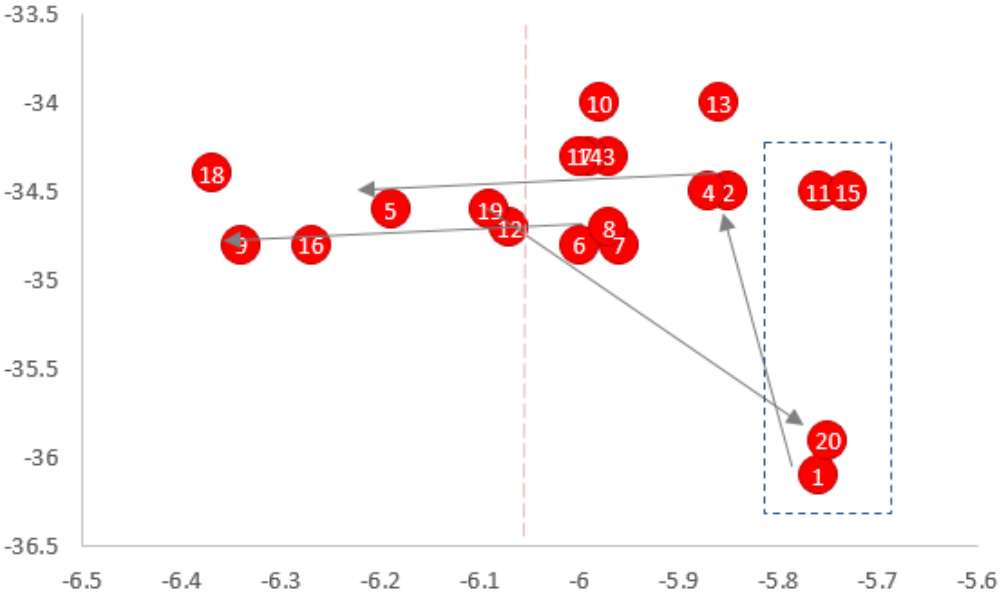


**Figure A.2.** February event hysteresis

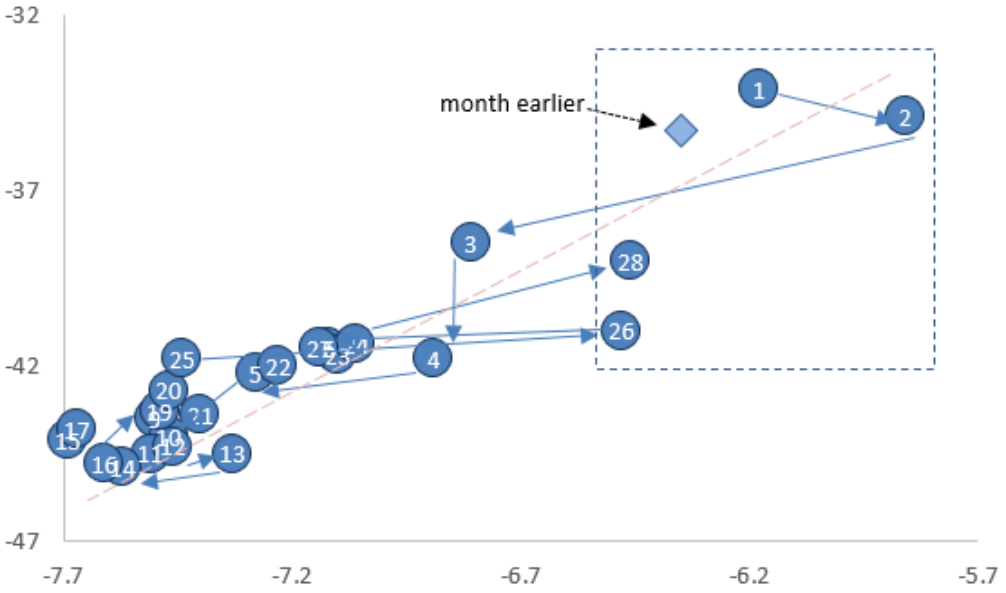


**Figure A.3.** July event hysteresis

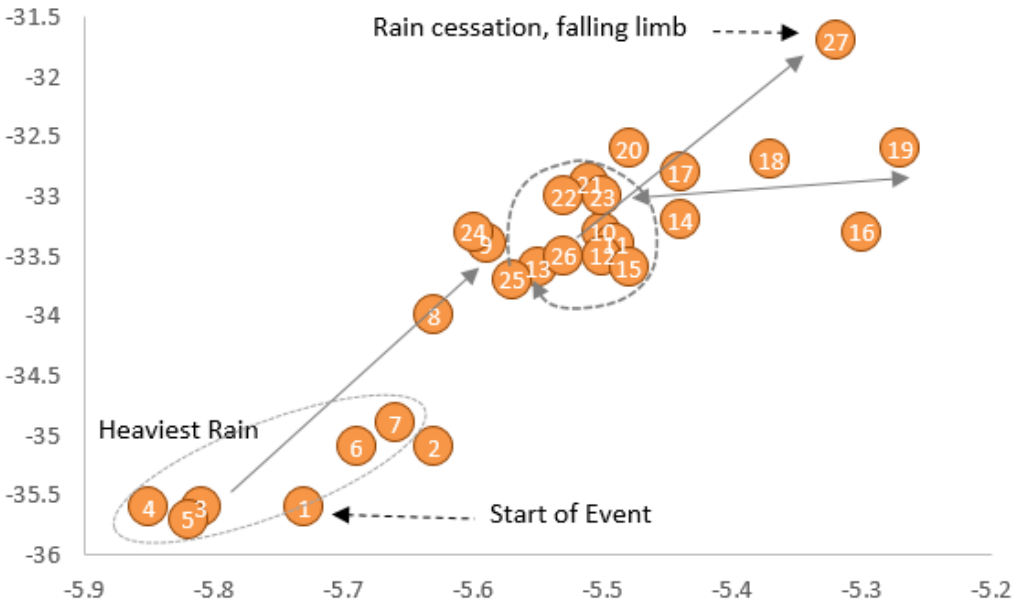


**Figure A.4.** December event hysteresis

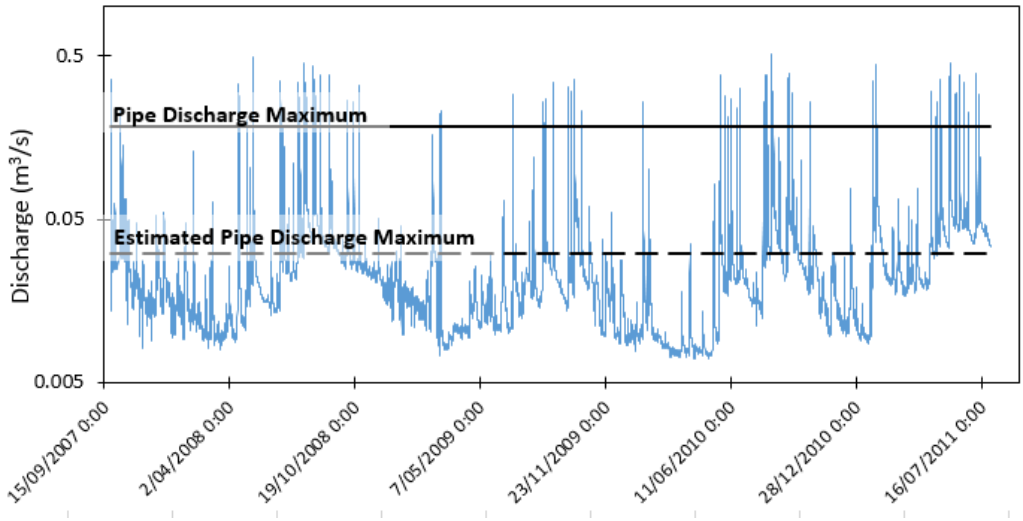


**Figure A.5.** Primary stream flow during wetland assessment period, showing visual proportions of stream flow that bypassed at the time (above pipe discharge maximum) and how much would bypass with the estimated maximum flowrate with a partially blocked pipe.

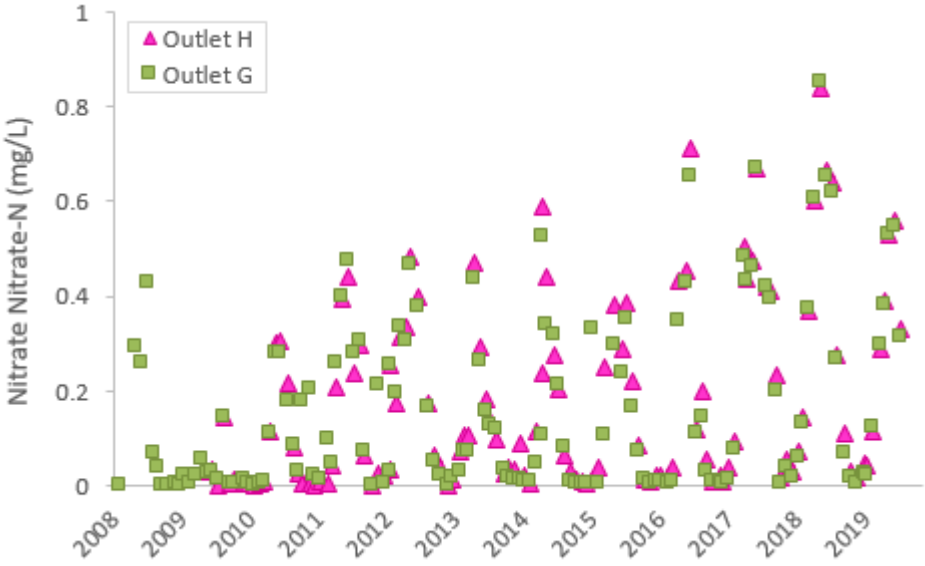


**Figure A.6.** Nitrate concentrations at the outlet of wetland and inlet to lake

## A.2 Photos

### A.2.1 Catchment Photos

**Figure A.7.** Riparian strip

**Figure A.8.** Main wetland

**Figure A.9.** Landslip revealing soil profile

**Figure A.10.** Soil profile at landslip

**Figure A.11.** Soil profiles along the rolling hills of the upper catchment showing variety of soil profiles; stream bottom texture at north stream confluence

**Figure A.12.** Hummocks in landscape, and rolling valleys slopes west of Lake Okaro

**Figure A.13.** Detention pond, regulates flows and traps silt

**Figure A.14.** Pipe draining detention bund at OK3

### A.2.2 July Storm

**Figure A.15.** High water level and overtopping of weir at OK1 during July 2019 storm event

**Figure A.16.** OK4 5th July 2019 - slug of sediment post event

**Figure A.17.** Increase in water level reaching Mayfly

**Figure A.18.** Rill erosion on a farm track after July event

## A.3 Soil Map

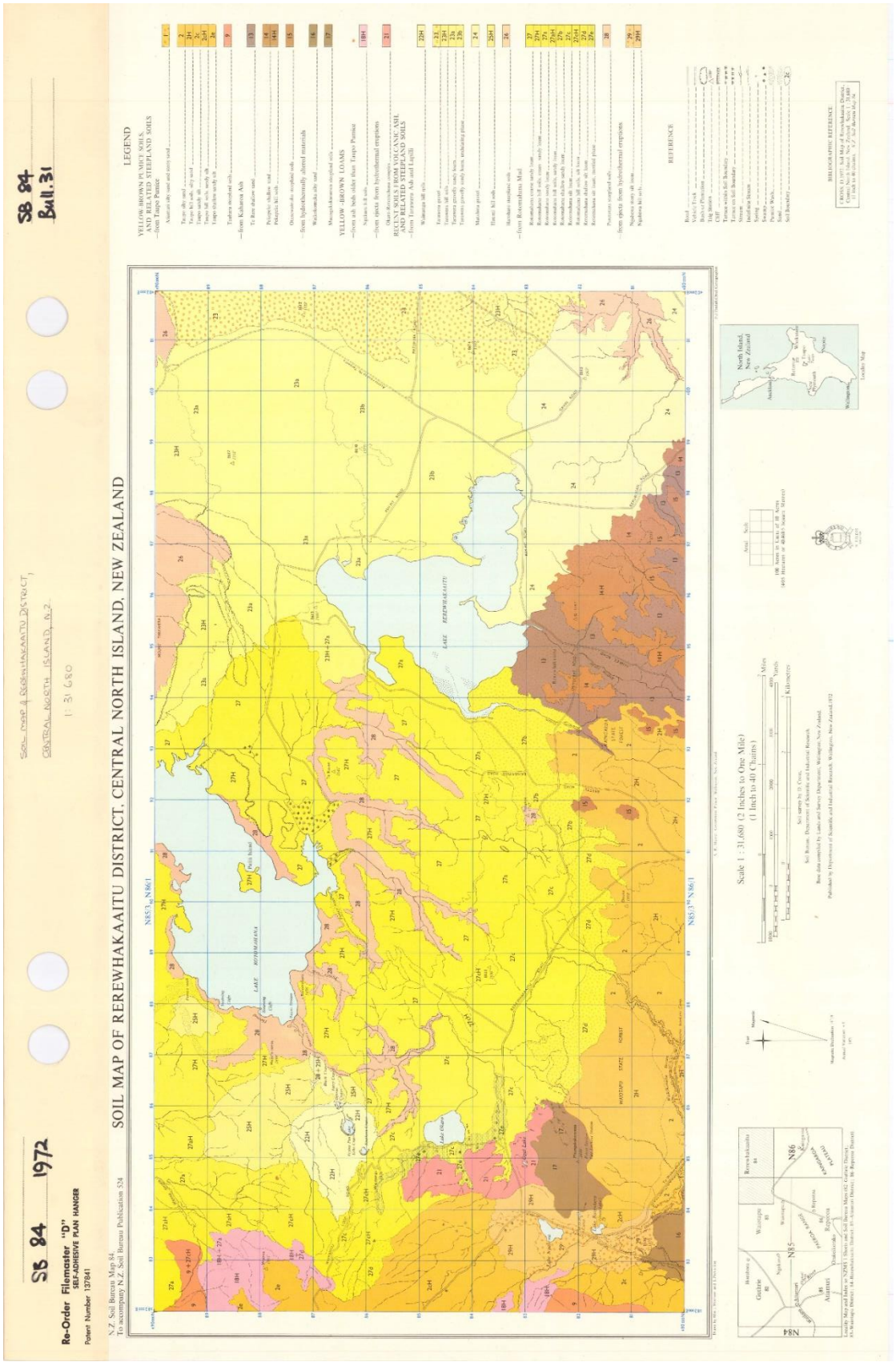


**Figure A.19.** Soil map of Rerewhakaaitu (Cross, 1972)